UCGE REPORTS
Number 20286

Department of Geomatics Engineering

Multichannel Dual Frequency GLONASS Software Receiver in Combination with GPS L1 C/A

(URL: http://www.geomatics.ucalgary.ca/research/publications)

by

Saloomeh Abbasiannik

April 2009

UNIVERSITY OF CALGARY

Multichannel Dual Frequency GLONASS Software Receiver

in Combination with GPS L1 C/A

by

Saloomeh Abbasiannik

A THESIS

SUBMITTED TO THE FACULTY OF GRADUATE STUDIES

IN PARTIAL FULFILMENT OF THE REQUIREMENTS FOR THE

DEGREE OF MASTER OF SCIENCE

DEPARTMENT OF GEOMATICS ENGINEERING

CALGARY, ALBERTA

April, 2009

Abstract

These days, Global Navigation Satellite System (GNSS) technology plays a critical role in positioning and navigation applications. Use of GNSS is becoming more of a need to the public. Therefore, much effort is needed to make the civilian part of the system more accurate, reliable and available, especially for safety-of-life purposes.

With the recent revitalization of Russian Global Navigation Satellite System (GLONASS), with a constellation of 20 satellites in February 2009 and the promise of 24 satellites by 2010, it is worthwhile to concentrate on the GLONASS system as a method of GPS augmentation to achieve more reliable and accurate navigation solutions. The use of GLONASS, in addition to GPS, provide very significant advantages such as increased satellite signal observation, and reduced horizontal and vertical dilution of precision factors. In particular, because of the limited number of GPS satellites, urban canyons and other locations with restricted visibility, such as forested areas, have problems acquiring and tracking a sufficient number of GPS signals. However, with the availability of combined GPS and GLONASS receivers, users will eventually have access to a 48-satellite constellation and the performance in these types of areas will improve accordingly.

Acknowledgement

The research presented in this thesis could not be completed without the generous and kind support of some special people. I wish to express my heartfelt gratitude to:

- Dr. Mark Petovello, my supervisor, for his continuous encouragement, guidance, and patience. He was not only my teacher in subject matter, but also my mentor in other aspects of my life during my graduate studies. He is my role model in research and professional career.

- Dr. Gérard Lachapelle, who offered me the opportunity to study in the PLAN group, for his insight, directions, and support. By providing a comfortable research environment, he facilitated accomplishing this research. Also, this thesis is improved using his comments and suggestions as he was in my oral exam committee.

- Ali Broumandan, who was there whenever I needed help and support. Thanks Ali for bringing me peace, happiness, encouragement, and constant love.

- My family, who tolerated all the seconds I have been away. This thesis is a dedication to them and their unconditional love. Thanks for giving me the wings to fly to pursue my dreams.

- Dr. Kyle O'Keefe and Dr. Michel Fattouche, who were in my M.Sc. oral exam committee, for their valuable suggestions and comments that improved this thesis.

- PLAN research engineers, Dr. Cillian O'Driscoll and Dr. Daniele Borio for their generous knowledge sharing, suggestions and helpful pieces of advice.

Table of Contents

List of Tables

List of Figures and Illustrations

List of Symbols

Symbol	Definition
f_{PBB}	Pseudo-base-band frequency
I	In phase
Q	Quadrature phase
I^{DR}	Doppler removed I
Q^{DR}	Doppler removed Q
I^{DRC}	Doppler removed and correlated I
Q^{DRC}	Doppler removed and correlated Q
$R(t)$	Auto-correlation function
$f_{carrier}$	Carrier frequency
IF	Intermediate frequency
E	Early
P	Prompt
L	Late
ϕ	Phase
C_k	Cross product
D_k	Dot product
C/N_0	Carrier to noise density ratio
T_{up}	Upper threshold
T_{low}	Lower threshold
T_{coh}	Coherent integration time
P_{esc}	Probability of error in sign change
b_i	Data bits
β_i	Check bits
C_i	Checksums
X, Y, Z	Satellite coordination
$\dot{X}, \dot{Y}, \dot{Z}$	Satellite velocity
$\ddot{X}, \ddot{Y}, \ddot{Z}$	Satellite acceleration
K	Channel number

List of Abbreviations

Abbreviation	Definition
ADC	Analog to Digital Convertor
ATAN	Arctangent
C/A	Coarse / Acquisition
CDMA	Code Division Multiple Access
CLL	Carrier Lock Loop
DLL	Delay Lock Loop
FDMA	Frequency Division Multiple Access
FFT	Fast Fourier Transform
FLL	Frequency Lock Loop
FPGA	Field Programmable Gate Array
GLONASS	Global Navigation Satellite System
GNSS	Global Navigation Satellite System
GPS	Global Positioning System
GSNRx	GNSS Software Navigation Receiver
ICD	Interface Control Document
IF	Intermediate Frequency
IonF	Ionosphere Free
NBP	Narrow Band Power
NCO	Numerically Controlled Oscillator
NP	Normalized Power
PLAN	Position, Location And Navigation
PR	Pseudo Random
PRN	Pseudo Random Noise
RF	Radio Frequency
RMS	Root Mean Square
STD	Standard Deviation
SV	Satellite Vehicle
SU	Soviet Union
UTC	Coordinated Universal Time

CHAPTER ONE: INTRODUCTION

1.1 Chapter outline

In this Chapter, a general background of GPS and GLONASS systems is reviewed. Then, the previous works related to this research is discussed. The Chapter continues with defining the objective of this research. At the end of this Chapter, thesis outline is presented.

1.2 Background

The Global Positioning System (GPS) provides accurate, continuous, worldwide, three dimensional position and velocity information to users with the appropriate receiving equipment (Spilker & Parkinson 1996). The GPS constellation nominally consists of 24 satellites arranged in six orbital planes with four satellites per plane. The satellites operate in 20,200-km orbits at an inclination of 55°, and each satellite completes the orbit in approximately 11 hours and 58 minutes. GPS can provide service to an unlimited number of users. The satellite broadcast navigation data and ranging codes on two frequencies using a technique called CDMA (Code Division Multiple Access). At the time of writing, there are only two frequencies in use by the system, called L1 (1,575.42 MHz) and L2

(1,227.6 MHz). Each satellite transmits on these frequencies, but with a unique set of codes compared to the other satellites. Each satellite generates a short code referred to as the coarse/acquisition or C/A code and a long code denoted as the precision or P(Y) code. Navigation data provides the means for the receiver to determine the location of the satellite at the time of signal transmission. The ranging code enables the user's receiver to determine the transit time of the signal and hence determine the satellite-to-user range. If the receiver clock were synchronized with the satellite clock, only three range measurements would be required. However, a low cost quartz clock is usually employed in navigation receivers to minimize the cost, complexity, and size of the receiver. Thus, four measurements are required to determine the user latitude, longitude, height, and receiver clock offset from internal system time.

The Russian counterpart of GPS is called GLONASS. GLONASS is a radio-based satellite navigation system, developed by the former Soviet Union and now operated by Russian Space Forces (Feairheller & Clark 2006).

The purpose of GLONASS is to provide an unlimited number of air, marine, and any other type of users with all-weather three-dimensional positioning, velocity measuring and timing anywhere in the world or near-earth space. A completely deployed GLONASS constellation is composed of 24 satellites in three orbital planes. Eight satellites are equally spaced in each plane. The satellites operate in circular 19,100-km orbits at an inclination of 64.8°, and each satellite completes the orbit in approximately 11 hours and 15 minutes (GLONASS ICD 2002).

User equipment measures pseudorange and pseudorange rate of generally four or more GLONASS satellites.

It also receives and processes navigation messages contained within navigation signals of the satellites. The navigation message describes the position of the satellites. Processing of the measurements and the navigation messages of the four or more GLONASS satellites allow users to determine three position coordinates, three velocity vector constituents, and to refer user time scale to the National Reference of Coordinated Universal Time UTC (SU). The interface between the space segment and the user equipment consists of radio links of L-band. At the time of writing, each GLONASS satellite transmits navigation signals in two sub-bands of L-band (with centre frequency of L1 ≈ 1.6 GHz and L2 ≈ 1.2 GHz). GLONASS uses FDMA (Frequency Division Multiple Access) in both L1 and L2 sub-bands. This means that each satellite transmits a navigation signal and raging code on its own carrier frequency in the L1 and L2 sub-bands (Feairheller & Clark 2006). Two GLONASS satellites may transmit navigation signals on the same carrier frequency if they are located in antipodal slots of a single orbital plane. GLONASS satellites provide two types of ranging code signals in the L1 and L2 sub-bands: standard accuracy signal and high accuracy signal. The standard accuracy signal is available for any users equipped with proper receivers and having visible GLONASS system satellites above the horizon (GLONASS ICD 2002).

GLONASS consists of satellites in medium Earth orbit (MEO), a ground control segment, and user equipment. GLONASS system was designed mainly for military purposes and was fully deployed in 1995 with a constellation of 24 satellites without any selective availability for civilian users (Polischuk & Revnivykh 2003). Commitments of the Russian Government to sustain the free use of GLONASS for the following 10 years were presented to the world community in 1995. However, between 1995 and the end of

1998, due to the lack of the federal budget funding, the GLONASS constellation was degraded. By the Presidential Decree in 1999, GLONASS was used only in the Ministry of Defense and Russian Aviation and Space Agency. After the evolution in the GNSS industry, when Europe introduced Galileo for civilian use and GPS modernization, on 20th August 2001, the Russian Government adopted the long-term program of GLONASS sustainment, modernization and application. The goal was to give more reliable and accurate navigation solution in combination with other GNSS systems and to share this market for civilian users (Polischuk & Revnivykh 2003).

While Russia's economic problems have slowed its ability to replenish failing or failed GLONASS satellites with the latest GLONASS-M models, Russia has continued to update and distribute the public GLONASS Interface Control Document (ICD). The GLONASS Coordination Scientific Information Center (KNITS), the Scientific and Production Association of Applied Mechanics (NPO PM) and the Research Institute of Space Device Engineering (RNII KP) must all agree on changes, additions, and amendments to the ICD. The current ICD states that GLONASS is made available for all-weather three-dimensional positioning, velocity measuring, and timing anywhere in the world or near-earth space (Polischuk & Revnivykh 2003).

The largest GLONASS user community outside the Russian Federation is composed of academics, engineers, geographers, cartographers, surveyors, and geologists who use GLONASS for increased accuracy in surveying, mapping, and tracking earth movements such as volcanoes, earthquakes, and glaciers (Leick 1995).

As designed, the ground support segments of GLONASS consists of a number of sites scattered throughout Russia that control, track, and upload ephemeris, timing information, and other data to satellites (Feairheller & Clark 2006).

Following the GLONASS modernization process, the second generation of GLONASS satellites, GLONASS-M, was launched. After completing on-orbit tests, the first GLONASS-M satellite was marked "healthy" on December 9, 2004, and is now broadcasting a new civil L2 signal as well as additional GLONASS-M navigation data that improves the performance of GLONASS significantly (Zinoviev 2005). The property of having a civil L2 signal is very useful in achieving more reliable and accurate navigation solution, because of the ability to mitigate ionosphere error in a dual frequency GNSS systems. Moreover, a narrow band interference that affects L1 may not affect L2. In total, with the help of the mentioned characteristics and other factors, the accuracy of GLONASS-M navigation signal is 2-2.5 times better than the original GLONASS navigation signal (Bartenev et al 2005).

GLONASS is on the way to its revival. The launches of third generation satellites, GLONASS-K, will begin in 2010. Along with the extended life-time of 12 years, GLONASS-K will be capable of broadcasting L3 civil signals, on which integrity information for safety-of-life applications will be available (Zinoviev 2005).

It is clear that a GPS+GLONASS receiver might provide advantages over a single-system (GPS-only or GLONASS-only) receiver (Ryan 2002), but in this integration, some issues must be resolved. The most important issues are the differences in coordinate systems and time reference frames between GPS and GLONASS channels (Zinoviev 2005).

GLONASS has better coverage in high latitudes because of its higher orbital inclination. GPS coverage is superior near the equator (Chachis 2001).

The GPS system has begun the process of modernization to expand its capabilities to include a new civilian code on the L2 frequency and eventually on the L5 frequency. GLONASS has launched modernized satellites (GLONASS-M) and a new L3 signal in GLONASS-K. In the near term, a receiver design will have to weigh the pros and cons of developing complex hardware chips to take the advantage of the rapidly evolving signal environment.

A software receiver can utilize the new signals without the need for a new hardware. Given a suitable front-end, new frequencies and ranging codes can be used simply by making software changes (Ledvina et al 2006). The software receiver idea is to use an analog-to-digital converter (ADC) to change the input radio frequency (RF) signals into digital data at the earliest possible stage in the receiver. In other words, the input signal is digitized as close to the antenna as possible. Once the signal is digitized, software-based digital signal processing will be used to obtain and process the digitized received signal. The primary goal of the software receiver is to minimize the hardware used in a receiver. A great flexibility can be achieved by using a software receiver (Bao & Tsui 2000a).

The following table shows the original and modernized signals of GPS, GLONASS, and Galileo.

Table 1-1 Original and Modernized Signals of GNSS Systems

	Original Signals	Modernized Signals
GPS	L1 (C/A), L1 (P), L2 (P)	L2 (C/A), L5
GLONASS	L1 (C/A), L1 (P), L2 (P)	L2 (C/A), L3
Galileo	E1, E2 ,E5, E6	N/A

1.3 Literature review

As mentioned above, there has been a recent effort to convert all or some parts of the hardware of a GNSS receiver to software and provide a software-based GNSS receiver. This helps in reducing the size and the price of a receiver besides some other advantages.

Besides some software receivers presented for the GPS system, there are some researches on other GNSS systems such as Galileo. Heinrichs et al (2007) developed the first interactive GPS/Galileo L1/E1 software receiver. Macchi & Petovello (2007) presented the development of a one-channel Galileo L1 software receiver and tested the software using real data. Ledvina et al (2006) developed and tested a real-time GPS and Galileo software receiver. The receiver has 12 channels for tracking GPS satellites and 12 channels for tracking Galileo satellites. Moreover, Normark & Ståhlberg (2005) describe a software hybrid GNSS receiver capable of real-time acquisition and tracking of GPS C/A and Galileo BOC(1,1) data and pilot channel.

Furthermore, some software developments have been done on new GPS signals. Muthuraman et al (2007) evaluated different data/pilot tracking algorithms for GPS L2C

signals using a software receiver. Ledvina et al (2005) demonstrated a real-time software receiver operation for GPS L2 civilian signal. This GPS civilian L1/L2 software receiver tracks 12 channels in real-time and has a navigation accuracy of 1-3 meters.

Some software receivers can be operated in a microprocessor, a Field-Programmable Gate Array (FPGA) or Digital Signal Processor (DSP). Itaca is a scientific GNSS software receiver (Tomatis et al 2007). The input data stream is processed by the acquisition block, which is based on the Fast Fourier Transform (FFT). The tracking block implements a coupled loop composed of a second order Costas Phase Lock Loop (PLL) and a second order Delay Lock Loop (DLL). One advantage of this software is the ability to monitor the signal at every stage. Since it was a part of Galileo receiver for high dynamic application, it focuses on the Galileo and GPS more than other GNSS systems. The software is going to be updated in order to make Itaca a valuable tool for the analysis of the next generation of GNSS signals (Tomatis et al 2007). Namuru is the name given to the open GNSS receiver research platform developed at the University of New South Wales, Australia (Mumford et al 2006). The platform includes three aspects; 1) a custom circuit board, 2) baseband processor (correlator block) logic design and 3) application firmware. Both the circuit board and baseband processor designs are available in the public domain. The custom circuit board has an L1 GPS RF front-end and contains an Altera ´Cyclone´ FPGA chip, 3-axis accelerometer and various input/output and memory components. The board has been carefully designed to keep noise around the sensitive RF front-end as low as possible. This software uses a Frequency Locked Loop (FLL) for carrier tracking. The cross product discriminator is used and the loop filter is a discrete second-order filter. Code tracking is achieved with a first-order Delayed Locked Loop

(DLL) with carrier aiding. The dot product early-late discriminator is used with bandwidth of 1 Hz (Mumford et al 2006).

A real-time GPS L1 C/A code software receiver has been implemented on a Digital Signal Processor (DSP) by Humphreys et al (2006). The receiver exploits FFT-based technique to perform acquisition. Efficient correlation algorithms and robust tracking loops enable the receiver to track an equivalent of 43 L1 C/A code channels in real-time. The FLL is used as a bridge between signal acquisition and Phase Locked Loop (PLL) tracking. The first-order FLL employs a four-quadrant arctangent discriminator. The PLL is a variable-bandwidth third-order Costas loop with a decision-directed discriminator and the DLL is a standard first-order carrier-aided 0.5-Hz-bandwidth code tracking loop with a dot product discriminator (Humphreys et al 2006). Kovar et al (2004) presented a software receiver implemented in an FPGA. For this purpose, a two-channel RF unit, a DSP unit based on FPGA device, and a high power computer unit are used. A powerful FPGA called Virtex-II Pro from Xilinx is used to integrate all digital processing parts (Kovar et al 2005). Spelat et al (2006) utilized FPGA and DSP for combined GPS and Galileo software receiver. Although FPGAs are powerful, they are relatively expensive. In addition, there is always a limitation for the capacity of the FPGA applied in this research. It is possible that this FPGA does not have enough capacity for the integrated GPS, GLONASS, and Galileo systems.

Won et al (2006) presented an efficient and practical way of general purpose high performance signal tracking software for a multi-frequency GNSS receiver by using a Maximum likelihood Estimation (MLE) technique. The cost function of the MLE for estimating signal parameters such as code phase, carrier phase, and Doppler frequency is

used to derive a discriminator function for creating error signals from incoming and reference signals. The designed MLE tracking algorithm is implemented in C++. The use of C++ with Object-Oriented Programming (OOP) in combination with software engineering techniques makes it possible to use the tracking software for multiple frequencies and modulation schemes, for example, to track GPS and Galileo signals using the same lines of source code. In addition, Petovello & Lachapelle (2006) presented an efficient new method of Doppler removal and correlation with application to software-based GNSS receivers.

The Purdue Software Receiver (PSR) is a real-time software GPS receiver developed at the University of Purdue. The PSR is programmed in C++ and this has made the objects to encapsulate functions and related data together and to reduce unnecessary copying of data. The PSR has an FFT acquisition module presented in the code. The early and late correlations are utilized to generate the early-minus-late (EML) signal, which enables DLL tracking of the code. The prompt correlation is used directly for FLL/PLL tracking of the carrier frequency (Heckler & Garrison 2004). The software receiver starts after the acquisition card in the method proposed by Sharawi & Korniyenko (2007). The raw GPS data which was collected on rooftop was sent to an RF front-end and then to a data acquisition card that sampled the data and stored it on a hard drive. The whole software receiver is provided using Matlab™ code. Although there is a claim on GLONASS system on this research, no results for GLONASS are presented at the time of writing this thesis.

The PLAN (Position, Location And Navigation) Group in the Department of Geomatics Engineering at the University of Calgary developed its first software receiver

(GNSS_SoftRx™) in 2003 (Ma et al 2004). Numerous PLAN Group members (e.g. Skone et al 2005, Zheng & Lachapelle 2005) have used the post-mission version of this software for many research projects. The second version of the software was developed in 2005. In this version, real-time operation capability was achieved by using optimized algorithm to perform Doppler removal and code correlation (Charkhandeh et al 2006). This receiver was expanded and optimized for a real-time acquisition method and interfacing the software with hardware. Inside the recent GPS receiver, a second-order loop filter DLL is used to track the C/A code of the signals. Carrier tracking is performed using a second-order loop filter. The decision-directed cross product discriminator has been implemented for FLL. An FLL-assisted PLL is also implemented in the receiver and the ATAN carrier phase discriminator is used for the PLL (Charkhandeh et al 2006). Petovello et al (2008) completed the software receiver in a modular design, wrote it entirely in C++, and renamed it GSNRx™. This software operates in post-mission mode and generates pseudorange; Doppler frequency and carrier phase observation for further processing and generates a stand alone Position, Velocity and Time (PVT) solution.

These are just some examples of the research that have been done on GNSS software receivers but none of the work mentioned above – either using a pure software receiver or those implemented in microprocessor, FPGA or DPS – have presented a solution for GLONASS system.

1.4 Research objective

The objective of this research is to develop a combined GPS and GLONASS software receiver capable of providing a position solution. The software receiver generated in the PLAN group at the Geomatics Engineering department of the University of Calgary called GSNRx™ is modified to include the GLONASS system (Petovello et al 2008). To this end, the following sub-objectives are identified:

1. Providing acquisition and tracking methods for GLONASS L1 and L2 signals,

2. Providing a method to decode GLONASS navigation data, and

3. Combining GLONASS with GPS in order to compute the best position solution

1.5 Thesis outline

In Chapter one, the GLONASS system background was presented. Moreover, the previous researches in the relevant areas, along with their limitations, were described. Finally, the objective of this thesis was presented.

In Chapter two, the historical evolution of GLONASS, its constellation and orbits are discussed in detail. Because of the enhanced number of GLONASS-M satellites launches and close plan for GLONASS-K satellites launches; these types of GLONASS satellites are reviewed. The characteristics of GLONASS radio frequency signals including signal structure, correlation characteristics, ranging code and navigation data bits are explained, too. The objective of any Global Navigation Satellite System (GNSS) signal processing is

generating a local signal which exactly matches the incoming pseudo-base-band signal. The signal processing procedure is as follows (Lachapelle 2007):

- Signal acquisition in which a local signal is generated and approximately matches the incoming signal. GLONASS signal acquisition is explained in Chapter three.

- Signal tracking in which a local signal is generated in a way that closely matches the incoming signal and GLONASS tracking steps are explained in Chapter four for both GLONASS L1 and GLONASS L2 signals.

- Navigation message demodulation where the navigation data bits are decoded. GLONASS navigation data demodulation is explained in Chapter five.

The combination of GPS and GLONASS for more accurate and reliable navigation solution is explained in Chapter six. In the last Chapter, seven, the conclusion and summary along with the future work are discussed.

CHAPTER TWO: GLONASS THEORY

2.1 Chapter outline

This Chapter begins with a short review of GLONASS history. Then, the GLONASS orbit and constellation is briefly discussed. A short explanation of the legacy generation, type M generation and type K generation GLONASS spacecraft is presented. The Chapter continues with GLONASS signal characteristics and in this section the GLONASS Radio Frequency (RF) signals in L-band, Pseudo Random (PR) ranging codes, Intra-system interference and signals power level are explained. The GLONASS navigation message in terms of its content and structure are then explained in detail. At the end, the GLONASS time system and coordinate frame are discussed.

2.2 Historical evolution

The Soviet military initiated the GLONASS program in the mid-1970s to support military requirements. The test of the system showed that they could use GLONASS for civilian users while concurrently meeting the Soviet defense needs. The first GLONASS satellite was launched in October 1982 and an initial test constellation of four satellites was deployed by January 1984. However, the Soviet launched ballast payloads, instead of real

satellites, to save production costs, while the system was under development (Feairheller & Clark 2006).

According to Feairheller & Clark 2006, in 1988, the free use of GLONASS navigation signal was offered. In 1990-1991, after the demise of the Soviet Union, the Russians tested the GLONASS constellation with 10-12 satellites. During the development, it became clear that GLONASS signals interfered with radio astronomy observation in the 1610.6-1613.8 MHz band. The international scientific community protested and the Russians agreed to modify the future GLONASS frequency plan in November 1993. In April 1994, the Russians initiated the first of seven launches to complete the constellation. In December 1995, the Russians successfully launched the last set of three satellites to complete the 24-satellite constellation. In February 1995, these satellites were declared operational and the constellation was fully populated for the first time. However, a number of older satellites began to fail and constellation quickly degraded. From 1996 to 2001, the Russians only launched two sets of three satellites. This was insufficient to maintain the constellation. The constellation degraded to six to eight satellites in 2001. In August 2001, the Russian government passed Decree Number 587 entitled "Federal Dedicated Program (FTsP) Global Navigation system-2002-2011." This decree established a 10-year program to rebuild the GLONASS program. The GLONASS FTsP is a comprehensive program to fund the space segment, ground segment, user equipment, manufacturing industry, transportation application industry, and geodetic application industry. Under this program, the GLONASS constellation will be replenished with 10-12 modernized GLONASS-M satellite and 18-27 new lightweight GLONASS-K

satellites. The first GLONASS-M satellite was launched in late 2003 (Feairheller & Clark 2006).

Moreover, GLONASS will continue to broadcast FDMA signals at its current frequencies as well as new ones in the future at L3 (1201-1208 MHz) in CDMA format. Use of FDMA signals has complicated the design of combined receivers, because all the other GNSS receivers use CDMA. As a result, this equipment has been more expensive and typically limited to professional or commercial application. Improved timing and orbit determination are planned to enable the system to match GPS system performance by 2012. At the time of writing, GLONASS was in the seventh year of its 10-year plan for rebuilding its constellation. Russia also plans to expand the GLONASS constellation from the current fully operational capability (FOC) of 24 satellites to 30 satellites at a minimum. Terrestrial and space-based augmentation systems are also under development to improve real-time accuracy of GLONASS (GNSS Program Updates 2008).

At the time of writing, there are 20 GLONASS satellites in the constellation of which 19 are GLONASS-M satellites (GLONASS Constellation Status 2009).

Figure 2-1 shows GLONASS constellation status on 21th February 2009 (GLONASS Constellation Status 2009).

Orbital plane	Orbital slot	RF channel	#GC	Operation begins	Comments
	2	01	728	20.01.09	In operation
	3	05	727	17.01.09	In operation
I	4	06	795	29.01.04	In operation
	6	01	701	08.12.04	Maintenance
	7	05	712	07.10.05	In operation
	8	06	729	12.02.09	In operation
	9	-2	722	25.01.08	In operation (L1 only)
	10	04	717	03.04.07	In operation
II	11	00	723	22.01.08	In operation
	13	-2	721	08.02.08	In operation
	14	04	715	03.04.07	In operation
	15	00	716	12.10.07	In operation
	17	-1	718	04.12.07	In operation
	18	-3	724	26.10.08	In operation
	19	03	720	25.11.07	In operation
III	20	02	719	27.11.07	In operation
	21	-1	725	05.11.08	In operation
	22	-3	726	13.11.08	In operation
	23	03	714	31.08.06	In operation
	24	02	713	31.08.06	maintenance

Figure 2-1 GLONASS Constellation status on 21th of February 2009

2.3 Constellation and orbit

The GLONASS constellation nominally consists of 21 active satellites plus three active on-orbit spares. The 24 satellites will be uniformly located in three orbital planes 120° apart in right ascension. A 21-satellite constellation provides continuous four-satellite visibility over 97% of the Earth's surface (Feairheller & Clark 2006). Under the 21-satellite concept, the performance of all 24 satellites will be determined by GLONASS controllers and the best 21 will be activated. The remaining three will be held for back up or in reserve.

Each GLONASS satellite is in a 19,100 km altitude circular orbit with an inclination of 64.8°. The orbital period is 11 hours and 15 minutes (GLONASS ICD 2002). The current orbital configuration and overall system design provide navigation service to users up to 2,000 km above the Earth's surface (Feairheller & Clark 2006).

Table 2-1 shows the difference between the nominal GPS and GLONASS constellations.

Table 2-1 GLONASS and GPS constellation comparison

	GLONASS	GPS
Number of satellite	24	24
Number of orbital plane	3	6
Orbital inclination	64.8°	55°
Period of revolution	11 h 15 m	11 h 58 m
Orbital altitude	19,100 km	20,200 km

2.4 Spacecraft description

At the time of writing, there are two types of GLONASS spacecraft in the constellation; the first-generation GLONASS satellite and GLONASS-M satellites. As discussed earlier, there will also be GLONASS-K satellites in the constellation in the next two years. A brief explanation of each type is presented here.

2.4.1 First-generation GLONASS

From 1982, the Russians planned to launch the first generation of GLONASS satellites. Although these are normally referred to as "GLONASS" satellites, the term "first-generation GLONASS" is used herein to avoid confusion with the proper name of the GNSS and from the use of "GLONASS satellite" to refer to any combination of satellites within the system. The primary function of first-generation GLONASS satellites is recording the satellite ephemeris and almanac data which are uploaded from ground stations and also controlling of navigation signal formulation. Moreover, the onboard clock has a critical role in all types of GLONASS satellites. The first-generation GLONASS spacecraft carry three "Gem" cesium-beam frequency standards (Feairheller & Clark 2006).

2.4.2 GLONASS-M

In 2003, the Russians began launching GLONASS-M satellites, where "M" stands for "Modernized". These satellites use more modern electronics and support a number of new features. In comparison with the previous satellite, GLONASS-M offers some advantages such as:

- Extended guaranteed life-time (seven vs. three years)

- More stable clock

- Additional GLONASS-M navigation data

- Inter-satellites radio link

One of the advantages of GLONASS-M satellite is the ability to transmit civil L2 signal (Zinoviev 2005). Moreover, GLONASS-M satellites broadcast new navigation data and have some differences relative to first-generation GLONASS satellite in both immediate and non-immediate data. These new navigation data greatly improve overall system performance (Zinoviev 2005).

2.4.3 GLONASS-K

The Russians plan to start launching the new GLONASS-K satellites in 2010. Currently, there is a plan to produce 18-27 GLONASS-K satellites. These newer satellites weigh about half of the GLONASS-M satellites. The lighter satellite will allow the Russians to launch GLONASS-K satellites six at a time on a single Proton launch vehicle, or two at a

time on a Soyuz launch vehicle. GLONASS-K offers some advantages such as (Feairheller & Clark 2006):

- Longer life-time, namely around 10-12 years

- More stable clock

- Third civil and military signals in the 1201-1208 MHz frequency range

2.5 GLONASS signal characteristics

In GPS, each satellite transmits the ranging code on the same frequency using Code Division Multiple Access (CDMA). In GLONASS however, each satellite transmits the same ranging code signal on different frequencies using Frequency Division Multiple Access (FDMA) technique. Although there are some disadvantages in using an FDMA technique such as larger and more expensive receivers because of the extra front-end components to process multiple frequencies, some advantages are available. In particular, a narrowband interference source that disrupts only one FDMA signal would disrupt all CDMA signals simultaneously.

2.5.1 GLONASS navigation RF signal characteristics

The interface between space segment and user equipment consists of radio links of L-band. Each GLONASS satellite transmits a navigation signal in two sub-bands of L-band referred to as L1 and L2, the frequencies of which are defined by the following expressions:

$$f_{k1} = f_{01} + K.\Delta f_1 \qquad\qquad 2\text{-}1$$

$$f_{k2} = f_{02} + K.\Delta f_2 \qquad\qquad 2\text{-}2$$

where K is the frequency number (frequency channel) of signals transmitted by GLONASS satellites in the L1 and L2 sub-bands and

a) f_{01}= 1602 MHz; Δf_1= 562.5 kHz, for L1 sub-band

b) f_{02}= 1246 MHz; Δf_2= 437.5 kHz, for L2 sub-band

The channel number K for any particular GLONASS satellite is provided in the almanac (non-immediate data of navigation message). K is a unique integer for each satellite and varies from -07 to 13. The plan is to have satellites on opposite sides of the Earth (antipodal) share the same frequency number.

Carrier frequencies L1 and L2 are generated from a common onboard time/frequency standard in each satellite. The nominal value of this frequency is equal to 5.0 MHz (GLONASS ICD 2002).

Figure 2-2 shows a general block diagram for generating GLONASS signals (Feairheller & Clark 2006). As it is shown, this signal generator is for first-generation GLONASS satellites which transmit standard accuracy signal on the L1 sub-band only. For GLONASS-M satellites, standard accuracy signal must be added to the L2 sub-band.

$$A(t) = C_{HA}(t) D_{HA}(t) Cos(\omega_1 t + \theta)$$
$$B(t) = C_{SA}(t) D_{SA}(t) Sin(\omega_1 t + \theta)$$

$$S2(t) = C_{HA}(t) D_{HA}(t) Cos(\omega_2 t + \theta)$$

$$S1(t) = A(t) + B(t)$$
$$S2(t) = C_{HA}(t) D_{HA}(t) Cos(\omega_2 t + \theta)$$

BPF: Band-pass Filter

SA: Standard Accuracy

HA: High Accuracy
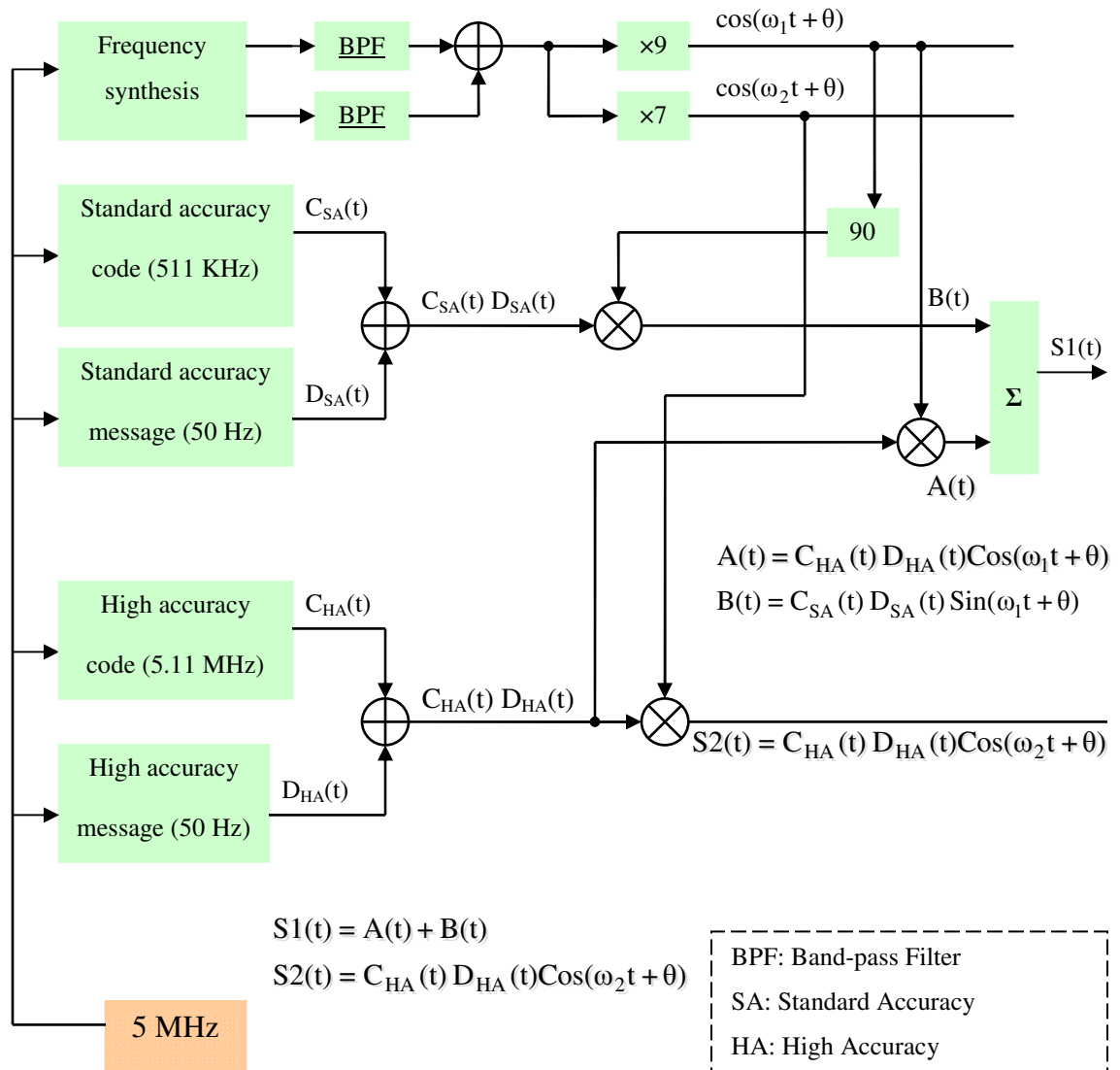
Figure 2-2 GLONASS signal generator (modified Feairheller & Clark 2006)

2.5.2 GLONASS signal modulation

The sequence used for modulation of the carrier frequencies when generating standard

accuracy signals on L1 for first-generation GLONASS satellites and on L1 and L2 for

GLONASS-M satellites is generated by modulo-2 addition of the flowing three binary signals:

- Pseudo random (PR) standard accuracy ranging code transmitted at 511 kHz

- Navigation message transmitted at 50 Hz

- 100 Hz auxiliary meander sequence

2.5.3 GLONASS ranging code

GLONASS ranging code is a sequence of the maximum length (M-length) shift register. GLONASS satellites provide two types of ranging code: standard accuracy and high accuracy which are discussed in more details in next sections.

2.5.3.1 Standard accuracy ranging code

The standard accuracy signal is available for any users equipped with the proper receivers and having a sufficient number of visible GLONASS system satellite above the horizon. In fact, the standard accuracy code is designed for use by civil users worldwide. (GLONASS ICD 2002).

Standard accuracy ranging code is sampled at the output of the 7th stage of a 9-stage shift register. The initialization vector to generate this sequence is (111111111). The generating polynomial which corresponds to the 9-stage shift register is:

$$G(X) = 1+X^5+X^9 \qquad\qquad 2\text{-}3$$

A simplified block diagram of the standard accuracy ranging code generation is given in

Figure 2-3 (GLONASS ICD 2002).
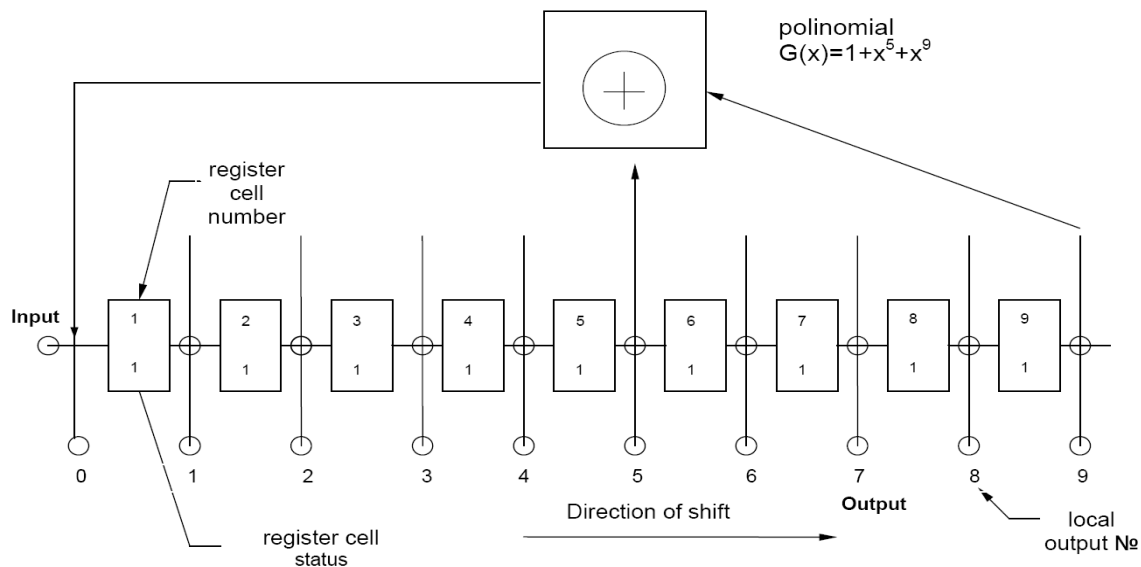
Figure 2-3 Simplified block diagram of standard ranging code generation (from GLONASS ICD 2002)

The GLONASS standard accuracy ranging code characteristics are shown in Table 2-2

(Beser & Danaher 1993).

Table 2-2 GLONASS standard accuracy ranging code characteristics

Code type	M-length 9-bit shift register	
Code rate	0.511 MHz	
Code length	511 bits	
Repeat rate	1 ms	
Navigation message	Super-frame	2.5 minutes
	Frame	30 seconds
	String	2 seconds

The 511-bit code is clocked at 0.511 MHz and repeats every one millisecond. This short code allows a receiver to search a maximum of 511 code phase shifts and consequently a quick acquisition is achieved. Each code phase represents approximately 587 m (Feairheller & Clark 2006).

The standard accuracy ranging code signal consists of a super-frame of 2.5 minutes containing five frames of 30 second each. Each frame consists of 15 strings, each two seconds long (Beser & Danaher 1993). More details regarding the navigation message are given in section 2.6.

2.5.3.2 High accuracy ranging code

The Russians have not publicly published any specifics on high accuracy ranging code. They have emphatically stated that this code is a military signal, and military signal is not the interest of this thesis. Interested reader is referred to Feairheller & Clark 2006.

2.5.4 Intra-system interference

This interference is caused by inter-correlation properties of ranging code and FDMA technique used in GLONASS system. When a navigation signal is transmitted on frequency channel K=n, then in the receiver there is an interference between this signal and signals transmitted on frequency channel K=n+1 and K=n-1. However, this interference is conditional to the simultaneous visibility of the satellites with adjacent frequencies (GLONASS ICD 2002).

2.5.5 Power level of the received signal

If the elevation mask is 5° or more, the power level of received GLONASS signal from GLONASS satellite at the output of a 3 dBi linearly polarized antenna is not less than -161 dBW for the L1 sub-band. For GLONASS-M satellites, the power is not less than -161 dBW for L1 sub-band and not less than -167 dBW for L2 sub-band if the satellite is observed at an angle of 5° or more (GLONASS ICD 2002). As such, the level of GLONASS signal on L2 sub-band for GLONASS-M satellite is expected to be lower than L1. This will have an impact on acquisition and tracking results. In other words, acquisition and tracking of the L1 signal does not ensure acquisition and tracking of the L2 signal from the same satellite.

Figure 2-4 shows the received power level as a function of angle of elevation of satellite for user located on the ground.
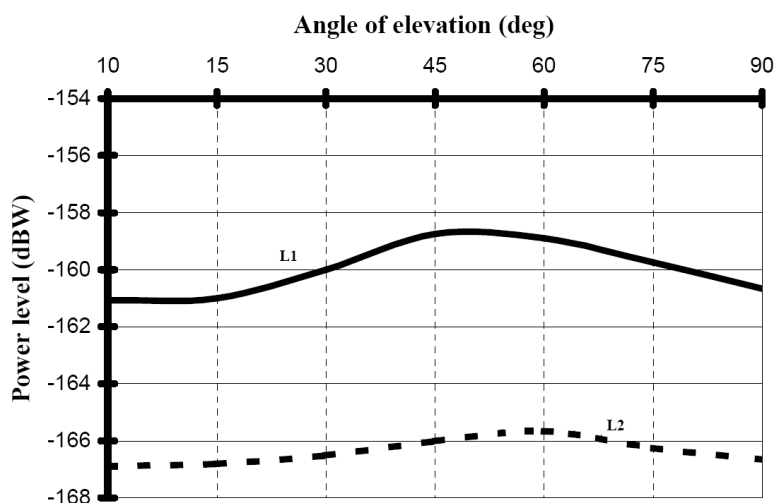
Figure 2-4 Relationship between minimum received power level and topocentric elevation angle (from GLONASS ICD 2002)

2.6 GLONASS navigation message

The purpose of the navigation message is to provide users with requisite data for positioning, timing and planning observations. The navigation message includes immediate and non-immediate data transmitted at 50 bits per second.

The GLONASS navigation message is generated as continuously repeating super-frames. A super-frame consists of frames and a frame consists of strings. Each of these units are explained in detail in next sections.

2.6.1 Super-frame structure

Within each super-frame, a total content of non-immediate data (almanac for 24 satellites) and the immediate data (for the satellite being tracked) are transmitted. Each super-frame consists of five frames and has a duration of 2.5 minutes.

2.6.2 Frame structure

Within each frame the total content of immediate data for the satellite being tracked and a part of non-immediate data are transmitted. Each frame consists of 15 strings, each with duration of two seconds. As such, a frame is 30 seconds.

Data in strings 1-4 of each frame contain the immediate data related to the satellite transmitting the navigation message. The immediate data are the same for all the frames in a super-frame. Strings 6-15 of each frame contain non-immediate data for all 24

satellites. Frame 1-4 contain non-immediate data for 20 satellites and 5th frame contains the non-immediate data for the remaining four satellites. Non-immediate data for each satellite occupies two strings. Data contained in 5th string of each frame are the same in one super-frame and relate to non-immediate data. Figure 2-5 and Figure 2-6 show the structure of frames 1-4 and frame 5, respectively. Figure 2-7 shows the super-frame structure.
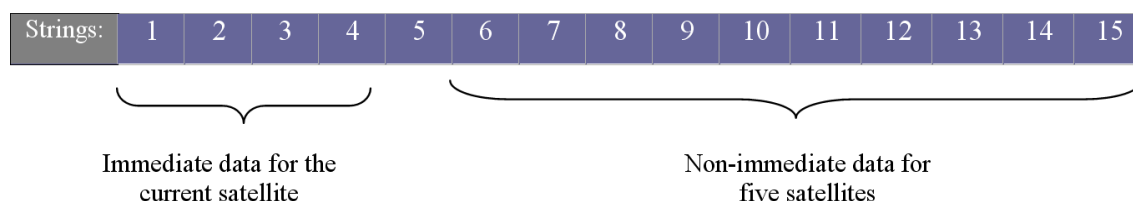
Figure 2-5 Frame 1, 2, 3, and 4 structure
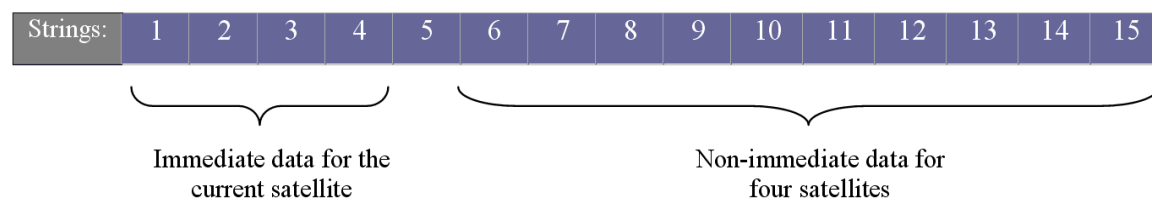
Figure 2-6 Frame 5 structure

Frame number	String number		2 s		
			1.7 s		0.3 s
I	1	0	Immediate data	KX	MB
	2	0	for	KX	MB
	3	0	transmitting	KX	MB
	4	0	satellite	KX	MB
	. .		Non-immediate data (almanac)for		
	15	0	five satellites	KX	MB
II	1	0	Immediate data	KX	MB
	2	0	for	KX	MB
	3	0	transmitting	KX	MB
	4	0	satellite	KX	MB
	. .		Non-immediate data (almanac)for		
	15	0	five satellites	KX	MB
III	1	0	Immediate data	KX	MB
	2	0	for	KX	MB
	3	0	transmitting	KX	MB
	4	0	satellite	KX	MB
	. .		Non-immediate data (almanac)for		
	15	0	five satellites	KX	MB
IV	1	0	Immediate data	KX	MB
	2	0	for	KX	MB
	3	0	transmitting	KX	MB
	4	0	satellite	KX	MB
	. .		Non-immediate data (almanac)for		
	15	0	five satellites	KX	MB
V	1	0	Immediate data	KX	MB
	2	0	for	KX	MB
	3	0	transmitting	KX	MB
	4	0	satellite	KX	MB
	. .		Non-immediate data (almanac) for four satellites		
	14	0	Reserved bits	KX	MB
	15	0	Reserved bits	KX	MB

85 | 84................9 | 8...... ...1

30 s

30s x 5 = 2.5 minutes

bit number within string

data bits in relative bi-binary code

Hamming code bits in relative bi-binary code

Figure 2-7 Super-frame structure (from GLONASS ICD 2002)

2.6.3 String structure

In standard accuracy signal, the navigation message is generated as a pattern of two-second repeating strings. Each string contains data bits and time mark. The data bits occupy 1.7 seconds and the time mark has duration of 0.3 seconds. Thus, each string is two seconds long. During the first 1.7 seconds within two seconds intervals, 85 data bits are transmitted. In fact, the original data bits have bit positions 9…84 and check bits are in positions 1…8. The data of each string is separated from the data of adjacent string by the time mark (GLONASS ICD 2002). Figure 2-8 shows a general view of a string structure.
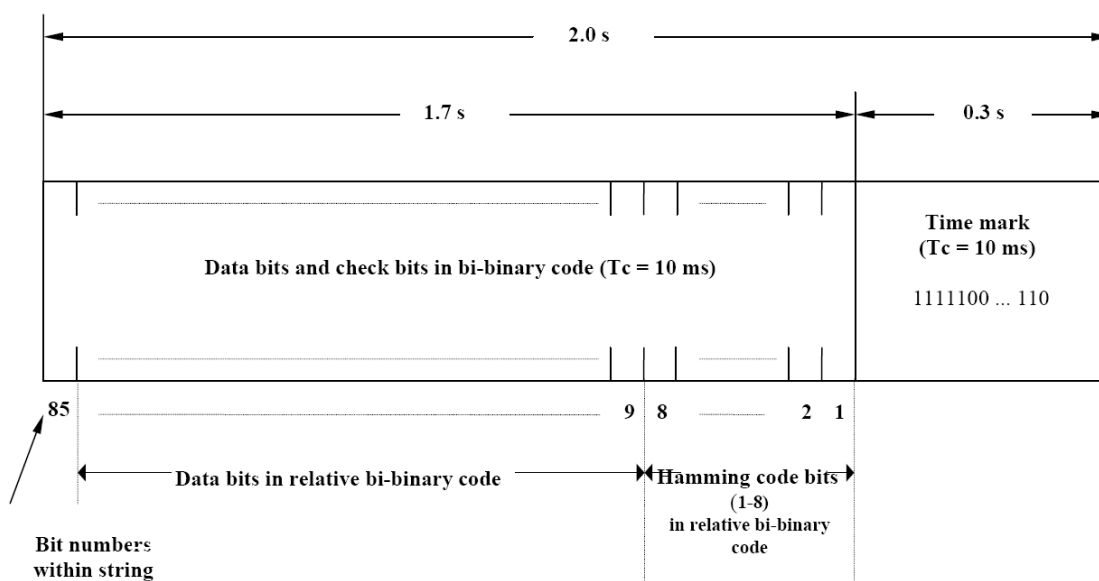
Figure 2-8 String structure (from GLONASS ICD 2002)

The binary code of the time mark is a pseudo random sequence of 30 bits when the duration of one bit is equal to 10 ms. This sequence is described by the following polynomial:

$$G(x) = 1+X^3+X^5$$ 2-4

or may be shown as :

$$111110001101110101000010010110$$

The first bit of the digital data in each string is always "0" (GLONASS ICD 2002).

Figure 2-9 shows a block diagram of GLONASS data sequence generation.
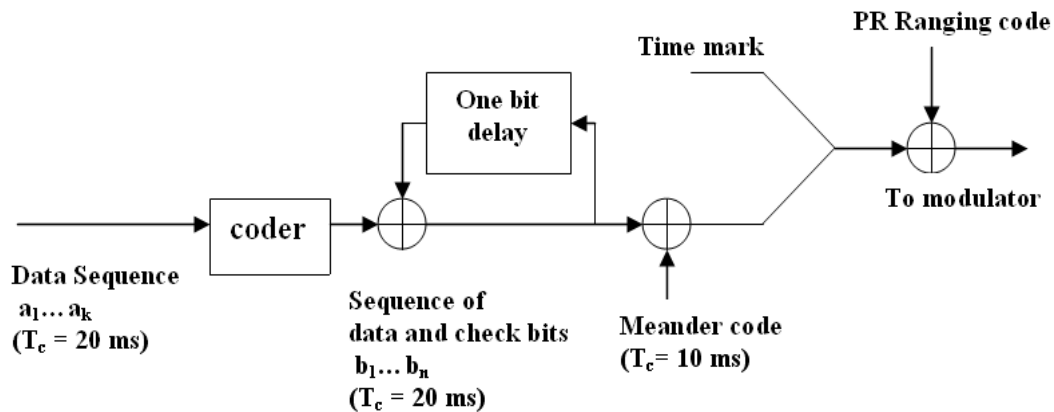
Figure 2-9 Block diagram of GLONASS data sequence generation (from GLONASS ICD 2002)

The original GLONASS navigation data bits are 20 ms long. A sequence of check bits Hamming code with a code length of four is added to the navigation data bits for verification. The original navigation data bits plus the check bits are transformed into relative code by a one-bit delay and modulo-2 addition of each bit with the previous one as shown in Figure 2-9. Then the meander code (100 Hz) is modulo-2 added to the data

bits. Because of the effect of meander code, the data bit duration is now 10 ms. Time mark bits which are 10 ms long are appended to the data bits, thus generating the two-second long string. The string is sent to the modulator for modulation with standard accuracy ranging code.

2.6.4 Navigation message content

According to GLONASS ICD 2002, the navigation message includes immediate data and non-immediate data.

Immediate data relates specifically to the GLONASS satellite broadcasting the data and includes:

- Difference between onboard time scale of satellite and GLONASS time
- Relative difference between carrier frequency of the satellite and its nominal value
- Ephemeris parameters

The non-immediate data contain almanac of the system and includes:

- Data on status of all satellites within space segment
- Coarse correction to the onboard time scale of each satellite relative to GLOASS time
- Orbital parameters of all satellites within space segment
- Correction to GLONASS time relative to UTC (SU)

2.7 GLONASS time

GLONASS satellites are equipped with clocks which exhibit a daily instability not worse than 5×10^{-13} for first-generation GLONASS satellites and 1×10^{-14} for the GLONASS-M satellites. GLONASS time can be defined as (GLONASS ICD 2002):

$$t_{GLONASS} = UTC(SU) + 03 \text{ hours } 00 \text{ minutes} \qquad \text{2-5}$$

To re-compute satellite ephemeris at the moment of measurement in UTC(SU) the following equation shall be used:

$$t_{GLONASS} = t + \tau_c + \tau_n (t_b) - \gamma_n(t_b)(t-t_b) \qquad \text{2-6}$$

where 't' is time of transmission of the navigation signal in the onboard time scale. 'τ_c' is the GLONASS time scale correction to UTC (SU) time. '$\tau_n(t_b)$' is the correction to n^{th} satellite time relative to GLONASS time at time t_b. '$\gamma_n(t_b)$' is the relative deviation of predicted carrier frequency value of n-satellite from nominal value at time t_b (GLONASS ICD 2002).

2.8 GLONASS reference frame

Before 1993, GLONASS provided data in the Soviet Geodetic System 1985 (SGS-85). From August 1993 to September 2007, GLONASS transmitted ephemeris data in the Earth Parameter System 1990 (PZ-90). PZ-90 is similar in quality to the Earth model employed in WGS-84 used by GPS (Feairheller & Clark 2006). The origin of this frame is located at the centre of the Earth's mass. The Z-axis is directed to the Conventional Terrestrial Pole as recommended by the International Earth Rotation Service (IERS). The X-axis is directed to the point of intersection of the Earth's equatorial plane and the zero

meridians. The Y-axis completes coordinate system to the right-handed one (GLONASS ICD 2002).

In June 2007, Russian government decided on the implementation of PZ-90.02. Thus, from 20 September 2007, GLONASS satellites broadcast ephemeris information in PZ-90.02 reference frame. With the new system, the GLONASS orbit accuracy is improved by 15-25%. To transform PZ-90.02 coordination to ITRF (Inertial Terrestrial Reference Frame) no rotation is needed but an offset of -36 cm, +8 cm, and +18 cm in the X,Y and Z directions is required (Revnivykh 2007). On the other hand, the WGS-84 reference frame and ITRF closely match. As such, a transformation from PZ-90.02 to WGS-84 can be provided.

CHAPTER THREE: ACQUISITION

3.1 Chapter outline

In this Chapter a general view of a GNSS receiver is presented. The incoming GNSS signal structure and the process on it, is explained. Then, the acquisition theory is briefly discussed and a few acquisition methods are reviewed. The differences between GPS and GLONASS signals affecting acquisition are highlighted. At the end, a data collection set-up is described and some acquisition results are presented.

3.2 GNSS receiver overview

The final goal of a GNSS receiver is computing the position and velocity of the receiver or at least providing some measurements which can be used to compute these values. For this purpose, the received signals at antenna must be acquired and tracked. After tracking, navigation message can be extracted and utilized to generate some measurements that are useful in computing the navigation solution.

Figure 3-1 illustrates a block diagram of a GNSS receiver. The received signal at the antenna is amplified and then down converted to the desired intermediate frequency (IF). The down converted signal is sampled and sent to the signal processor block. Amplification, down conversion and sampling are performed in the radio frequency (RF)

front-end block. The signal processor block consists of tracking loop as well as navigation message extraction and measurement generation components. One signal processing block is assigned for each satellite signal being tracked and is herein simply called a "channel". Generally, a signal tracking loop consists of the following components (Petovello & O'Driscoll 2007):

- Doppler removal component in which the carrier part of the received signal is removed as is explained in section 3.4.1

- Correlation component in which the ranging code part of the received signal is removed as is explained in section 3.4.2

- Discriminator component which can compute the difference (error) between the locally generated signals and the received ones

- Loop filter component which smoothes the output of the discriminators

The latter two points are discussed in Chapter four.

Figure 3-2 illustrates a general tracking loop block diagram. Although tracking is the subject of the next Chapter, the entire tracking loop diagram is presented here because many of the computations required for signal tracking also apply to signal acquisition.
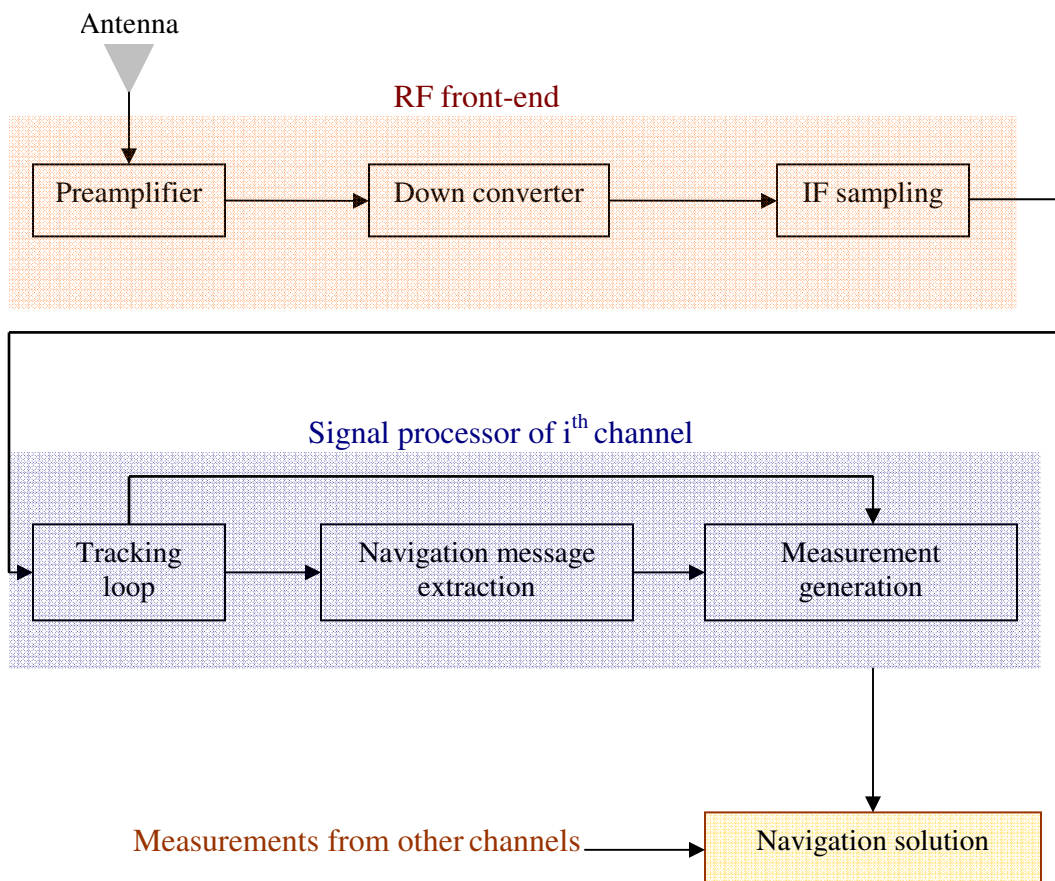
Figure 3-1 GNSS receiver overview

Samples from RF front-end
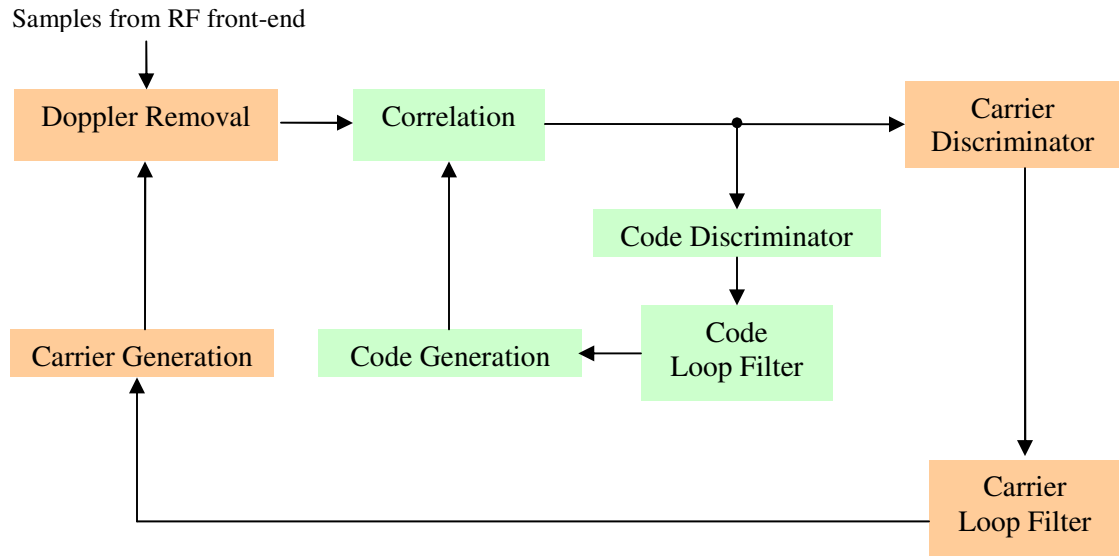
Figure 3-2 General signal tracking block diagram (modified Petovello & O'Driscoll 2007)

3.3 Incoming GNSS signal structure

In this section, the incoming signal structure is overviewed. Furthermore, the signal processing steps from the antenna to the sampling is explained.

Generally, a GNSS signal structure can be presented by the following equation (Lachapelle 2007):

$$S(t) = A.C(t).D(t).\cos(2\pi f_R t + \phi) \qquad\qquad 3\text{-}1$$

where

- S(t) represents the signal received at the antenna,

- A represents the amplitude of the received signal,

- C(t) represents the received ranging code,

- D(t) represents the received navigation data message,

- f_R represents the frequency of the received carrier signal, and

- ϕ is the phase of the received carrier signal

Considering the Doppler effect, the received signal frequency is not the same as the frequency which is transmitted by the satellite. This difference is detected and compensated during the tracking process. Similarly, navigation data and ranging code are modulated onto carrier signal and are extracted during tracking.

A simplified received GNSS signal can be presented as follows:

$$S(t) = A(t).\cos(2\pi f_R t + \phi) \qquad\qquad 3\text{-}2$$

This equation is the simplified version of equation 3-1 where the signal amplitude, ranging code, and navigation data are summarized in A(t).

In the RF front-end, the received signal must be down converted after amplification. For this purpose, a frequency mixer multiplies the incoming signal with a locally generated sinusoid signal that can be represented as:

$$LO(t) = B.\cos(2\pi f_{LO} t) \qquad\qquad 3\text{-}3$$

A simplified block diagram of a frequency mixer is shown in Figure 3-3. At the mixer output, a sinusoidal signal with an intermediate frequency (IF) appears. In fact, this intermediate frequency is the difference between incoming signal frequency and the locally generated signal frequency (IF = f_R- f_{LO}).
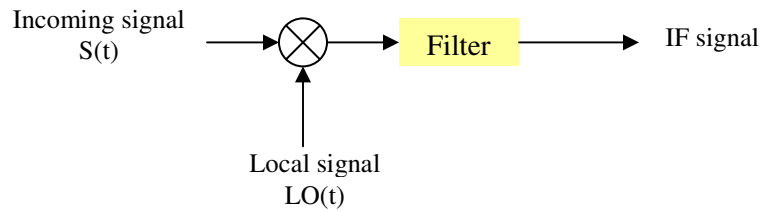
Figure 3-3 Simplified block diagram of a frequency mixer

In signal acquisition and tracking of a GNSS receiver, In-phase (I) channel and Quadra-phase (Q) channel of the down converted signal are used. These signals are generated by the same method as down conversion in frequency mixer as is shown in Figure 3-4. The locally generated signal is mixed with the input intermediate frequency signal to generate I channel signal which is a sinusoidal signal with a pseudo-base-band frequency. This pseudo-base-band frequency (f_{PBB}) equals to the difference between the input intermediate frequency and the locally generated signal frequency. The local signal phase is shifted 90° and then is mixed with the input signal to generate the Q channel. The frequency of the Q channel signal is equal to the frequency of I channel signal and that is the pseudo-base-band frequency.
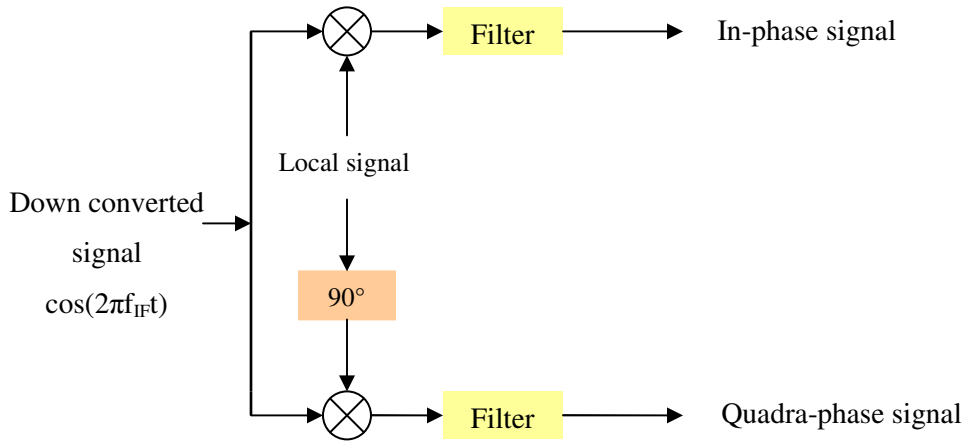
Figure 3-4 I and Q signal generation (modified Lachapelle 2007)

The final step in an RF front-end is to sample the continuous signal with a sampling frequency f_s (= $1/T_s$). Therefore, the kth complex samples at the output of RF front-end are I_k^{raw} and Q_k^{raw} and can be defined as:

$$I_k^{raw} = I(kT_s) = A_k.D_k.C_k.\cos(2\pi f_{PBB}kT_s + \phi)$$

$$Q_k^{raw} = Q(kT_s) = A_k.D_k.C_k.\sin(2\pi f_{PBB}kT_s + \phi) \qquad 3\text{-}4$$

The superscript "raw" is chosen for these samples because these are unprocessed samples which are transmitted to the signal processor block for Doppler removal and correlation. For the purpose of this paper, the data bits are assumed constant during an integration interval and will therefore be omitted from the following equations

3.4 Doppler removal and correlation

This section describes the Doppler removal and correlation (DRC) process in a GNSS receiver.

3.4.1 Doppler removal

In Doppler removal process, the Doppler frequency is removed from the incoming carrier signal by mixing it with a locally generated signal. Using the traditional rigorous method, the Doppler removed I and Q can be presented as follow (Petovello & Lachapelle 2006):

$$I_k^{DR} = I_k^{raw}.\cos(2\pi\hat{f}T_sk + \hat{\phi}) + Q_k^{raw}.\sin(2\pi\hat{f}T_sk + \hat{\phi})$$
$$= A_k.C_k.\cos(2\pi\delta fT_sk + \delta\phi)$$

$$Q_k^{DR} = Q_k^{raw}.\cos(2\pi\hat{f}T_sk + \hat{\phi}) - I_k^{raw}.\sin(2\pi\hat{f}T_sk + \hat{\phi})$$
$$= A_k.C_k.\sin(2\pi\delta fT_sk + \delta\phi) \qquad\qquad 3\text{-}5$$

where,

- $\hat{f}$ represents the frequency of the locally generated signal,

- $\hat{\phi}$ represents the phase of the locally generated signal,

- δf represents the frequency error between the locally generated and incoming signal,

- $\delta\phi$ represents the phase error between the locally generated and incoming signal, and

- DR superscript represents "Doppler removal"

If the locally generated signal matches the incoming pseudo-base-band signal, the errors will be zero and the effect of Doppler frequency is removed.

3.4.2 Correlation

To remove the ranging code from the incoming signal, correlation is required. For this purpose, the Doppler removed samples of the incoming signal are multiplied by the locally generated ranging code and then are summed as follows (Petovello & Lachapelle 2006):

$$I_k^{DRC} = \sum_{k=1}^{N} \hat{C}_k . I_k^{DR}$$
$$Q_k^{DRC} = \sum_{k=1}^{N} \hat{C}_k . Q_k^{DR}$$

3-6

where,

- $\hat{C}$ represents the locally generated ranging code,
- N represents the number of samples, and
- DRC superscript represents "Doppler removal and correlation"

Equation 3-6 can be written as ((Petovello & Lachapelle 2006) :

$$I_k^{DRC} = A.N.R(\delta\tau).\frac{\sin(\pi\delta f T_s N)}{\pi\delta f T_s N}.\cos(\pi\delta f T_s N + \delta\phi)$$

$$Q_k^{DRC} = A.N.R(\delta\tau).\frac{\sin(\pi\delta f T_s N)}{\pi\delta f T_s N}.\sin(\pi\delta f T_s N + \delta\phi)$$

3-7

where, $R(\delta\tau)$ represents the auto-correlation of the ranging code with an difference of $\delta\tau$ between the incoming and locally generated ranging codes.

3.5 GNSS signal acquisition

Acquisition is the process of detecting the presence of a GNSS signal. When the signal is detected, the necessary parameters can be obtained and passed to the tracking process described in Chapter four.

A variety of GNSS signal acquisition methods are presented in different references (e.g. Ward et al 2006; Bao & Tsui 2000b, Van Dierendonck 1996). Bao & Tsui (2000b) present the cell-by-cell search, the fast Fourier transformation (FFT), and the delay and multiplication method for GNSS signal acquisition. Each method has some advantages and disadvantages. For example, the delay and multiplication method is faster than FFT method but in case of weak signals, it has a lower performance. Therefore, there is a trade-off between speed and sensitivity. If the signal is strong, the fast-low sensitivity acquisition method can detect it but if the signal is weak, the FFT method is better able to find it (Bao & Tsui 2000b). However, in case of weak signals, some other methods are presented (e.g. O'Driscoll 2007, Psiaki 2001). For the purpose of this work, only the cell-by-cell search method and FFT method are explained in next sections.

3.5.1 Cell-by-cell search method

In the cell-by-cell search method, the correlation is performed in the time domain, where the locally generated ranging code is shifted and accumulated for all possible shifts. Therefore, for GPS signal acquisition, all 1023 C/A ranging code chips are examined. Typically, code chip is searched in increments of half chip and each code phase value to

be searched is considered a code bin. This process is repeated for all Doppler bins. In fact, the entire range of Doppler frequency search is divided into smaller cells called Doppler bin. For example, if the entire Doppler frequency search range is assumed ±5 kHz for static antenna, it can be divided to smaller 5-Hz bins for search. One code bin and one Doppler bin create a cell (Ward et al 2006). The search starts from a particular code bin and particular frequency bin. If the signal is not detected, another code bin is examined. It continues until all code bins for that particular frequency bin are exhausted. Then, the search continues on the adjacent frequency bins and for all code bins until all the cells are examined or the signal is detected, whichever happens first (Ray 2007). This search is shown in Figure 3-5.
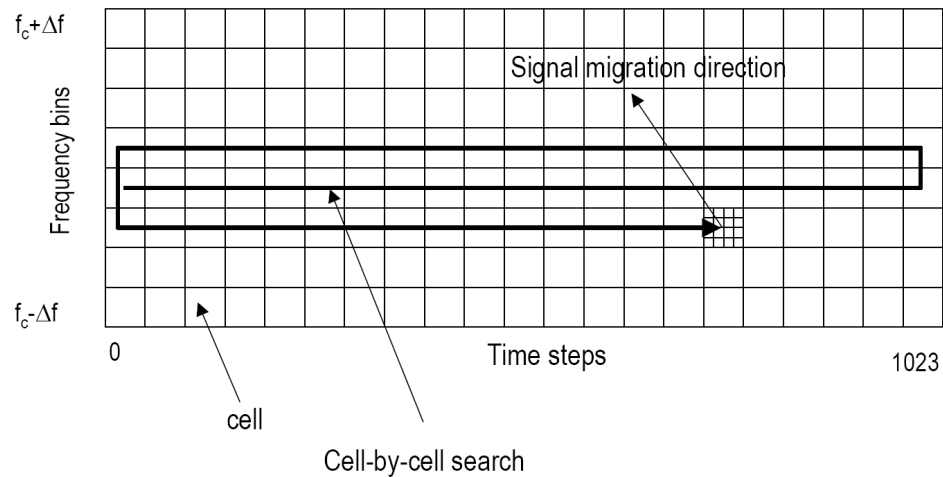
Figure 3-5 cell-by-cell search diagram (from Ray 2007)

3.5.2 Fast Fourier Transform method

The Fast Fourier Transform (FFT) method lessens the computation process and thus decreases the time-to-first-fix (TTFF), but it needs additional memory space to store signal samples for FFT computation. This is an efficient technique when a receiver has a digital signal processor (DSP) and software signal processing loop. Therefore, FFT method is preferred for software-based receivers (Lachapelle 2007).

The incoming samples are Doppler removed and then FFT is performed on them. This is shown in the following equation assuming x being the Doppler removed signal:

$$X(f) = FFT\{x\} \qquad\qquad 3\text{-}8$$

The local signal, y , is generated and sampled then FFT is computed:

$$Y(f) = FFT\{y\} \qquad\qquad 3\text{-}9$$

The conjugate multiplication in frequency domain is performed using X(f) and Y(f):

$$Z(f) = X(f) \times Conjugate(Y(f)) \qquad\qquad 3\text{-}10$$

This signal must be transformed back to the time domain:

$$z(t) = IFFT \{Z(f)\} \qquad\qquad 3\text{-}11$$

where IFFF is the inversed FFT and z(t) represents the correlation of input signal and the locally generated signal (Bao & Tsui 2000b).

3.6 GLONASS signal acquisition

For GLONASS signal acquisition, FFT method is used and for convenience, the initial GLONASS signal acquisition process was performed in Matlab™. There are some major

differences between GPS and GLONASS signals which affect the acquisition process. The first one is GLONASS ranging code and the second one is the effect of FDMA technique which GLONASS uses for multiplexing. They are explained more in next sections. Table 3-1 summarizes these differences.

Figure 3-6 shows the block diagram for the acquisition process used for acquiring the GLONASS L1 and L2 signals.

Table 3-1 Main differences between GPS and GLONASS affecting acquisition

Item	GPS	GLONASS
Multiplexing	CDMA	FDMA
Ranging code type	Gold Code	M-Length

```
┌─────────────────────┐
│  Read input signal  │
└─────────────────────┘
           │
           ▼
┌─────────────────────┐
│   Initialization    │
└─────────────────────┘
           │
           ▼
      ╱─────────╲            No      ┌──────────────────────────┐
     ╱ Frequency  ╲ ─────────────────▶│  Check the peak value of │
     ╲  range?    ╱                   │ correlation and output its│
      ╲─────────╱                     │  code offset and Doppler  │
           │ Yes                      │        frequency         │
           ▼                          └──────────────────────────┘
┌─────────────────────┐
│ Generate local carrier│
└─────────────────────┘
           │
           ▼
┌─────────────────────┐
│   Doppler removal   │
└─────────────────────┘
           │
           ▼
┌─────────────────────┐
│  Generate local code │
└─────────────────────┘
           │
           ▼
┌──────────────────────────┐
│  Take 1 ms from incoming  │
│  signal and 1 ms local code│
└──────────────────────────┘
           │
           ▼
┌──────────────────────────┐
│   Perform correlation     │
│   in frequency domain     │
└──────────────────────────┘
           │
           ▼
┌──────────────────────────┐
│        Compute            │
│   correlation value       │
│      and store it         │
└──────────────────────────┘
```
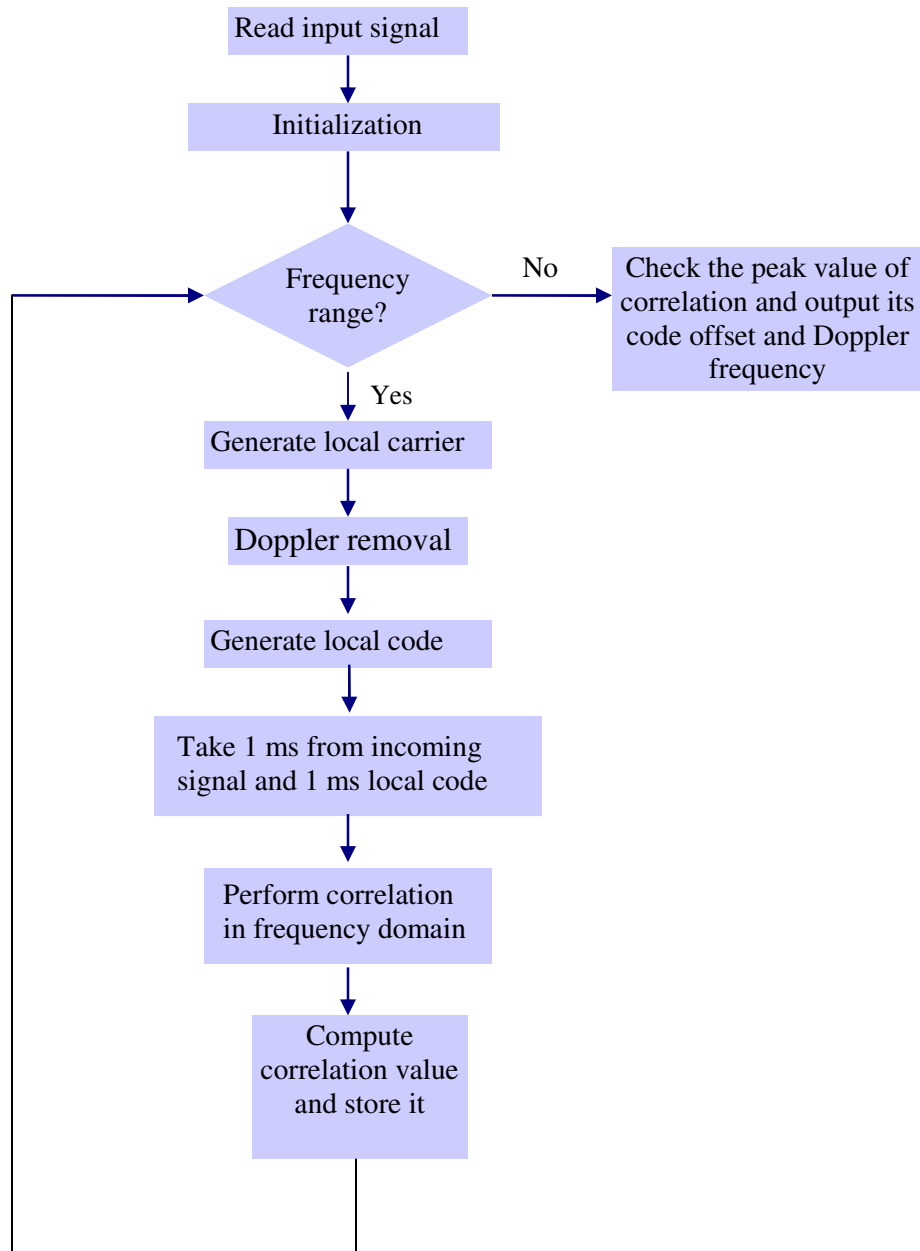
Figure 3-6 GLONASS acquisition process block diagram

3.6.1 Effect of ranging code

As discussed in section 2.5.3, the GLONASS ranging code is different from GPS ranging code. In fact, all the GLONASS satellites in the constellation transmit the same ranging code; however each GPS satellite has a unique ranging code. GPS C/A ranging code signal belongs to a family of Pseudo Random Noise (PRN) codes which are called Gold codes. These codes are generated from the product of the output of two maximum length 10-stage shift registers which are driven by a 1.023 MHz clock and each one includes 1023 bits (Spilker 1996). On the other hand, GLONASS ranging code is not a Gold code but is a maximum length 9-stage shift register sequence. A maximum length sequence is a type of pseudo random binary sequence which is generated from an m-stage shift register with linear feedback. In maximum length sequence, an m-stage shift register produces a sequence with the length of 2^m-1. In case of GLONASS ranging code, because the shift register has nine stages, a 511-bit sequence is generated (2^9-1= 511). The auto-correlation of a GLONASS ranging code takes two values: 511 and -1.

For GLONASS signal acquisition, one and only one ranging code must be generated for all the GLONASS satellites as a replica ranging code.

3.6.2 Effect of FDMA

GLONASS uses Frequency Division Multiple Access technique. This means that each satellite transmits its own carrier frequency. For this purpose, the carrier frequency with channel number zero (i.e., 1602.00 MHz) is down converted to intermediate frequency

(IF) in the front-end as discussed in section 3.2 and the other GLONASS satellites' carrier frequencies are generated accordingly:

$$f_{Carrier} = IF + K \times \Delta f_{1or2}$$ 3-12

where,

- IF is the intermediate frequency,

- K is the channel number, and

- Δf_{1or2} is the frequency offset for GLONASS L1 and L2 as is discussed in section 2.5.1.

Considering that each GLONASS satellite is transmitting its own frequency, some of the Doppler removal and correlation methods which are used for GPS can not be implemented for GLONASS. For example, in look-up table Doppler removal and correlation method, the sine and cosine values of the possible phases are generated and stored in a table (Charkhandeh et al 2006). This provides considerable processing improvements because the local carrier phase does not need to be generated on the fly. For GLONASS however, the desired sine and cosine values must either be computed on the fly which is not efficient for real-time operation, or a separate table must be used for every GLONASS satellite. Although the latter is possible, it requires considerable memory requirements and was therefore avoided in this case..

Moreover, in the simultaneous Doppler removal method for GPS presented by Petovello & Lachapelle (2006), instead of a look-up table, a single frequency table is generated. Considering that only one locally generated frequency is used for Doppler removal of all the GPS satellites, it is required that the removal be performed just once for all the

satellites. However, this method cannot be effectively utilized for GLONASS because the resulting power attenuation would be too large.

3.7 Data collection

To validate the acquisition strategy, a data collection is planned using Trimble Office Planning™ software. The data collection was conducted on 10th October 2008 at 3:13 pm, Calgary time for 10 minutes under open-sky conditions on the roof of CCIT building on the University of Calgary campus.

During this period, there were about seven GLONASS satellites visible above the $10°$ elevation angle. Figure 3-7 and Figure 3-8 show the GLONASS and GPS satellites visibility respectively. The dotted red lines approximately indicate the time range of this data collection.
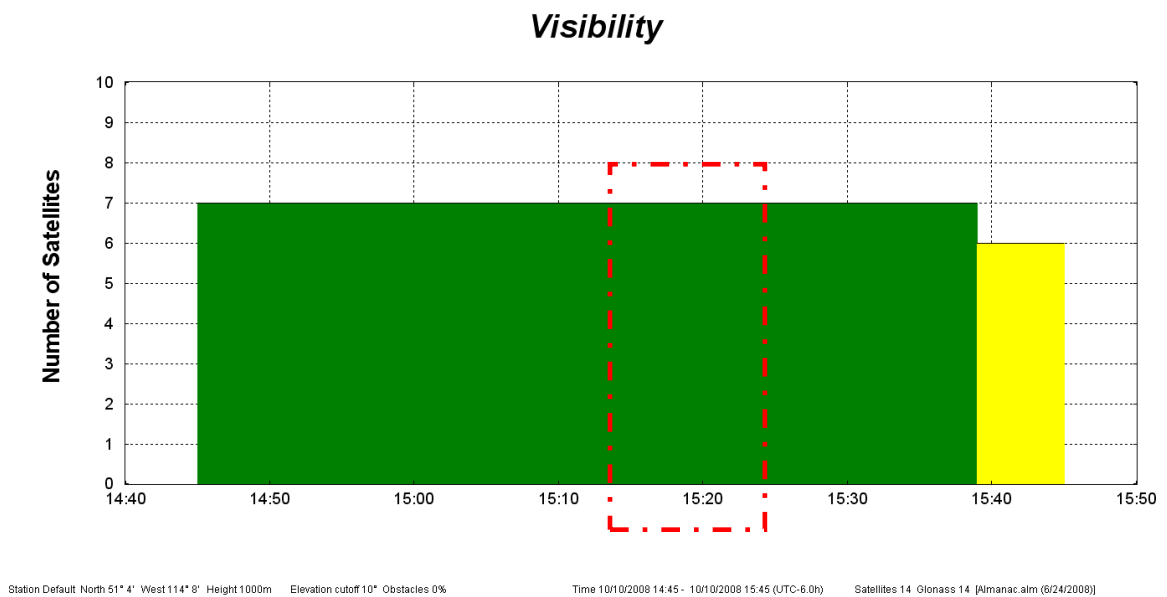
Figure 3-7 GLONASS satellites visibility

Visibility

Station Default North 51° 4' West 114° 8' Height 1000m   Elevation cutoff 10° Obstacles 0%   Time 10/10/2008 14:45 - 10/10/2008 15:45 (UTC-6.0h)   Satellites 31 GPS 31 [almanac.alm (10/30/2008)]
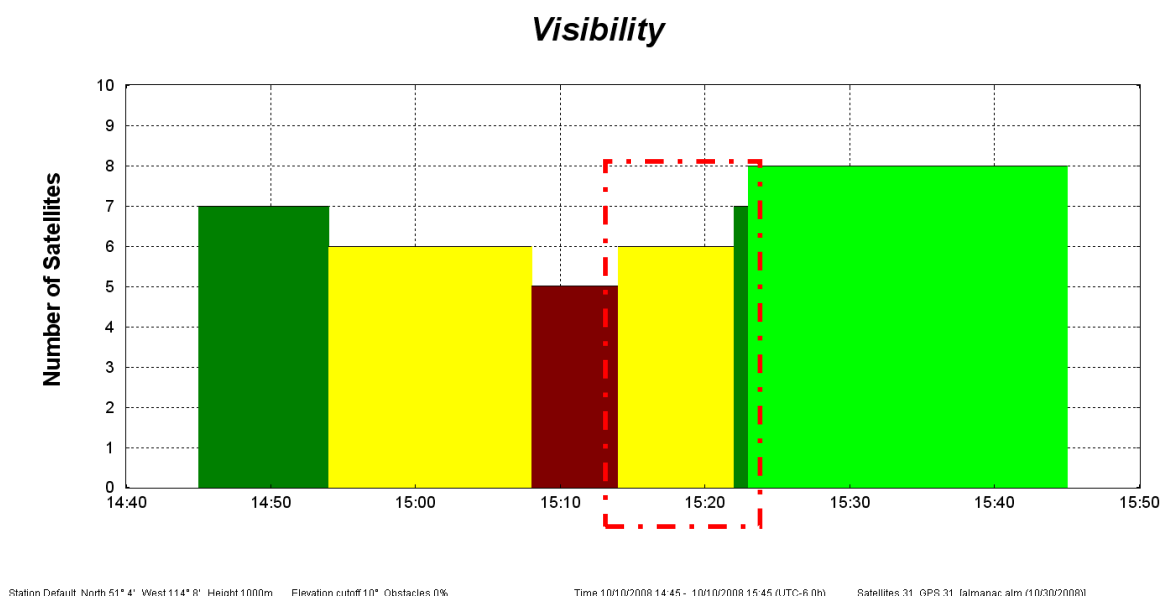
Figure 3-8 GPS satellites visibility

The data collection set-up is shown in Figure 3-9. The antenna used was a NovAtel™ GPS-GG702 model which can receive GPS and GLONASS L1 and L2 signals. The received signal was sent into a splitter where it was divided into three signals. These three signals were sent to the three channels of the RF front-end for collecting GPS L1, GLONASS L1 and GLONASS L2 signals. In the font-end, the signals were sampled and down converted into desired intermediate frequency. The sampling rate which was chosen for both GPS and GLONASS signals was 12.5 MSps.

GPS SV

GLONASS SV

date: 10th October 2008

time: 3:13 pm, Calgary time

duration: 10 minutes

Antenna

RF Front-end

GPS L1

GLONASS L1

Splitter

GLONASS L2
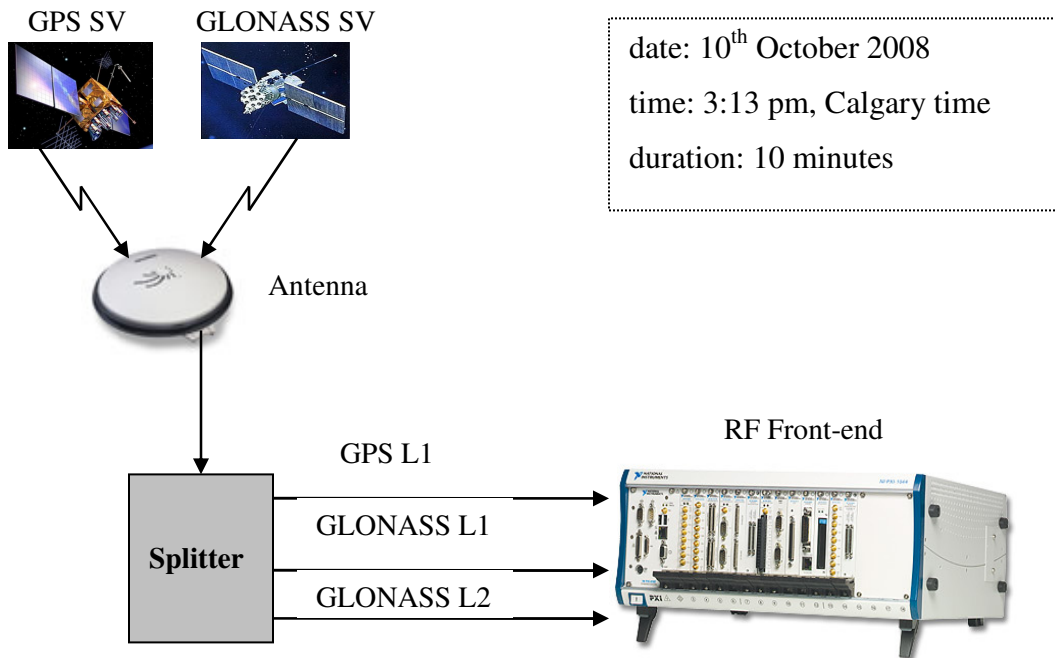
Figure 3-9 Data collection set-up

3.8 Acquisition results

The GPS signals acquired by the FFT method are presented in Table 3-2. Figure 3-10 shows the elevation angle of each GPS satellite during the data collection period. The L1 signal for all the visible GPS satellites was acquired except G15 and G14 which were below 10° elevation angle and so weak. Although, the L1 signals for almost all GPS satellites at elevation angle below 10° were acquired, these signals are weak and during the tracking process may lose lock.

Table 3-2 Acquired GPS L1 signals

GPS PRN	L1 signal acquired	Comments
G02	Yes	Below 10° elevation angle
G04	Yes	---
G05	Yes	Below 10° elevation angle
G09	Yes	---
G11	Yes	Below 10° elevation angle
G12	Yes	---
G17	Yes	---
G20	Yes	---
G28	Yes	---
G32	Yes	Below 10° elevation angle
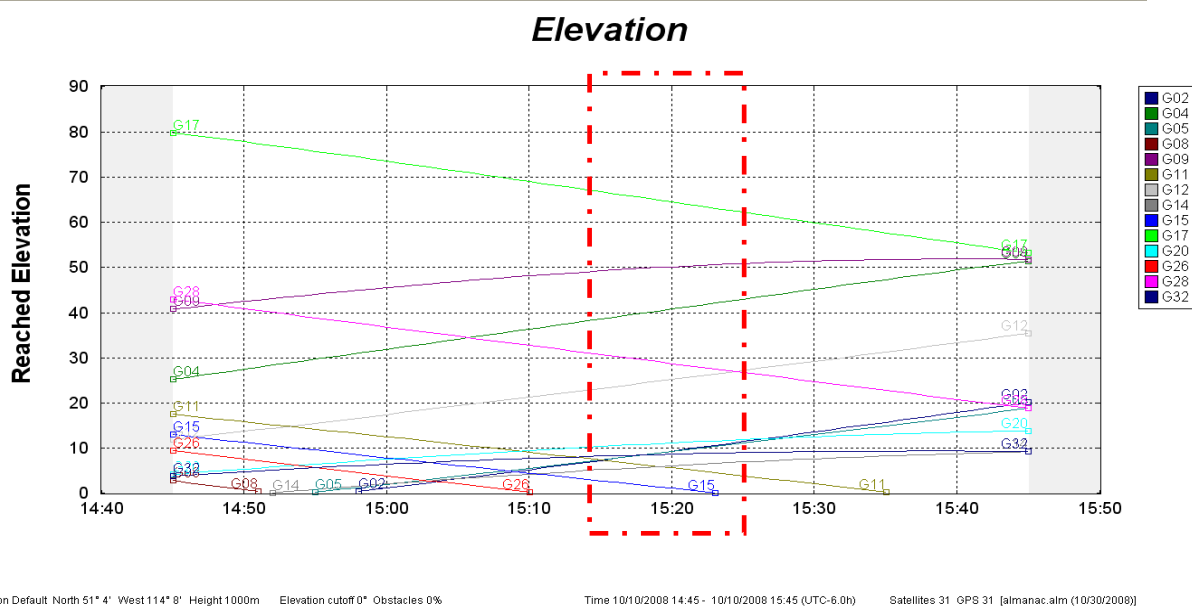
Figure 3-10 GPS satellites elevation

Table 3-3 shows the acquired GLONASS L1 and L2 signals. It is noted that the L2 signal of GLONASS satellite at orbital slot 07 is not acquired because this satellite is in low elevation and its L1 and L2 signals are weak. Generally, GLONASS L2 signal is weaker than GLONASS L1 signal as discussed in section 2.5.5. Therefore, although L1 is acquired, L2 can not be detected in this case.

Figure 3-11 shows the elevation angle of each GLONASS satellite during the data collection period.

Table 3-3 Acquired GLONASS L1 and L2 signals

Orbital slot	Channel Number	L1 signal acquired	L2 signal acquired	SV type
R07	05	Yes	No	M
R13	-2	Yes	Yes	M
R15	00	Yes	Yes	M
R17	-1	Yes	Yes	M
R23	03	Yes	Yes	M
R24	02	Yes	Yes	M

Elevation

Station Default North 51° 4' West 114° 8' Height 1000m   Elevation cutoff 0° Obstacles 0%   Time 10/10/2008 14:45 - 10/10/2008 15:45 (UTC-6.0h)   Satellites 15 Glonass 15 [almanac.alm (10/30/2008)]
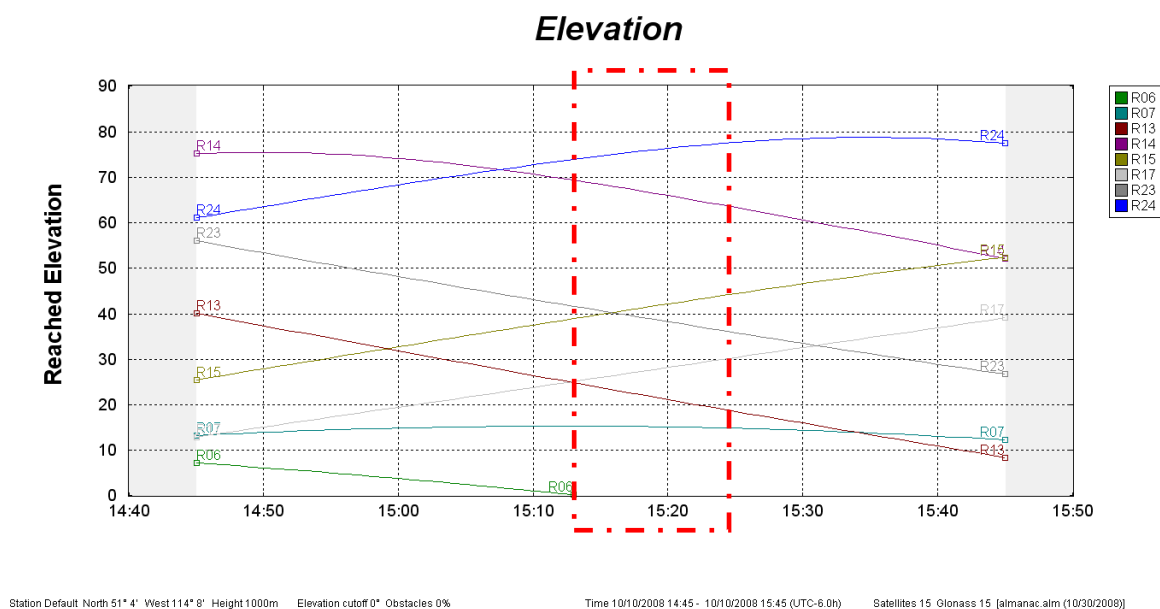
Figure 3-11 GLONASS satellites elevation

The acquisition figures for GPS L1, GLONASS L1 and GLONASS L2 are shown in Figure 3-12, Figure 3-13, and Figure 3-14.

Acquisition result for GPS PRN=9
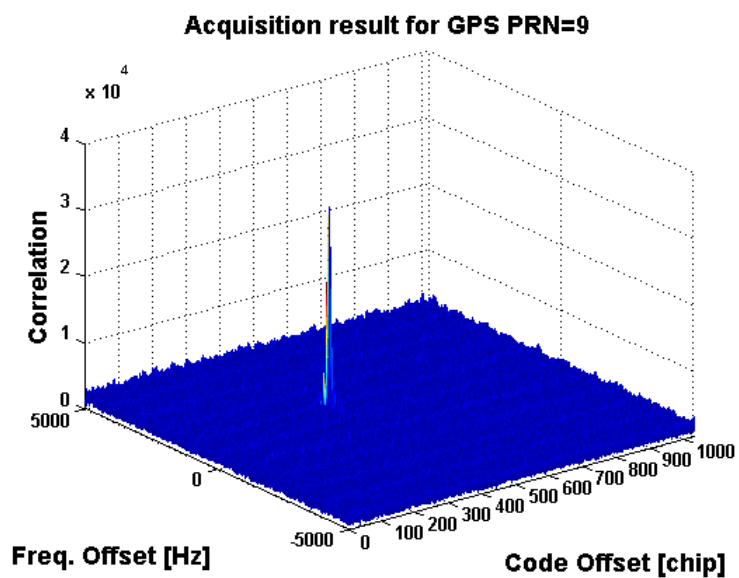
Figure 3-12 Acquisition result for GPS signal with PRN 9
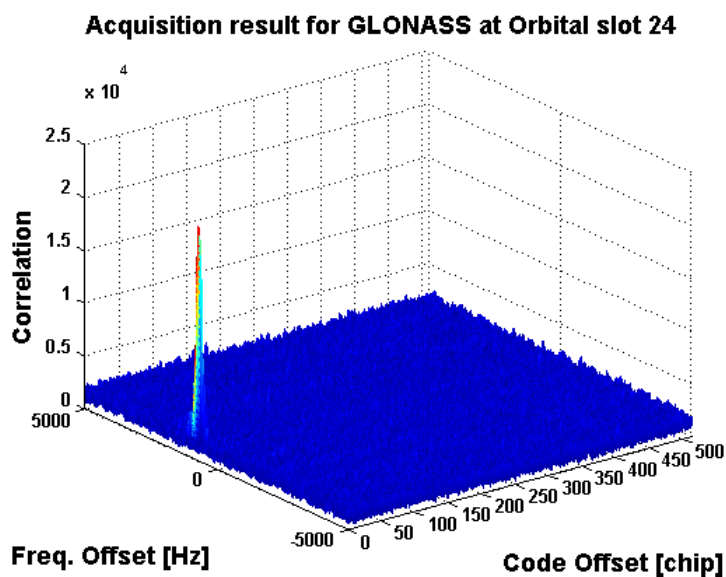
Figure 3-13 Acquisition result for GLONASS L1 signal at orbital slot 24
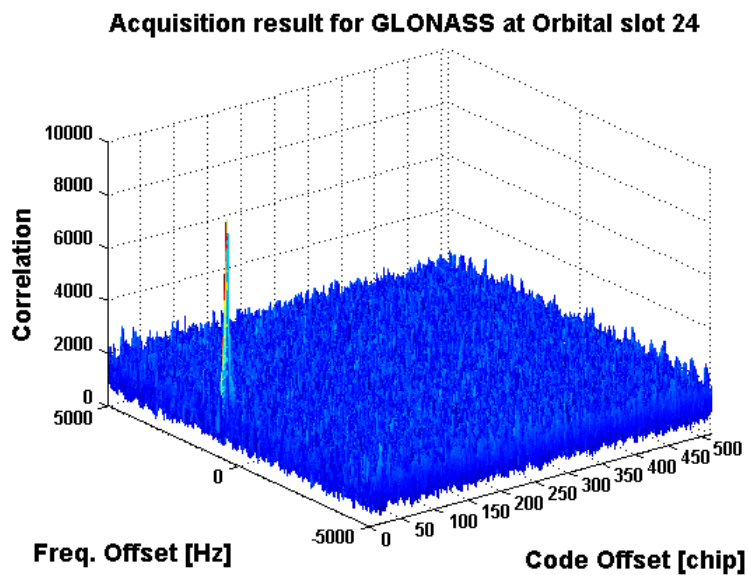
Figure 3-14 Acquisition result for GLONASS L2 signal at orbital slot 24

Acquisition results for GLONASS L1 and L2 show that the correlation peak is lower for GLONASS L2 signal which is related to the power of received L2 signal that is weaker than L1 signal. However, there are correlation peaks with acceptable power for GPS, GLONASS L1 and GLONASS L2 which helps in finding the initial value of Doppler frequency and ranging code offset.

From the acquisition process, code phase offset and Doppler frequency are obtained and sent to the tracking process. Tracking is discussed in Chapter four. An example of these values is presented in Table 3-4. These values correspond to the plots above. The code phase offset for GLONASS L1 and L2 from the same satellite are almost the same. The ranging code is the same for L1 and L2 signals and these similar values are expected. The Doppler frequency is proportional to the carrier frequency (Ray 2007), thus the Doppler frequency for GLONASS L1 and L2 are different.

Table 3-4 Example of acquisition process output

	Doppler frequency (HZ)	Code offset (Chips)
GPS PRN 9	825	395.2
GLONASS L1 orbital slot 24	775	2.3
GLONASS L2 orbital slot 24	575	2.3

CHAPTER FOUR: TRACKING

4.1 Chapter outline

This Chapter begins with a description of the signal tracking process. Both carrier and code loops are explained in detail. Phase lock loop, frequency lock loop, and delay lock loops along with different type of discriminators and loop filters are reviewed. A brief discussion on tracking loop aiding is presented after that. The Chapter continues with the introduction of the software which is developed to track GLONASS L1 and L2 signals. The corresponding modifications to the GPS software receiver are then reviewed. At the end of the Chapter, some results are presented for the tracked GLONASS L1 and L2 signals.

4.2 Tracking loop overview

The objective of a tracking loop is determining the difference between the locally generated signal and the incoming pseudo-base-band signal, filtering that estimate and sending new information to the signal generators. In a tracking loop process, both carrier and code signals are accurately reproduced inside the receiver. For each carrier and code portion of the received signal, a tracking loop exists. The code tracking loop is called a delay lock loop (DLL) and must provide an estimate of code phase of the ranging code being tracked. The carrier tracking loop is called carrier lock loop (CLL) and it must

track the incoming carrier phase via a phase lock loop (PLL) or a carrier frequency via frequency lock loop (FLL). The carrier phase yields more accurate information needed for navigation message decoding. Two tracking loops can be coupled in some cases where the DLL needs an accurate estimate of the incoming carrier frequency which the CLL can provide (Ward et al 2006).

Figure 4-1 shows a general view of a tracking loop. This figure is the simple view of Figure 3-2. Discriminators, loop filters, and signal generators are the basic components of a tracking loop. Each of these components will be explained in detail in this Chapter.
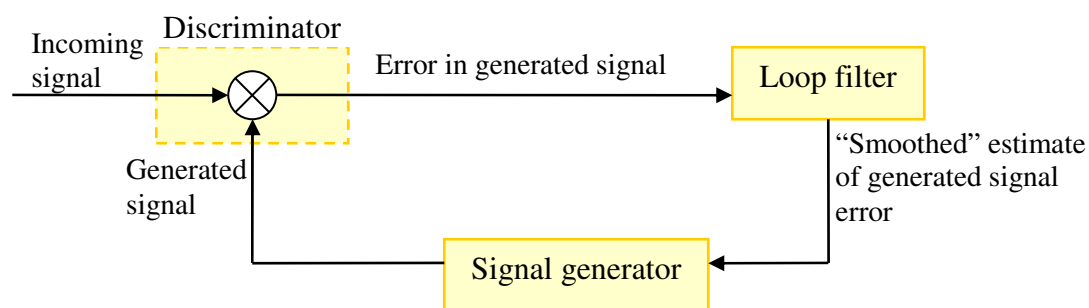
Figure 4-1 A general tracking loop (modified Lachapelle 2007)

Figure 4-2 illustrates a generic block diagram of a receiver channel showing both carrier and code lock loops. The received samples are applied as input. At first step, samples are stripped of the carrier by replica carrier signal. The replica carrier signals are synthesized by the carrier numerically controlled oscillator (NCO) and sine and cosine mapping functions (Ward et al 2006). I channel and Q channel values are then correlated with early, prompt and late replica codes. These replica codes are generated by the code

generator, 2-bit shift register, and the code NCO. In this loop, the code NCO produces twice the code generator clocking rate ($2f_{co}$) and sends it to the clock input of the 2-bit shift register. The code generator clocking rate (f_{co}) is provided by code NCO too. The 2-bit shift register generates two phase-shifted version of the code generated by code generator (presented by 'E' in the diagram). As such, there are three replica codes designated as early (E), prompt (P), and late (L). If the incoming signal is tracked, the maximum correlation of the prompt replica code and the incoming signal code is produced. Under the same circumstance, the correlation of early and late replica codes with the incoming signal code produces half of the maximum correlation value.
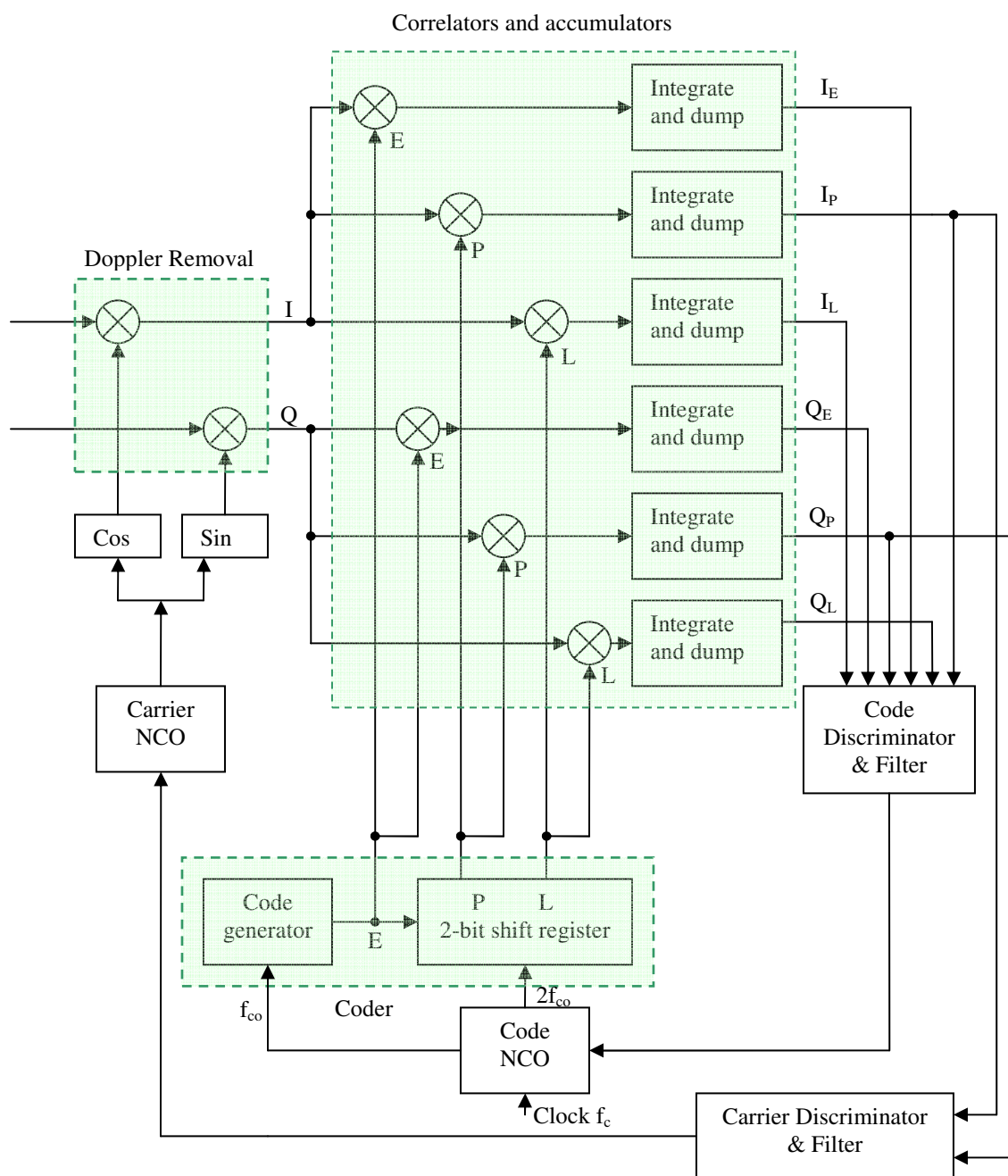
Figure 4-2 Generic digital receiver channel block diagram (modified Ward et al 2006, Lachapelle 2007, and Ray 2007)

4.3 Phase lock loop

The objective of a phase lock loop (PLL) is to generate the carrier portion of the locally generated signal. The discriminator in phase lock loop determines the difference between the phase of the locally generated carrier signal and the received pseudo-base-band signal. The output of the discriminator is sent to the NCO to generate a new reference signal. In Figure 4-3, the carrier tracking loop is highlighted with green color. PLL is sensitive to data bit transitions. Specifically, when the navigation data bit changes from one to zero or from zero to one, a 180° phase change is detected by the PLL and it therefore attempts to correct the perceived error. As such, a discriminator that is insensitive to bit transitions is preferred. These types of discriminators are termed Costas discriminators. In Costas discriminators, Doppler removed and correlated I channel and Q channel are used. Some of the algorithms for Costas discriminators are shown in Table 4-1 where $\delta\phi = \phi - \phi_{ref}$.

The PLL discriminator used for GLONASS phase lock loop is a two-quadrant arctangent Costas discriminator.

Table 4-1 Common Costas loop discriminators (from Ward et al 2006)

Discriminator	Output phase error	Remarks
Sign(I)×Q	$\sin(\delta\phi)$	- Decision directed Costas - Near optimal for high SNR - Least computational burden
I×Q	$\sin(2\delta\phi)$	- Classic Costas analog discriminator - Near optimal for low SNR - Moderate computational burden
Q/I	$\tan(\delta\phi)$	- Suboptimal, but works well for Low and high SNR - Higher computational burden
atan(Q/I)	$\delta\phi$	- Two-quadrant arctangent - Optimal (Maximum-likelihood estimator) for both low and high SNR - Highest computational burden
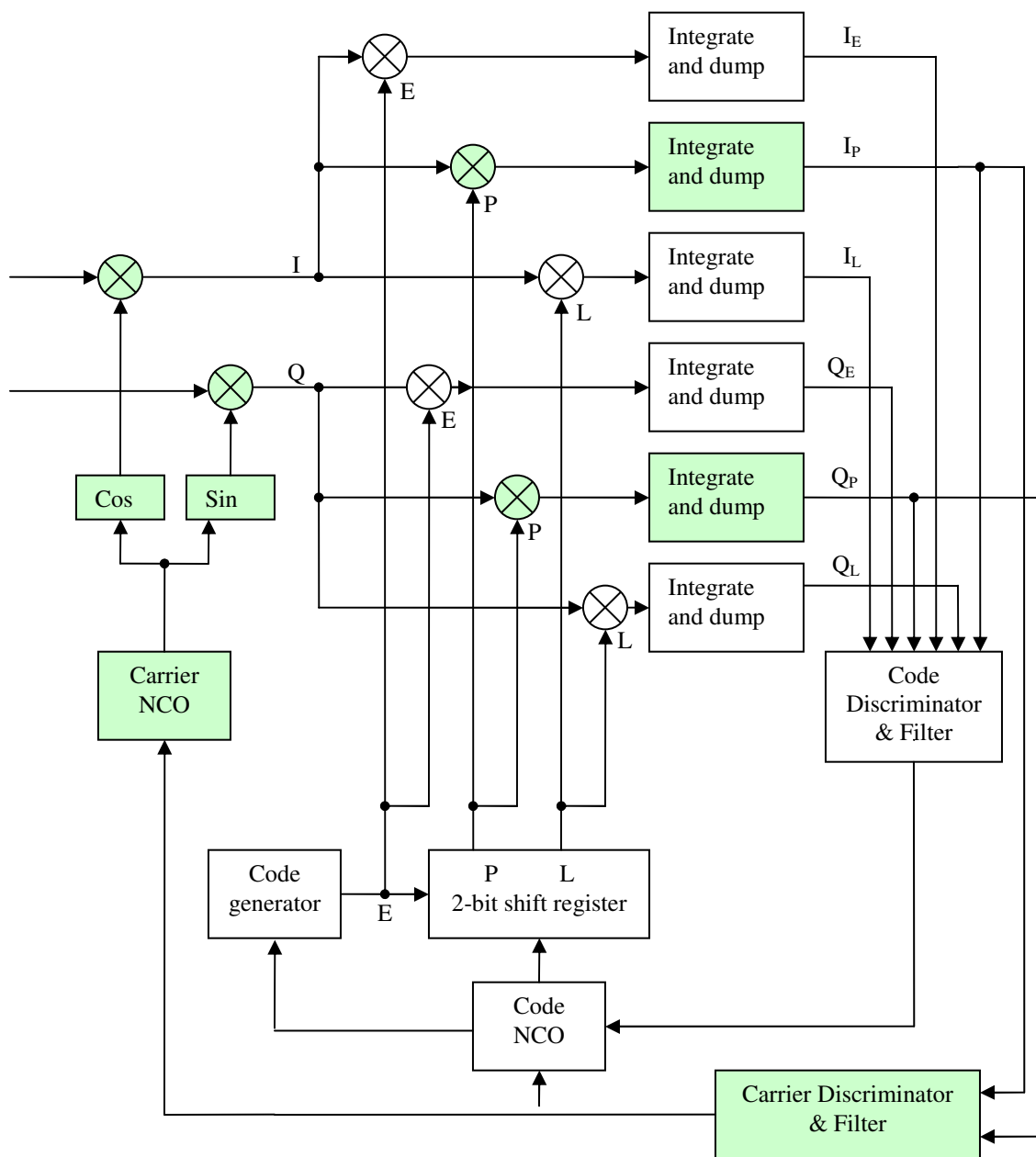
Figure 4-3 Block diagram of carrier tracking loop

4.4 Frequency lock loop

The objective of a frequency lock loop (FLL) is to generate the carrier portion of the locally generated signal. The difference between PLL and FLL is that FLL only tracks the frequency of the incoming signal not the phase. In fact, FLL tries to match the frequency of the locally generated carrier signal with the incoming pseudo-base-band signal. The frequency error signal can be used to drive the carrier NCO in the same way as phase error signal does in a PLL. However, FLL can perform better in high receiver dynamics (Ward et al 2006). A combined FLL and PLL tracking loop can be used as an initial step and then switch to PLL. To estimate the frequency error, the cross and dot product of two consecutive correlator outputs are used. These values are shown in the following equations:

$$\text{Cross}_k = C_k = [I_{k-1} \ Q_{k-1}] \times [I_k \ Q_k] = I_{k-1}. Q_k - I_k. Q_{k-1}$$

$$= A_{k-1}.A_k.B_k.B_{k-1}.\sin (\delta\phi_k - \delta\phi_{k-1}) \tag{4-1}$$

$$\text{Dot}_k = D_k = [I_{k-1} \ Q_{k-1}] \bullet [I_k \ Q_k] = I_{k-1}. Q_k + I_k. Q_{k-1}.$$

$$= A_{k-1}.A_k.B_k.B_{k-1}.\cos (\delta\phi_k - \delta\phi_{k-1}) \tag{4-2}$$

In the above equations I_k and Q_k are assumed to be presented by the following equations (i.e., simplified versions of Equation 3-7):

$$I_k = A_k.B_k.\cos(\delta\phi_k)$$

$$Q_k = A_k.B_k.\sin(\delta\phi_k) \tag{4-3}$$

where

- A represents the amplitude of the signal,

- B represents the data bits, and

- $\delta\phi$ represents the phase error

Table 4-2 summarizes several FLL discriminators, the output frequency errors and their characteristics.

Table 4-2 Common frequency lock loop discriminators (from Ward et al 2006)

Discriminator	Output frequency error	Remarks
$C_k / (t_k - t_{k-1})$	$\sin(\phi_k - \phi_{k-1})/(t_k - t_{k-1})$	- Near optimal at low SNR - Least computational burden
$(\text{Sign}(D_k) \cdot C_k) / (t_k - t_{k-1})$	$\sin(2(\phi_k - \phi_{k-1}))/(t_k - t_{k-1})$	- Decision directed - Near optimal at high SNR - moderate computational burden
$[\text{atan2}(C_k, D_k)]/(t_k - t_{k-1})$	$(\phi_k - \phi_{k-1})/(t_k - t_{k-1})$	- Four-quadrant arctangent - Maximum likelihood estimator - optimal at high and low SNR - highest computational burden

In GLONASS tracking loop, the FLL discriminator is a decision directed discriminator.

4.5 Delay lock loop

The objective of a delay lock loop (DLL) is to track the standard ranging code of the received pseudo-base-band signal by generating a local standard ranging code. This loop consists of correlator, accumulator, DLL discriminator and loop filter as is shown in Figure 4-4 in yellow color. The inputs to the DLL are Doppler removed samples modulated with navigation data and ranging code. To remove this ranging code, it is required to generate three pairs of I and Q values; early (I_E, Q_E), prompt or punctual (I_P, Q_P), and late (I_L, Q_L), where E, P, and L subscripts stand for early, punctual and late respectively. Early and late values are typically one chip away from each other and are half chip spaced from the prompt value (Ward et al 2007).

There are two types of DLL discriminators:

1. Coherent discriminator: where all power is on I channel, implying phase lock is achieved.

2. Non-coherent discriminator: where phase lock is not required.

Some types of DLL discriminators are presented in Table 4-3. In this table E and L represent the following equations:

$$E = \sqrt{I_E^2 + Q_E^2} \qquad\qquad 4\text{-}4$$

$$L = \sqrt{I_L^2 + Q_L^2} \qquad\qquad 4\text{-}5$$
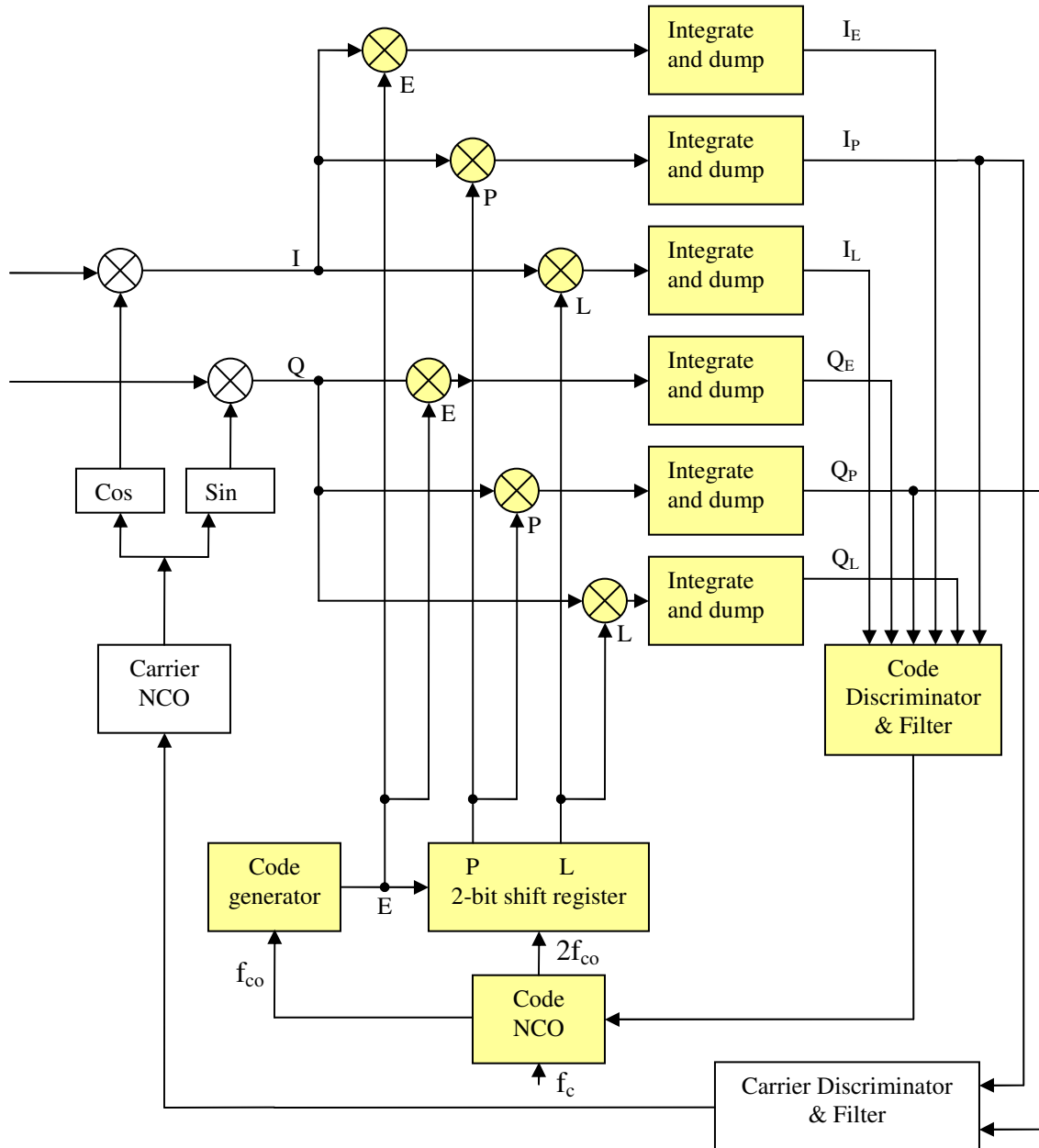
Figure 4-4 Block diagram of code tracking loop

Table 4-3 Common delay lock loop discriminators (from Ward et al 2006)

Type	Discriminator	Comments
Coherent	$0.5\ (I_E - I_L).I_P$	• Dot-product • Low computational load • Most accurate code measurement
Non-coherent	$0.5\ [(I_E - I_L).I_P +$ $(Q_E - Q_L).\ Q_P]$	• Dot-product power • Low computational load • For 1-chip early-late spacing, it produces nearly true tracking error output within ±0.5 chip of input error
	$0.5(E^2 - L^2)$	• Early-minus-late power • Moderate computational load • For 1-chip early-late spacing, it produces true tracking error within ±0.5 chip of input error
	$0.5\ [(E-L)/(E+L)]$	• Normalized-early-minus-late-envelope • Highest computational load • For 1-chip early-late spacing, it produces true tracking error within ±0.5 chip of input error • Becomes unstable at ±1.5 chip input error

The typical code tacking loop is a normalized-early-minus-late-envelope delay lock loop (Ward et al 2006). In this case, the difference between the power of early and late is calculated and sent to the discriminator. The result is filtered and sent to the code NCO for generating the local standard accuracy ranging code. This difference indicates which one (early or late ranging code) contains more energy and thus whether the NCO must

advance or delay the locally generated code. When the power of the early and late correlators is the same, the difference is zero and this is the objective of code tracking loop. By considering that the auto-correlation function has roughly a triangular shape with a typical two-chip space length (Figure 4-5), the early-minus-late correlator with and without tracking error is shown in Figure 4-6.
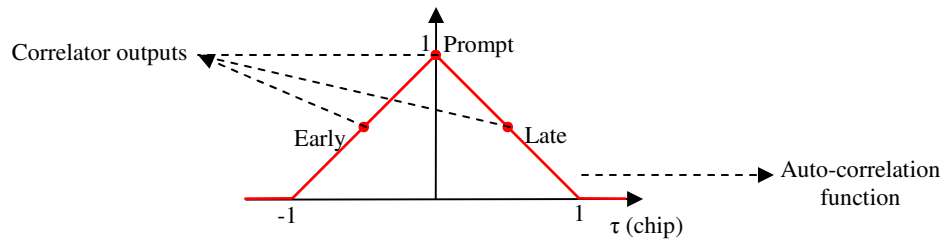
Figure 4-5 Standard code auto-correlation function
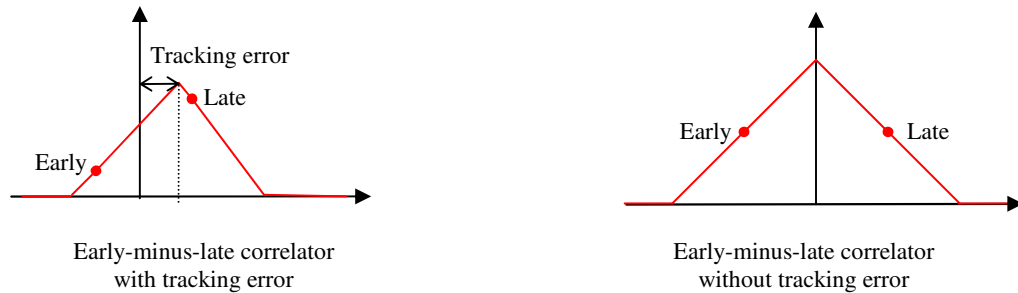
Figure 4-6 Early-minus-late correlators

The normalized-early-minus-late-envelope discriminator is used for tracking the standard ranging code of the received pseudo-base-band Doppler removed GLONASS samples.

4.6 Loop filters

The objective of a loop filter is to reduce the effect of noise on the discriminator output signal in order to generate an accurate and smooth estimate of the original signal at its output and to pass this information to the NCO. A loop filter rejects as much noise as possible and responds to the changes in signals which are caused by both receiver and satellite dynamics (Ward et al 2006). Satellites dynamics cause Doppler changes up to 0.9 Hz/s and receiver dynamics causes additional changes, wither higher acceleration causing faster changes in Doppler (Lachapelle 2007). The loop filter order and noise bandwidth are two main parameters of a loop filter. By carefully choosing these parameters, the performance of a tracking loop can increase significantly (Petovello & O'Driscoll 2007).

4.6.1 Loop order

Loop order defines the filter sensitivity to the dynamics (Ward et al 2006). These loop filters are summarized in Table 4-4.

Table 4-4 Loop filter characteristics (modified Lachapelle 2007)

Loop order	Characteristics	Best operation under	Tracking error proportional to
First	Senses high frequency noise and removes	Static condition	Velocity
Second	Senses velocity and adjust	Constant velocity	Acceleration
Third	Senses acceleration and adjust	Constant acceleration	Jerk

Figure 4-7 illustrates a third order loop filter in the Laplace, or "S", domain. Analog integrators are presented by 1/S which is the Laplace transform of the time domain integration function.
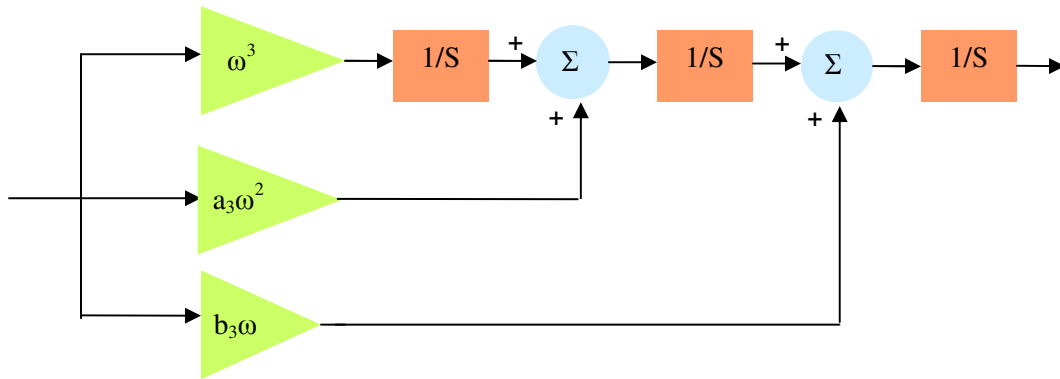
Figure 4-7 Third order analog loop filter (from Ward et al 2006)

In Figure 4-7, ω^3, $a_3\omega^2$, and $b_3\omega$ are the typical filter values. As such, the noise bandwidth (B_n) will be explained with these values. For the third order loop filter a_3, b_3, and B_n are 1.1, 2.4, and 0.7845ω respectively.

As it is shown in Figure 4-2, there are loop filters for both code lock loop and carrier lock loop. In carrier lock loop, the error in frequency lock loop (FLL) filter is one degree less sensitive than what is shown in Table 4-4 (Lachapelle 2007). This means that the first order FLL filter senses the velocity and adjusts it but is sensitive to the acceleration.

4.6.2 Loop bandwidth

The loop bandwidth must be set in a way that rejects as mush noise as possible. On the other hand, it must be wide enough to contain both satellite and receiver dynamics. For example, when the receiver is in static condition, the Doppler shift is approximately ±5 kHz, but for moving receiver it can be ±10 kHz or more (Lachapelle 2007). As such, the bandwidth must be sufficiently wide to pass true signal dynamics unchanged.

4.7 Tracking loop aiding

As discussed above, the loop bandwidth must be sufficiently wide to let actual signal dynamics pass and also be sufficiently narrow to prevent the noise to pass. Thus, there is always a compromise between having more noise and true signals. On the other hand, in some cases, the signal dynamics can be measured externally and removed. Then, the noise bandwidth can be reduced. This is the concept of tracking loop aiding. Figure 4-8 illustrates the block diagram of the code tacking loop aiding with carrier tracking loop. The carrier tracking loop is adjusted by a scale factor, then the code loop filter output is added to it. The result is sent to the code NCO. The scale factor is presented as the following equation (Ward et al 2006):

$$\text{Scale factor} = \frac{R_c}{f_L} \qquad \text{4-6}$$

where

- R_c represents code chip rate (Hz) plus C/A code Doppler effect, and

- f_L represents L-band carrier frequency (Hz)

The C/A code Doppler frequency can be calculated according to the carrier frequency.

Code Doppler [chip/s]= Carrier Doppler[cycle/s]. (L-band wavelength [m/cycle]/ chip length [m/chip])

This scale factor is required because the Doppler effect on signal is proportional inversely to the signal wavelength. As such, the Doppler effect on the code chip rate is much smaller than the Doppler effect on the carrier frequency for the same relative velocity between satellite and the receiver.
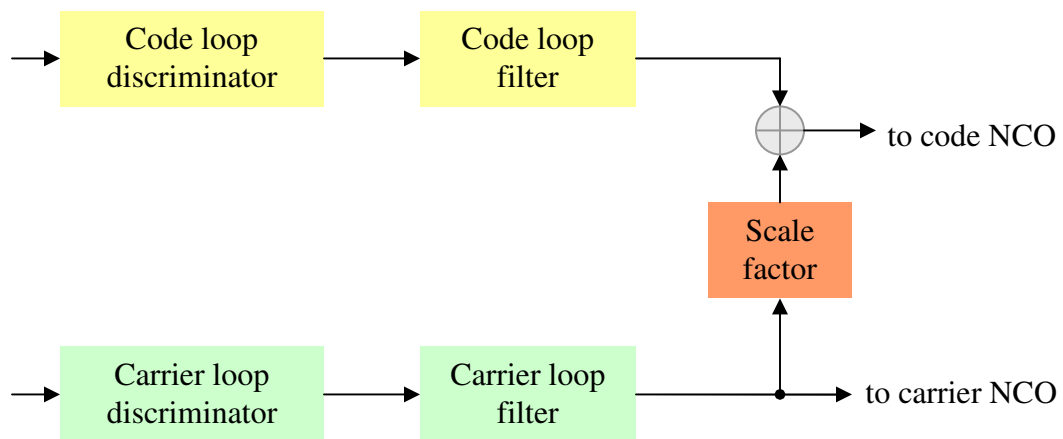
Figure 4-8 Carrier aiding of code loop (modified Ward et al 2006)

4.8 GLONASS tracking loop

The GLONASS L1 and L2 signals' tracking is performed in the modified GSNRx™ software. This software is explained more in section 4.8.1. The tracking software receives the approximate Doppler frequency and code offset for each GLONASS satellite being

acquired from the acquisition process explained in Chapter three. The tracking software uses these parameters to generate some measurements which can be used to generate a navigation solution.

4.8.1 GSNRx™

GNSS Software Navigation Receiver (GSNRx™) is a C++ class-based GNSS software receiver program developed in Position, Location And Navigation (PLAN) group at the University of Calgary (Petovello et al 2008). This software is basically developed for GPS L1 C/A signal and is capable of processing the raw samples from the RF front-end and generating measurements to be used in other data processing programs. Also, it can produce navigation solution in post-mission. GSNRx™ is used as the basis for tracking GLONASS L1 and L2 signals. A general view of this software receiver is shown in Figure 4-9.

The software is initialized using an option file in which different parameters can be set by the user. The fields of the option file that are relevant to this research are explained in section 4.8.2.

As part of this research, the GSNRx™ software was modified to allow tracking of the GLONASS L1 and L2 signals for as many GLONASS satellites as possible.
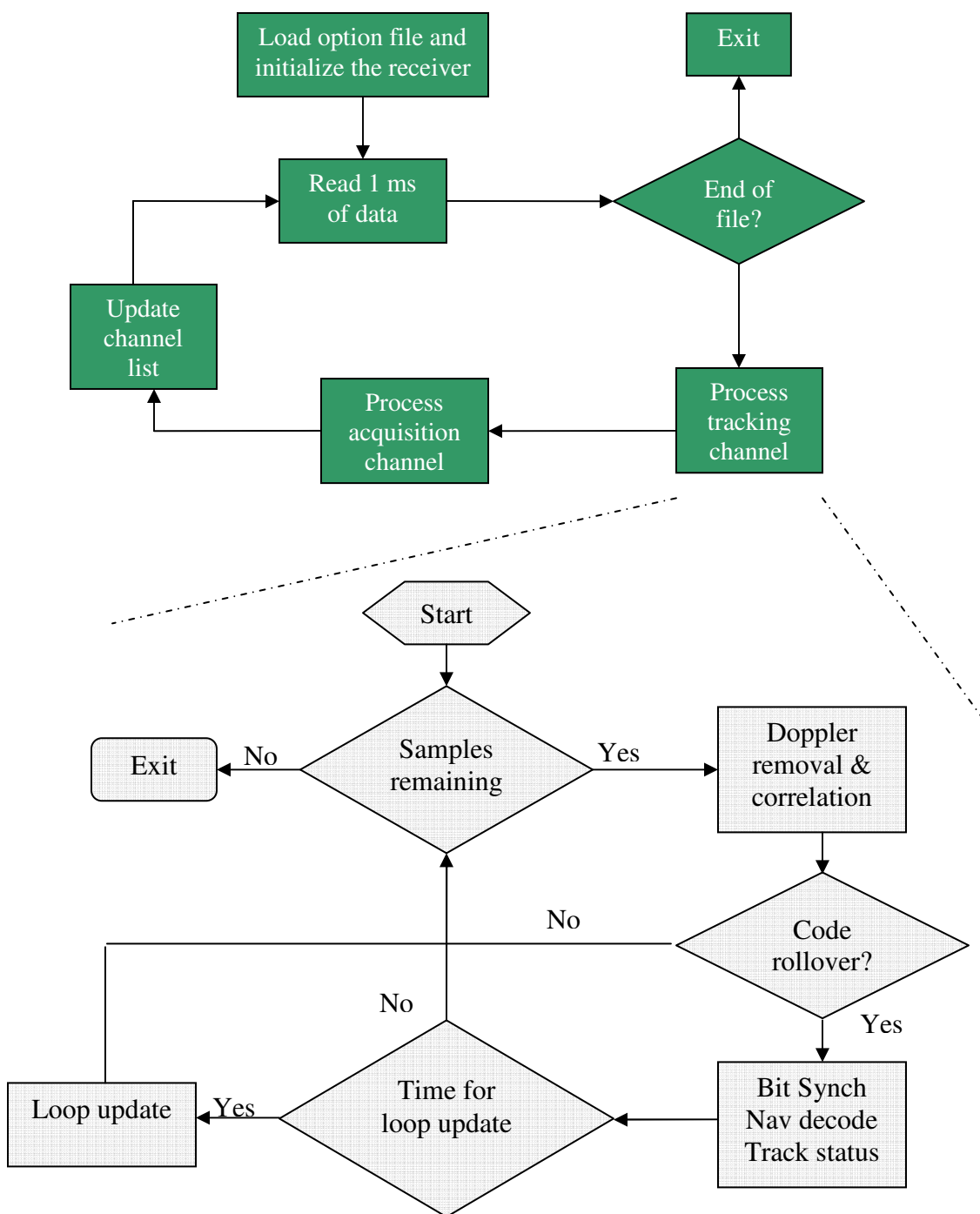
Figure 4-9 Block diagram of GSNRx™ (from Petovello & O'Driscoll 2007)

In GSNRx™ tracking, the received samples are first shifted to baseband (using Doppler removal) and correlated with the local code. Then, on each code rollover event, bit synchronization, navigation message decoding and tracking status updates are performed for each channel (Figure 4-9). Code rollover is an event specific to each tracking channel. The outputs of the Doppler removal and correlation are accumulated and when the accumulation period and tracking loop update periods are equal, the tracking loops are updated (Petovello & O'Driscoll 2007). For GLONASS tracking process, the Doppler removal and correlation component needs some modification. Different locally generated frequencies as discussed in section 3.6.2 are needed for each GLONASS satellite. Moreover, the locally generated ranging code for correlation must be in the format discussed in section 3.6.1. Considering the effect of meander code, the bit synchronization for GLONASS is different from GPS which is discussed in Chapter five. Also, the GLONASS navigation message needs its specific navigation message decoding algorithm which is explained in Chapter five.

4.8.2 Option file

The details of the relevant options for GLONASS (relative to GPS) are explained below. The values illustrated are for GLONASS L1 and L2 signals unless stated otherwise.

- Data file: This field contains the name of the raw data file. This file includes a stream of bytes. Each byte represents a sample from the RF front-end. GLONASS L1 and L2 feed two different raw files to the option file because of their different carrier frequencies.

- Intermediate frequency: This field represents the intermediate frequency of the samples in the file presented in data file field. This value is set 4 MHz.

- Sampling rate: this filed represent the sampling rate of the samples in the file presented in data file field. This value is set 12.5 MSps.

- Maximum coherent integration: This field represents the maximum length of the coherent integration in a channel. This value is set 10 ms for GLONASS because the received GLONASS navigation data bit is 10 ms.

- Type of carrier loop: The carrier loop can operate in PLL or FLL-assisted PLL mode. For GLONASS tracking loop, PLL is chosen.

- PLL bandwidth: As discussed in section 4.8, the loop bandwidth can be fixed or variable. This field is a space to change the bandwidth of the PLL. For GLONASS, the bandwidth of PLL is set 15 Hz.

- FLL bandwidth: In this field the bandwidth of FLL can be set. The bandwidth of FLL is set 8 Hz for GLONASS.

- Initial DLL bandwidth: In this field DLL bandwidth is set before the aiding with carrier lock loop. This value is set 2 Hz for GLONASS.

- Assisted DLL bandwidth: This field define the DLL bandwidth after aiding with carrier lock loop. This value is set 0.05 Hz for GLONASS.

- PRN: It indicates the satellite number which is going to be tracked. For GLONASS, this filed represents the satellites being acquired and are ready to be tracked. This field must be followed by approximate Doppler frequency (Hz) and

code phase (Chips) which are acquired in acquisition process discussed in Chapter three.

- Doppler: As explained above, this field indicates the Doppler frequency (Hz) of the satellite being acquired and is passed to this option file for tracking.

- Code phase: This field is dedicated to the code phase (Chips) of the satellite being acquired and is passed to this option file for tracking. It must follow the PRN and Doppler fields.

4.8.3 Tracking loop implementation in GSNRx™

The mode of the tracking loop can be reflected by a parameter called tracking state for each channel. The software uses two indicators called frequency lock indicator (FLI) and phase lock indicator (PLI) for the transition between tracking states. FLI (Mongredien et al 2006) and PLI (Van Dierendonck 1995) are defined by the following equations:

$$\text{FLI}_k = \frac{D_k^2 - C_k^2}{D_k^2 + C_k^2} = \cos(4\pi\delta f_k T_{\text{coh}}) \tag{4-7}$$

$$\text{PLI}_k = \frac{I_k^2 - Q_k^2}{I_k^2 + Q_k^2} = \cos\left(2\delta\phi_k\right) \tag{4-8}$$

D_k and C_k are explained in section 4.4 and T_{coh} is the coherent integration time. According to the equations 4-7 and 4-8, FLI and PLI range between minus one in the worse case and positive one in the best case.

Tracking states and a short description for each state is summarized in Table 4-5. To achieve phase lock loop which is the ultimate goal of a tracking loop, it is required to

achieve frequency lock loop at first to avoid false lock in PLL. On the other hand, loss of lock must be detected. By comparing the FLI and PLI values against different thresholds (that depend on the current tracking state), the software is able to successfully track signals in a robust manner.

Table 4-5 Tracking states summary

Tracking state	Description
Initialization	• Carrier tracking loop is performed using FLL alone • Gives time to FLI to converge before being used for decision making
Wideband FLL	• Carrier tracking loop is performed using FLL alone • A constant 1-ms integration time is used to maintain ±250 Hz pull-in range
Narrowband FLL	• Carrier tracking loop is performed using FLL alone • Integration time is maximized for fine frequency tracking
FLL-assisted PLL	• Carrier tracking loop is performed using FLL-assisted PLL • DLL aiding with CLL begins
PLL	• Carrier tracking loop is performed using PLL

4.9 Tracking Results

In this section, the tracking results for GLONASS L1 and L2 signals are presented beside the tracking status. The tracking statuses are defined by numbers in the tracking software as shown in Table 4-6. Presenting tracking status besides each result helps to more easily explain the result obtained.

Table 4-6 Tracking status in software

Tracking status	In software
Initialization	0
Wideband FLL	1
Narrowband FLL	2
FLL-assisted PLL	3
PLL	4

4.9.1 Doppler frequency

Figure 4-10 shows the Doppler frequency tracking for the GLONASS L1 signal transmitted from GLONASS satellite at slot number 24. In the initialization tracking status, the tracking is performed using only FLL. The software searches for the correct Doppler frequency. In wideband FLL status, the Doppler frequency is searched over a wide frequency range. This search becomes finer in narrowband FLL until the Doppler frequency is reliably tracked. In FLL-assisted PLL and PLL tracking status this Doppler frequency is tracked.
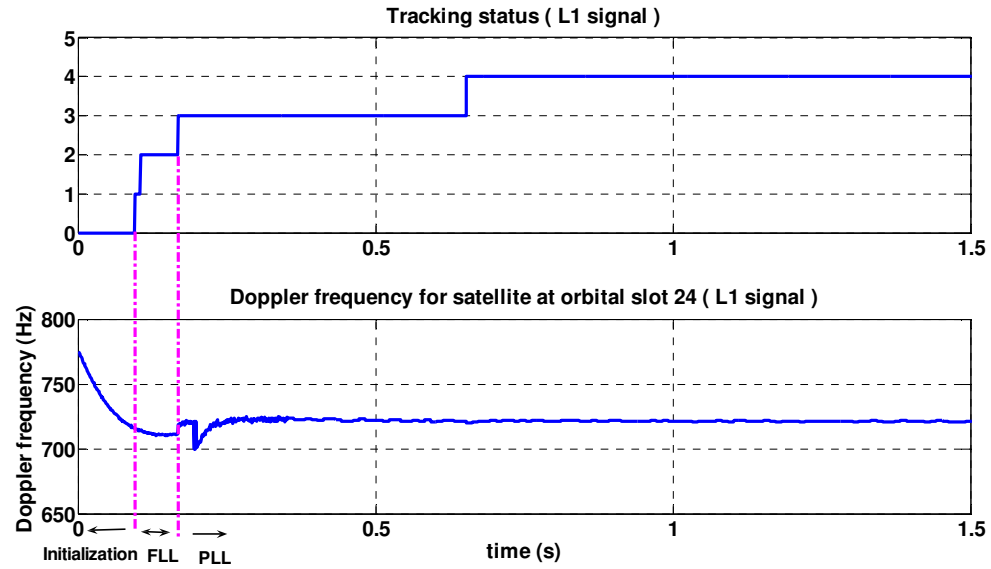
Figure 4-10 Doppler frequency for GLONASS L1 signal transmitted from satellite at orbital slot 24

Figure 4-11 presents the Doppler frequency tracking for GLONASS L2 signal transmitted from GLONASS satellite at orbital slot 24. Similar to the Doppler tracking for the L1 signal, after initialization, the Doppler frequency search continues in wideband FLL and after that in narrowband FLL. In FLL-assisted PLL and PLL tracking status, the found correct Doppler frequency is tracked.
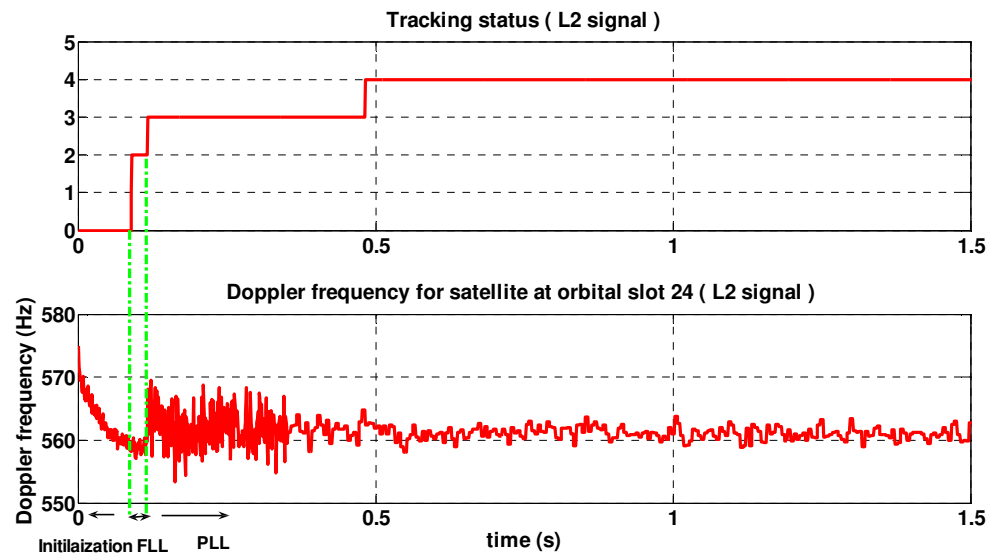
Figure 4-11 Doppler frequency for GLONASS L2 signal transmitted from satellite at orbital slot 24

In both figures, it is seen that the Doppler frequency becomes nosier in FLL-assisted PLL step. That is because of the PLL bandwidth (15 Hz) which is wider than FLL (8 Hz) bandwidth and allows more noise enter the system suddenly which affects the Doppler frequency search but it is maintained in tracking loop after a short time.

Moreover, the L2 Doppler frequency appears to converge more rapidly than L1 because the initial approximate Doppler frequency extracted from the acquisition process was closer to the Doppler frequency found in FLL step during tracking process.

To compare GLONASS L1 and L2 Doppler frequency, Figure 4-12 is presented. In this figure the Doppler values are scaled just to present a better comparison between L1 and L2 Doppler frequencies. As discussed above, L2 Doppler frequency converges more rapidly than L1. L2 Doppler frequency is noisier than L1, because the L2 signal is generally weaker than L1 signal.
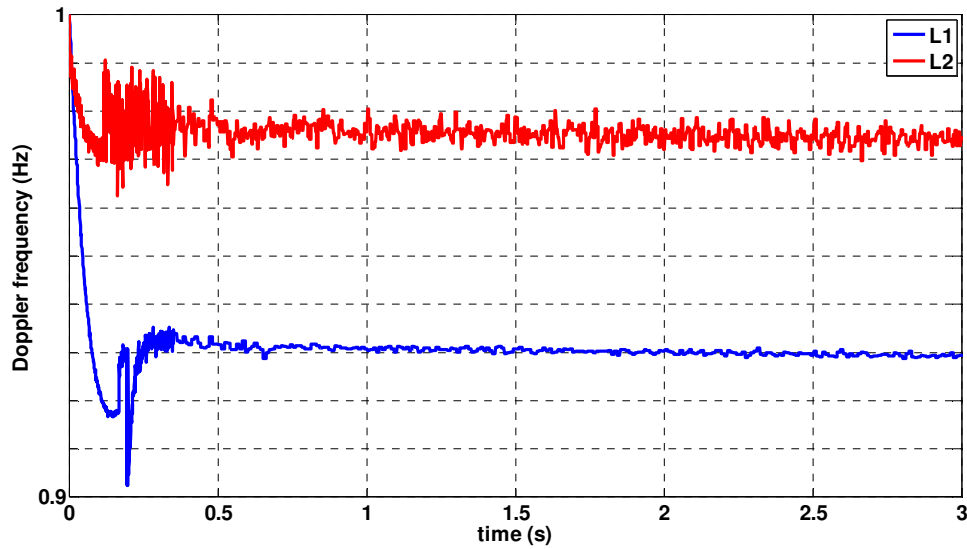
Figure 4-12 Doppler frequency tracking for L1 and L2 signal transmitted from GLONASS satellite at orbital slot 24

Doppler frequency tracking for other satellites signals tracked shows similar results.

4.9.2 Correlator outputs

Figure 4-13 presents the correlator outputs for the received L1 signal from the GLONASS satellite at orbital slot 24 (same satellite as in the previous section). In the period of initialization and FLL tracking status, the power is divided into I channel and Q channel. In the period of FLL-assisted PLL tracking status, the power is gradually transferred to the I channel and after achieving PLL status, all the power is in I channel and what remains in Q channel is just noise and this is the objective of a tacking status. Equation 3-7 can be re-written as:

$$I_k^{DRC} = A.N.R(\delta\tau).Sinc(\pi\delta f T_s N).Cos(\pi\delta f T_s N + \delta\phi)$$

$$Q_k^{DRC} = A.N.R(\delta\tau).Sinc(\pi\delta f T_s N).Sin(\pi\delta f T_s N + \delta\phi) \qquad \text{4-9}$$

According to these equations, when FLL tracking status is complete and the correct Doppler frequency is estimated, δf equals to zero and the Sinc function of zero is one. By achieving PLL, when the phase error is estimated, $\delta\phi$ equals to zero too. Thus, the sin term in Q^{DRC} is zero and only I^{DRC} will have a value.
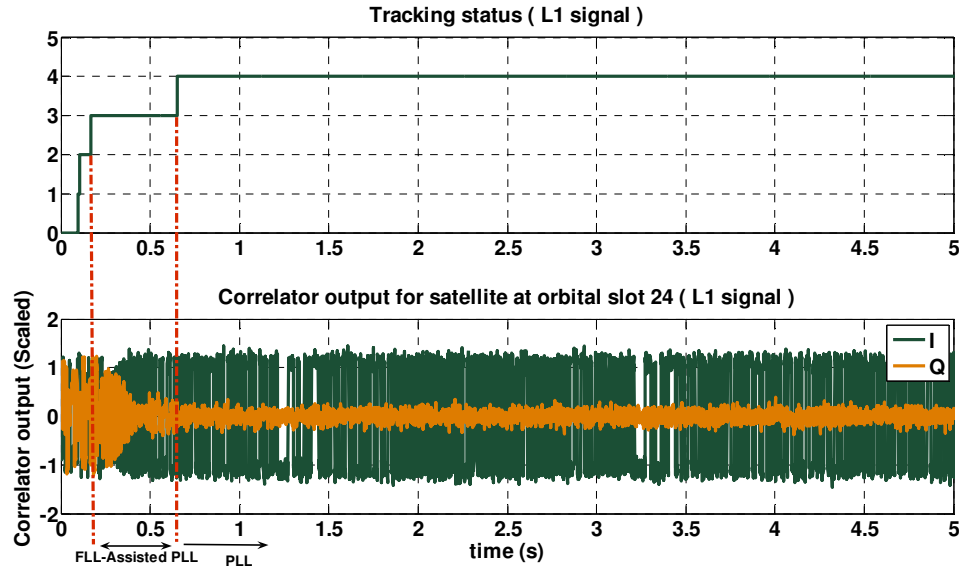
Figure 4-13 Correlator output for GLONASS L1 signal transmitted from GLONASS satellite at orbital slot 24
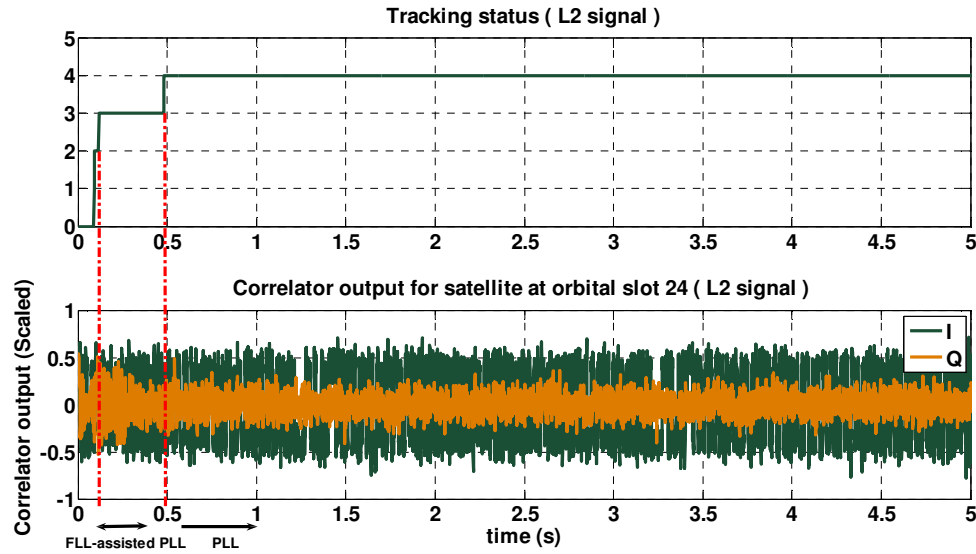
**Figure 4-14 Correlator output for GLONASS L2 signal transmitted from
GLONASS satellite at orbital slot 24**

Figure 4-14 presents the correlator outputs for the received L2 signal from the
GLONASS satellite at orbital slot 24. Similar to the L1 signal, the power is divided into I
and Q channel before PLL tracking status and after achieving PLL all the power is in I
channel.

There are similar results for the tracked L1 and L2 signals from the GLONASS satellites
at other orbital slots.

4.9.3 Carrier to noise density ratio estimation (C/N$_0$)

The carrier to noise density ratio estimation is performed using the power ratio method
(PRM) (Van Dierendonck 1995), as summarized below. In this method, the power of the
signal is computed over a wide bandwidth with a relatively short coherent integration

time. Then, the power is computed over a narrow bandwidth with a longer coherent integration time. Thus, the wideband power (WBP) is computed using 1 ms coherent integration time as follows:

$$WBP_k = \sum_{i=1}^{M} (I_i^2 + Q_i^2) \qquad \text{4-10}$$

And the narrowband power (NBP) is computed using M ms of coherent integration as the follows:

$$NBP_k = \left(\sum_{i=1}^{M} I_i \right)^2 + \left(\sum_{i=1}^{M} Q_i \right)^2 \qquad \text{4-11}$$

The ratio of equations 4-10 and 4-11 is called normalized power (NP) and is computed as:

$$NP_k = \frac{NBP_k}{WBP_k} \qquad \text{4-12}$$

These normalized values are averaged over h samples:

$$\mu_{NP} = \frac{1}{h} \sum_{k=1}^{h} NP_k \qquad \text{4-13}$$

Finally, C/N_0 is estimated with the following equation:

$$\frac{C}{N_0} = 10\log_{10} \left[\frac{1}{T_{coh}} \frac{\mu_{NP} - 1}{M - \mu_{NP}} \right] \qquad \text{4-14}$$

The value of M is set 10 for GLONASS signal.

Figure 4-15 compares the C/N_0 values for the received L1 and L2 signals from GLONASS satellite at orbital slot 24. As discussed in Chapter two in detail, GLONASS L2 signal is weaker than GLONASS L1 signal and this figure confirms this fact.
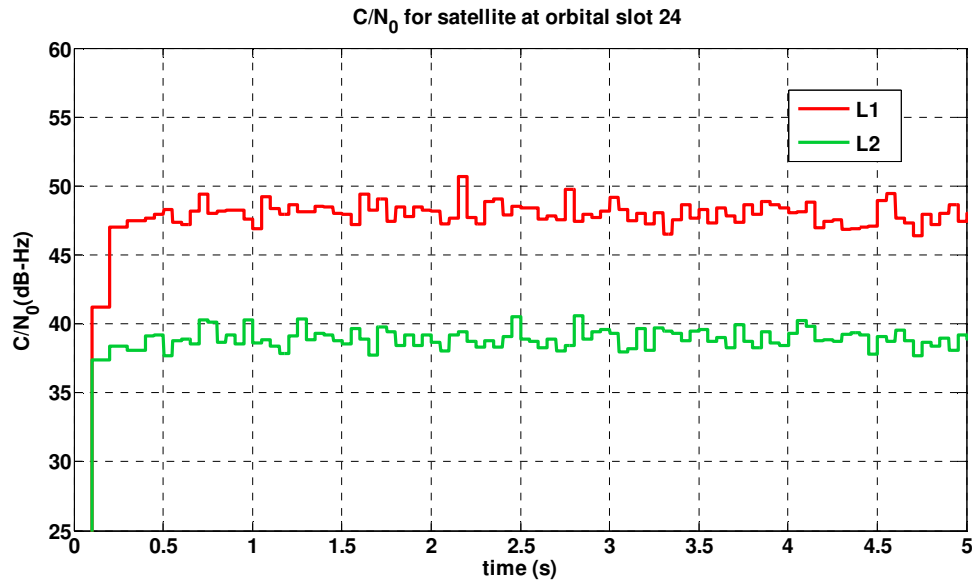
Figure 4-15 C/N$_0$ estimation for GLONASS L1 and L2 signal transmitted from GLONASS satellite at orbital slot 24

Table 4-7 summarizes the C/N$_0$ values for L1 and L2 signals being tracked. The values in the table represent average C/N$_0$ values over ten minutes. This table shows that the L2 C/N$_0$ values are lower than L1 values from the same satellite. The differences between L1 and L2 C/N$_0$ value are around 3 dB-Hz for all the satellites except for satellite at orbital slot 24. L1 signal received from GLONASS satellite at orbital slot 24 is strong.

Figure 4-16 presents the C/N$_0$ values for all the GLONASS L1 and L2 signals. This figure plus Table 4-7 confirm that L2 signal received from GLONASS satellite at orbital slot 23 is so weak (with average value of 35 dB-Hz over ten minutes) and the L1 signal received from GLONASS satellite at orbital slot 24 is the strongest signal.

Table 4-7 Average C/N$_0$ values for L1 and L2 signals

Orbital slot	Average C/N$_0$ value for L1 (dB-Hz)	Average C/N$_0$ value for L2 (dB-Hz)
R13	41.5	38.4
R15	43.2	40.4
R17	42	38.7
R23	38.8	35
R24	47	40.2
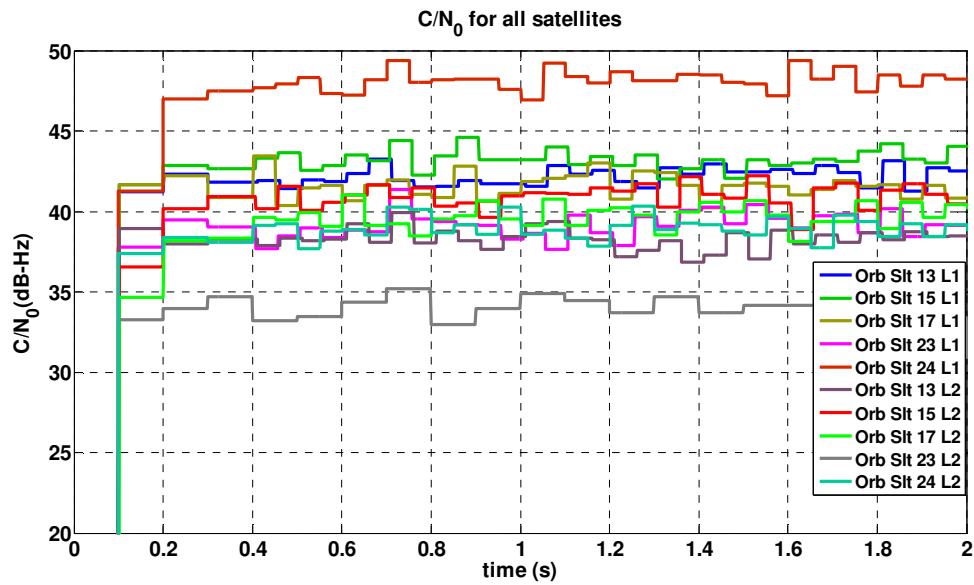
Figure 4-16 C/N$_0$ value for all the GLONASS L1 and L2 signals tracked

4.9.4 Frequency lock indicator

FLI has a critical role in switching from one tracking status to the other. Figure 4-17 illustrates the L1 FLI values in different region of tracking status.

During the initialization period, carrier loop tracking is performed using FLL alone. Initialization allows FLI to converge before being used for decision making. The value of FLI is checked periodically and this value makes the decision to switch to the next stage which is wideband FLL. In wide band FLL, narrowband FLL and FLL-assisted PLL the value of FLI is checked again and when it passes a defined threshold, the tracking status switches to the next tracking status. In FLL-assisted PLL period, besides FLI, the value of PLI is checked too. PLI results are shown in section 4.9.5. When the PLL is achieved, the value of FLI is not important anymore unless the PLI decreases below a lower threshold. In this case, the tracking status switches to wideband FLL.
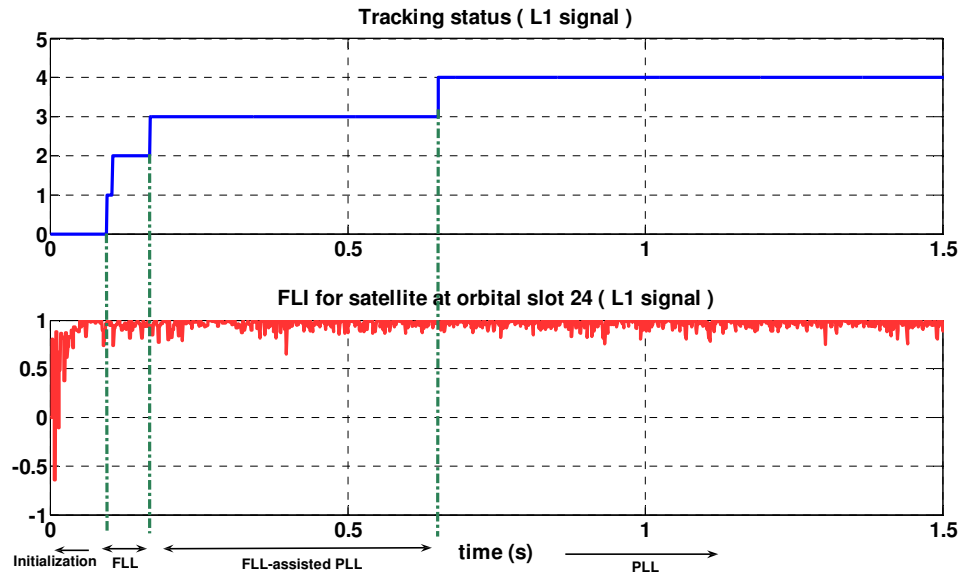
Figure 4-17 FLI for GLONASS L1 signal transmitted from GLONASS satellite at orbital slot 24

Figure 4-18 presents the FLI values in different regions of tracking status for GLONASS L2 signal.
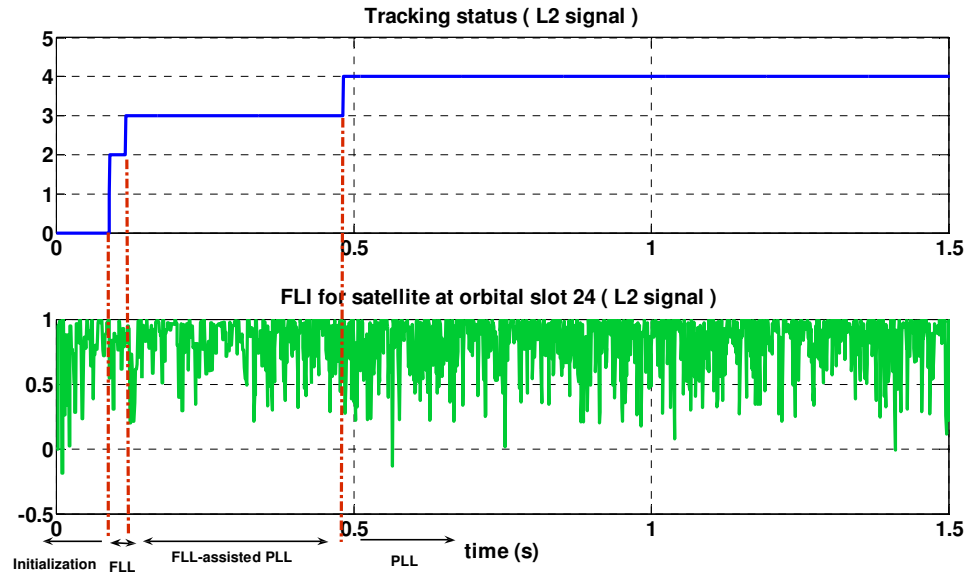
Figure 4-18 FLI for GLONASS L2 signal transmitted from GLONASS satellite at orbital slot 24

It is seen that during initialization period (tracking status = 0), FLI for the L2 signal converges faster than L1. Therefore, L2 passes the initialization period faster than L1. Moreover, FLI for L2 meet the condition of switching from wideband FLL to narrowband FLL more quickly than L1 and the same for switching from narrowband FLL to FLL-assisted PLL.

As discussed before, there was a good approximation of Doppler frequency for L2. As such, switching from FLL mode to PLL mode occurs more quickly for L2 than L1. Tracking status for L1 and L2 is presented in Figure 4-19.
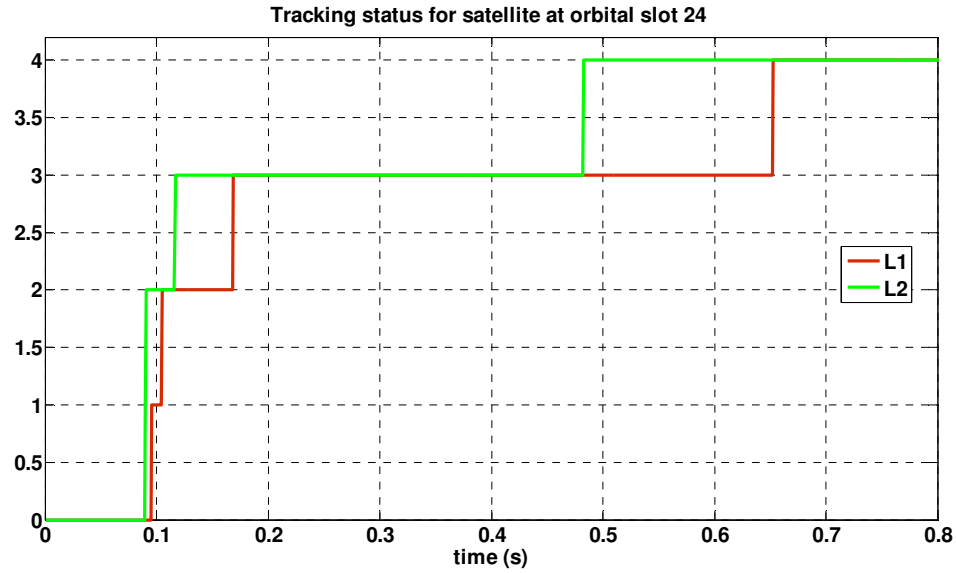
Figure 4-19 L1 and L2 tracking status for satellite at orbital slot 24

4.9.5 Phase lock loop

Figure 4-20 presents the PLI value for the GLONASS L1 signal transmitted from GLONASS satellite at orbital slot 24. In FLL-assisted PLL tracking status, the values of FLI and PLI are checked. When these values exceed a defined threshold, the tracking status switches from FLL-assisted PLL to PLL. Achieving PLL is the objective of the tracking process, and when it is lost it must be maintained as soon as possible. Thus, the value of PLI is checked during PLL tracking status. If the PLI value falls below a defined threshold, the tracking status will switch back to wideband FLL to maintain the lock on the signal.
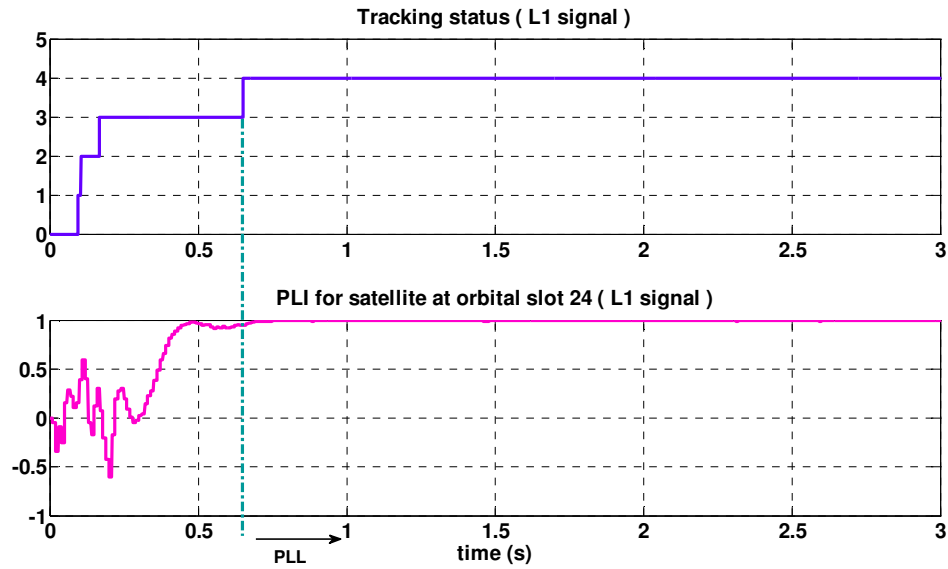
Figure 4-20 PLI for GLONASS L1 signal transmitted from GLONASS satellite at orbital slot 24.

Figure 4-21 presents PLI for GLONASS L2 signal transmitted from a GLONASS satellite at orbital slot 24.

Comparing L1 and L2 PLI, it is seen that L2 switches from FLL-assisted PLL to PLL faster than L1. During FLL-assisted PLL, FLI and PLI are both checked. Figure 4-21, Figure 4-18 and Figure 4-19 confirm that FLI and PLI for L2 reach the defined threshold for switching to PLL more quickly than FLI and PLI of L1. During PLL tracking status, although L2 PLI shows more fluctuations, it remains sufficiently high to preserve phase lock.
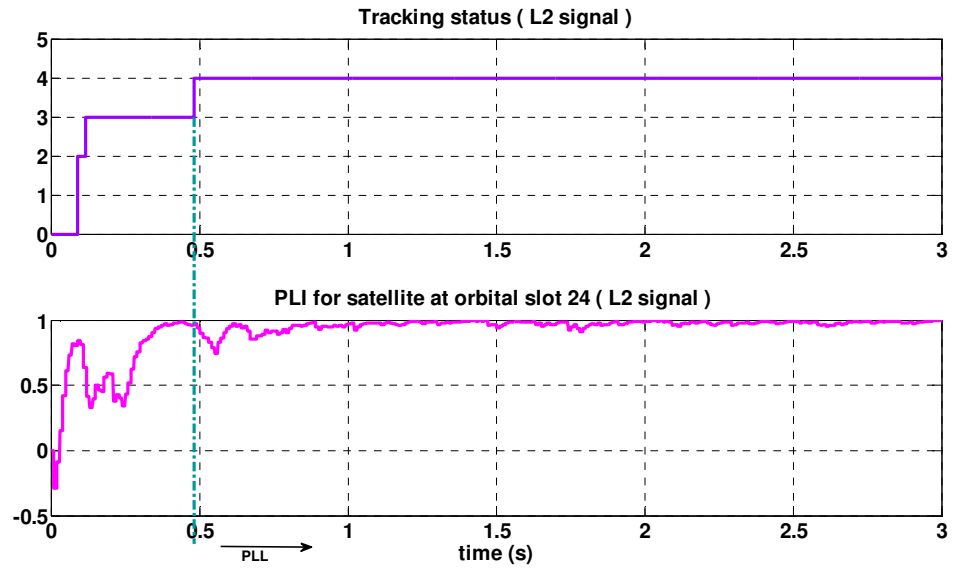
Figure 4-21 PLI for GLONASS L2 signal transmitted from GLONASS satellite at orbital slot 24.

CHAPTER FIVE: NAVIGATION SIGNAL PROCESSING

5.1 Chapter outline

At the beginning of this Chapter, the GLONASS navigation message structure is reviewed. After that, GLONASS navigation data bit synchronization is explained. The Chapter continues with an explanation of the method used for GLONASS navigation string synchronization. Then, the navigation data decoding is discussed and an experiment for verification of the whole process is illustrated. Then, the decoded GLONASS navigation message is compared with the navigation message from a commercial receiver and some results are presented. At the end of this Chapter, the ionosphere-free navigation solution is discussed and some results are presented.

5.2 GLONASS navigation message structure overview

The detailed GLONASS navigation message structure is explained in section 2.6.1. A summary of this section is presented here for convenience. According to GLONASS ICD (2002), the GLONASS navigation message is generated as a pattern of continuously repeating "strings" each with duration of two seconds. During the first 1.7 seconds of each two second interval (at the beginning of each string), 85 bits of navigation data are transmitted. During the last 0.3 seconds (at the end of each string) the time mark is transmitted. Navigation data bits are encoded using a Hamming code of length four. In

telecommunication, hamming code is a way of data error detection which named after its inventor, Richard Hamming. By hamming code, one single data bit is can be detected and corrected, and two simultaneous data bit errors can be detected. The coded sequence of data and check bits are then transformed into relative code. At the next step, the meander sequence is Modulo-2 added to the transformed data bits. The time mark, which separates data of one string from the data of adjacent string, is then appended. Finally, the ranging code is added prior to modulating the carrier.

Overall, 15 strings create one frame. Therefore, a frame is 30 seconds in duration. Each five frames create a super-frame with the duration of 2.5 minutes. Within each frame, all the immediate data for the given satellite and a part of the non-immediate data are transmitted.

Table 5-1 presents a comparison between GPS and GLONASS navigation message structure.

Table 5-1 Comparison between GPS and GLONASS navigation message

GNSS system	Data unit	Duration
GPS	Super-frame	12.5 minutes
	Page	30 s
	Sub-frame	6 s
	Word	600 ms
GLONASS	Super-frame	2.5 minutes
	Frame	30 s
	String	2 s

5.3 GLONASS navigation message decoding

GLONASS navigation message is a 50 Hz message which is modulated with a 100 Hz meander sequence by Modulo-2 addition (GLONASS ICD 2002). The GLONASS navigation message contains information related to the satellite being tracked and also information related to the GLONASS constellation. As such, the navigation message must be decoded to extract this information which is necessary for computing navigation solution. To this end, the following steps are required:

1. Bit synchronization
2. String synchronization
3. Navigation message decoding

These steps are explained more in the following sections.

5.3.1 Bit synchronization

To decode the navigation message, it is important to find the location of navigation data bit transition. To determine the data bit transition location, a few methods are proposed (Rambo 1989, Spilker 1977). The method which is used herein is the histogram method (Van Deirendonck 1996). In this method, a navigation data bit is divided into shorter bins. For GLONASS, a 10-ms data bit is divided into 10 1-ms bins. Then, the transitions between two successive bins are detected. These transitions are recorded in counters (one counter for each bin). The process continues until one of the three following conditions occurs:

a) One bin count exceeds the upper threshold (T_{up})

b) Two bin count exceeds the lower threshold (T_{low})

c) Loss of lock

If 'a' occurs, bit synchronization is successful. If 'b' occurs, the bit synchronization is failed because of low C/N_0 or lack of bit sign transition and bit synchronization is reinitialized. If 'c' occurs, the signal has been lost and must be reacquired.

The bit synchronization process is dependent on the C/N_0 estimation. As such, the lower and upper threshold should not be static. They must be dynamic and C/N_0 value dependent. The probability of making an error in determining a sign change is (Van Deirendonck 1996):

$$P_{esc} = 2P_e(1 - P_e) \qquad\qquad 5\text{-}1$$

where, the subscript 'esc' stands for the 'error in sign change' and P_e is calculated as follows:

$$P_e = \text{erfc}'[\sqrt{2(C/N_0)T_{coh}}] \qquad\qquad 5\text{-}2$$

In equation 5-2, T_{coh} is the coherent integration time and

$$\text{erfc}'(x) = \frac{1}{\sqrt{2\pi}} \int_x^\infty e^{-y^2/2} dy \qquad\qquad 5\text{-}3$$

If T_{search} represents the search time, upper threshold is defined as:

$$T_{up} = 25.T_{search} \qquad\qquad 5\text{-}4$$

and the lower threshold is defined as:

$$50.T_{search}.P_{esc} \leq T_{low} \leq 25.T_{search} - 3\sqrt{50.T_{search}.P_{esc}(1 - P_{esc})} \qquad\qquad 5\text{-}5$$

T$_{search}$ is defined one second in the software receiver.

For GPS in T$_{search}$ second, there are 25T$_{search}$ data bit transitions in average and for GLONASS in T$_{search}$ second there are 50 T$_{search}$ data bit transitions in average. As such, if the counter of a bin shows a value of 25T$_{search}$ or more for GPS and 50T$_{search}$ or more for GLONASS, the location of data bit transition is defined.

According to the above equations, the upper and lower thresholds are not common amongst all satellites being tracked.

Figure 5-1 illustrates the bit synchronization for different GLONASS satellites. In this figure, a status value of one represents the successful bit synchronization.
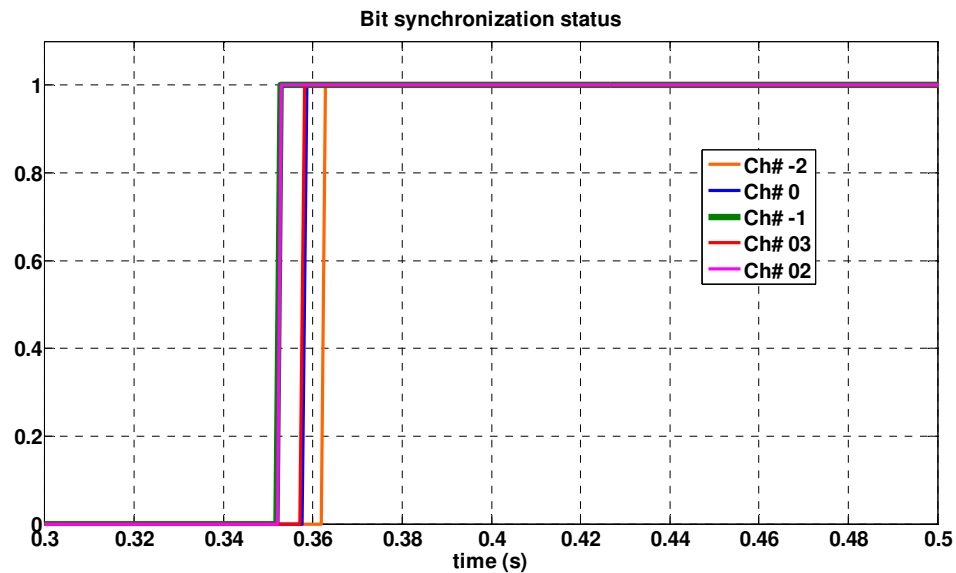
Figure 5-1 Bit synchronization status for different GLONASS satellites

algorithm for data verification allows correcting an error in one bit within a string and detecting (but not correcting) an error in two or more bits within string. To correct one bit in a string seven checksums are generated $(C_1 \dots C_7)$ and to detect two-bit error another checksum (C_Σ) is generated. These checksums are generated as follows (GLONASS ICD 2002):

$$C_1 = \beta_1 \oplus \left[\sum_i b_i \right]_{\text{mod } 2}$$

5-6

i = 9, 10, 12, 13, 15, 17, 19, 20, 22, 24, 26, 28, 30, 32, 34, 35, 37, 39, 41, 43, 45, 47, 49, 51, 53, 55, 57, 59, 61, 63, 65, 66, 68, 70, 72, 74, 76, 78, 80, 82, 84

$$C_2 = \beta_2 \oplus \left[\sum_j b_j \right]_{\text{mod } 2}$$

5-7

j = 9, 11, 12, 14, 15, 18, 19, 21, 22, 25, 26, 29, 30, 33, 34, 36, 37, 40, 41, 44, 45, 48, 49, 52, 53, 56, 57, 60, 61, 64, 65, 67, 68, 71, 72, 75, 76, 79, 80, 83, 84

$$C_3 = \beta_3 \oplus \left[\sum_k b_k \right]_{\text{mod } 2}$$

5-8

k = 10-12, 16-19, 23-26, 31-34, 38-41, 46-49, 54-57, 62-65, 69-72, 77-80, 85

$$C_4 = \beta_4 \oplus \left[\sum_l b_l \right]_{\text{mod } 2}$$

5-9

l = 13-19, 27-34, 42-49, 58-65, 73-80.

$$C_5 = \beta_5 \oplus \left[\sum_m b_m \right]_{\text{mod } 2}$$

5-10

$$m = 20\text{-}34,\ 50\text{-}65,\ 81\text{-}85$$

$$C_6 = \beta_6 \oplus \left[\sum_{n=35}^{65} b_n \right]_{\text{mod } 2}$$

5-11

$$C_7 = \beta_7 \oplus \left[\sum_{p=66}^{85} b_p \right]_{\text{mod } 2}$$

5-12

$$C_{\Sigma} = \left[\sum_{q=1}^{8} \beta_q \right]_{\text{mod } 2} \oplus \left[\sum_{q=9}^{85} b_q \right]_{\text{mod } 2}$$

5-13

The following rules are specified for correcting single errors and detecting multiple errors (GLONASS ICD 2002):

a) A string is considered correct if all the checksums ($C_1 \ldots C_7$ and C_{Σ}) are equal to zero or if only one of the checksum ($C_1 \ldots C_7$) is equal to zero but C_{Σ} is equal to one.

b) If two or more checksums are equal to one and C_{Σ} is equal to zero then b_{icor} is corrected to the opposite character. This character is in the following position:

$$i_{\text{cor}} = C_7 . C_6 . C_5 . C_4 . C_3 . C_2 . C_1 + 8 - K \qquad , \qquad \text{and } i_{\text{cor}} < 86$$

where, K is the ordinal number of the most significant checksum not equal to zero.

If the $i_{cor} > 85$, it indicates that there is odd number of errors greater than one. Thus, the data can not be corrected and must be ignored.

c) If at least one of the checksums $(C_1...C_7)$ is equal to one and C_Σ is equal to zero, or if all the checksums $(C_1...C_7)$ are equal to zero but C_Σ is equal to one, there are multiple errors and the data must be removed.

When the data verification is passed, the correct navigation data bits are revealed and information can be extracted from the data bits. The whole process mentioned above is the reverse process of GLONASS navigation data generation illustrated in Figure 2-9. Block diagram presented in Figure 5-2 summarizes the method used for GLONASS string synchronization.

```
                         ┌─────────┐
                         │  Start  │
                         └─────────┘
                              │
                              ▼
                     ╱─────────────────╲
                    ╱  Search for time   ╲      No
                    ╲  mark or its       ╱ ──────────┐
                     ╲  complement      ╱            │
                       ╲───────────────╱             │
                              │ Yes                   │
                              ▼                        │
                     ╱─────────────────╲              │
                    ╱  Search for time   ╲    No       │
                    ╲  mark after 2 s    ╱ ───────────┘
                       ╲───────────────╱
                              │ Yes
                              ▼
              ┌──────────────────────────────┐
              │ Convert the string from 10-ms │
              │ to 20-ms data bits (remove    │
              │ meander code effect)          │
              └──────────────────────────────┘
                              │
                              ▼
              ┌──────────────────────────────┐
              │ Remove time mark from the      │
              │ string                         │
              └──────────────────────────────┘
                              │
                              ▼
              ┌──────────────────────────────┐
              │ Transformation from relative   │
              │ code to sequence of data and   │
              │ check bits                     │
              └──────────────────────────────┘
                              │
                              ▼
                     ╱─────────────────╲    No      ┌──────────┐
                    ╱  Data bits         ╲ ────────▶│ Remove   │
                    ╲  verification      ╱           │ the data │
                       ╲───────────────╱             └──────────┘
                              │ Yes                       │
                              ▼                            ▼
              ┌──────────────────────────┐         ┌──────────────┐
              │ Sting synchronization is │         │ Report false │
              │ achieved                 │         │ data bits    │
              └──────────────────────────┘         └──────────────┘
                              │                            │
                              ▼                            │
                          ┌───────┐  ◀────────────────────┘
                          │  End  │
                          └───────┘
```

Figure 5-2 GLONASS navigation string synchronization algorithm

5.3.3 Navigation message decoding

After string synchronization, the data bits are stored in 85-bit strings. To extract the navigation data bits, it is necessary to find the first string in a frame. There are 15 strings in a frame and the number of each string is included within the data. Specifically, the string number is stored in data bit numbers 84, 83, 82, and 81 as illustrated in Figure 5-3.

Idle	String number				Ephemeris or part of almanac			Check bits								Time mark
85	84	83	82	81	80	…	9	8	7	6	5	4	3	2	1	

Figure 5-3 General view of a string structure

When the beginning of the frame is found (string number one), the other 14 strings in the frame are recognized. Then, the ephemeris information for the current satellite can be extracted from the strings. Moreover, in each frame a part of the almanac data is received (section 2.6.4). From the first four strings of a frame, all of the ephemeris data can be extracted. Strings six to 15 contain a part of the almanac for the current GLONASS constellation. With this method, the necessary information is extracted from the received navigation message.

5.4 Verification

To verify the GLONASS L1 and GLONASS L2 software receiver, from the acquisition process to the navigation solution, an experiment was performed. In this experiment, the GLONASS software receiver is compared to a commercial hardware receiver.

5.4.1 Experiment set-up

An experiment was set up on 7th of September 2008 for ten minutes to verify the GLONASS L1 and GLONASS L2 software receiver. The block diagram of this experiment is shown in Figure 5-4. In this experiment, the navigation solution from the GLONASS software receiver is compared to the navigation solution from a commercial receiver. The commercial receiver used for this purpose is a NovAtel™ OEMV-2 receiver.
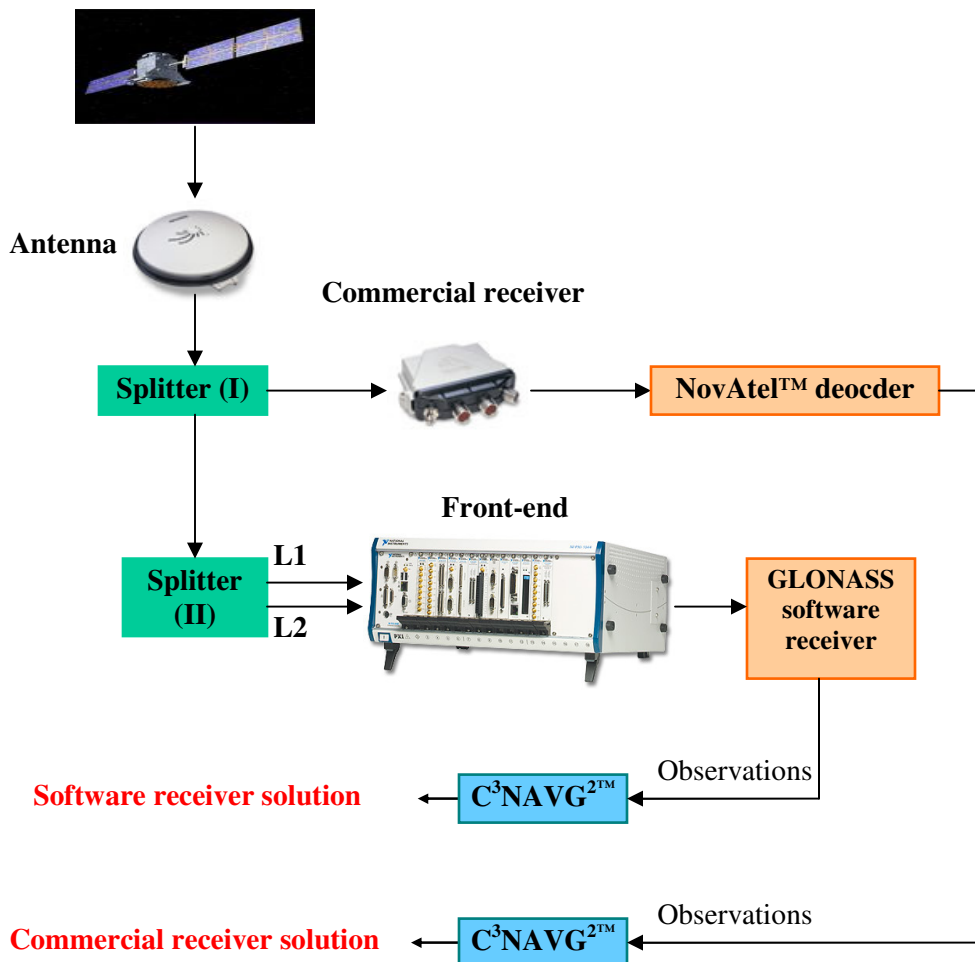
Figure 5-4 Experiment set-up for verification

The received signal from the antenna is sent to the splitter (I). One of the signals from the splitter is sent to the NovAtel™ receiver which was configured to log the raw measurement data. The other signal from the splitter is sent to yet another splitter (splitter II). The outputs of the second splitter are defined as L1 and L2 and sent to different RF input on the front-end.

In this experiment, raw measurement data is collected from the NovAtel™ receiver and sent to some NovAtel™ decoder software which is capable of generating GLONASS ephemeris and observation files in post-mission. The ephemeris file contains ephemeris information for all GLONASS satellites. The observation file contains pseudorange, carrier phase and Doppler frequency for L1 and L2 signals. These two files are fed into a software package called C^3NAVG^2™. This software was developed in the Position, Location And Navigation (PLAN) group at the department of Geomatics Engineering. C^3NAVG^2™ is a C program that processes GPS and/or GLONASS pseudorange data in both static and kinematic modes. One of the outputs of this software is the position of the antenna at each epoch. In this way, the position of the antenna determined by the commercial receiver is calculated.

In parallel with the NovAtel™ data collection, the GLONASS L1 and L2 samples were logged from the front-end. These samples were then processed by the GLONASS software receiver (GSNRx™) developed as part of this thesis.

5.4.2 Acquisition and tracking

Table 5-2 shows the GLONASS satellites available during the experiment and indicates whether their L1 and L2 signals were able to be acquired. Although the L1 signal of the satellite at orbital slot seven was acquired, the L2 signal for this satellite was not acquired. This satellite was at low elevation angle and the received signals are weaker for L2 than for L1 (see section 2.5.5). As such, L2 signal could not be acquired.

The acquisition method is the same as the method explained in section 3.4.

Table 5-2 Acquired GLONASS signals for 07 Sep 2008 data set

Orbital slot	Channel No	L1 acquired	L2 acquired
R07	05	Yes	No
R13	-2	Yes	Yes
R15	0	Yes	Yes
R23	03	Yes	Yes
R24	02	Yes	Yes

Using the initial tracking information (Doppler frequency and code offset) from the acquisition process, the tracking process was performed on the acquired signals.

5.4.3 Navigation data extraction

After successful tracking of the GLONASS signals, the navigation message was extracted from the received signal by the method explained in section 5.3.

Table 5-3 compares some of the ephemeris values for the GLONASS satellite at orbital slot 13. In GSNRx™ column, the ephemeris values extracted from the navigation message by the GLONASS software receiver (using the method described in this Chapter) are presented. In the NovAtel™ column, the ephemeris from the commercial receiver is presented. It is seen that the ephemeris values are the same for NovAtel™ and GSNRx™ receivers. This verifies that the proposed method for GLONASS navigation message decoding is working properly.

In Table 5-3, only a few of the ephemeris values are presented just as examples.

γ_n is the relative deviation of predicted carrier frequency value of nth satellite from the nominal value. τ_n is the correction to the nth satellite time relative to GLONASS time (GLONASS ICD 2002).

Table 5-3 Ephemeris comparison between NovAtel™ and GSNRx™ receiver

Ephemeris		GLONASS satellite at orbital slot # 13 / CH #-2	
		GSNRx™	NovAtel™
Satellite position (Km)	X	-1.519170e+004	-1.519170e+004
	Y	-2.045196e+004	-2.045196e+004
	Z	1.028575e+003	1.028575e+003
Satellite velocity (Km/s)	$\dot{X}$	-2.270088e-001	-2.270088e-001
	$\dot{Y}$	-1.514530e-002	-1.514530e-002
	$\dot{Z}$	-3.574990e+000	-3.574990e+000
Satellite acceleration (Km/s^2)	$\ddot{X}$	0.000000e+000	0.000000e+000
	$\ddot{Y}$	-9.313226e-010	-9.313226e-010
	$\ddot{Z}$	-1.862645e-009	-1.862645e-009
γ_n		-9.094947e-013	-9.094947e-13
τ_n		2.105907e-004	2.105907e-004

5.4.4 Results

The ephemeris data, as well as the observation data generated from the GLONASS software receiver, is processed using C^3NAVG^2™. In this way, the position of the antenna determined by the GLONASS software receiver is calculated and can be directly (and fairly) compared with the results from the NovAtel™ receiver.

Table 5-4 compares the root mean square (RMS) L1-only position error for GSNRx™ and NovAtel™ solutions obtained using five GLONASS satellites. The GSNRx™ solution is very similar to the NovAtel™ solution and at the level expected of a single point receiver. A part of their difference is related to the splitter (II) which attenuates the

signal processed by GSNRx™ be an additional 3 dB (relative to the NovAtel receiver). However, this is amplifier contained in the antenna (23 dB gain) should limit the difference in power to below this level. This confirms that the software receiver appears to be working well. Figure 5-5 illustrates the position error comparison between GSNRx™ (L1) solution and NovAtel™ (L1) solution. The large error in some epochs is related to the rejection of a weak GLONASS satellite in C^3NAVG^2™ program. It is also noted that the NovAtel solution is much smoother than that from GSNRx™. This is likely due to the fact that the NovAtel receiver uses narrower correlator spacing (relative to GSNRx™) and thus will inherently provide better multipath mitigation.
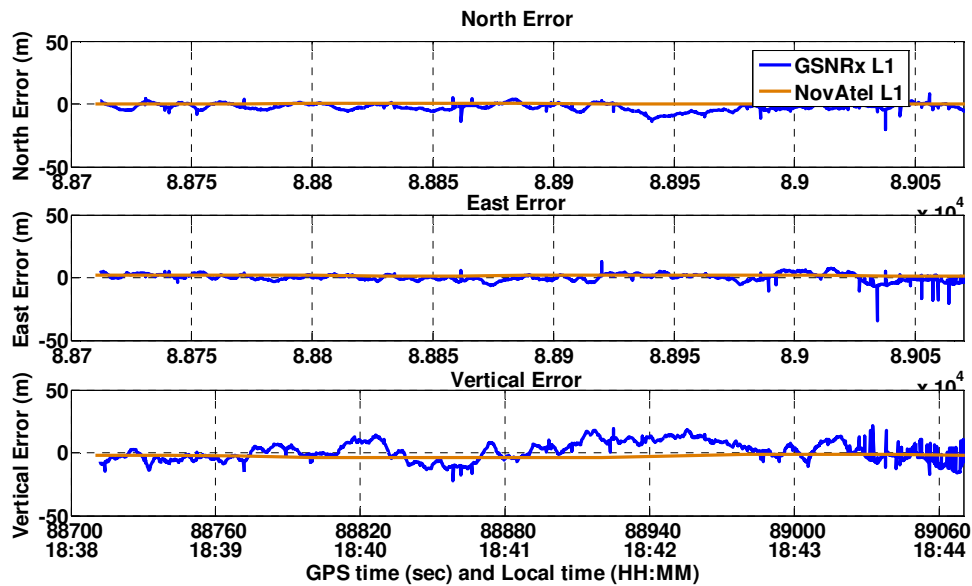
Figure 5-5 Position error comparison of GSNRx™ (L1) and NovAtel™ (L1)

Table 5-4 Root Means Square (RMS) position errors for GSNRx™ and NovAtel™

Solution	North	East	Vertical
GSNRx™ (L1)	2.1 m	2.8 m	7.5 m
NovAtel™ (L1)	0.5 m	1.7 m	2.8 m

Moreover, the position solution results for L1 and L2 from GSNRx™ are shown in Figure 5-6. The same satellites are tracked in both cases in order to remove any effect due to different satellite geometry.
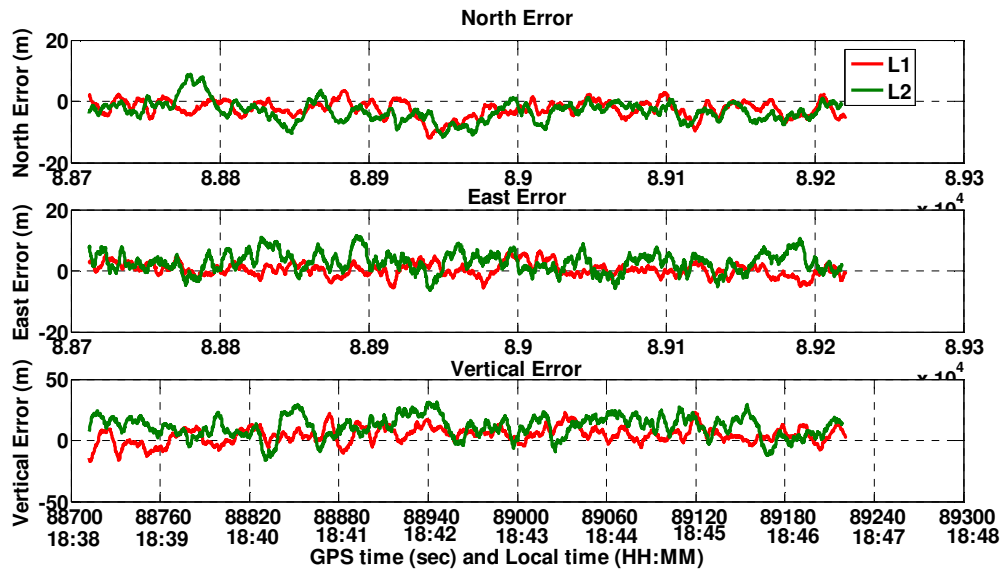
Figure 5-6 Position error comparison of L1 and L2 computed using GSNRx™

Table 5-5 compares the root mean square (RMS) value of the position error for L1-only and L2-only solutions. This table shows that the RMS position errors for L1-only and L2-only solutions are approximately the same which is expected under calm ionospheric condition which was present during the test. For these solutions, only the four satellites for which the L2 data is available are used (even for L1 solution) in order to avoid effects

due to different satellite geometry. Given the above, the small differences in the L1-only solution in table Table 5-4 are expected. Referring to Table 5-2, L2 signal for one GLONASS satellite (at orbital slot 07) could not be acquired. The considerable difference in vertical error is related to the one satellite signal which was rejected in some epochs during the processing of L2 solution.

Table 5-5 Root Means Square (RMS) position errors for L1 and L2 solution

Solution	North	East	Vertical
GSNRx™ (L1)	3.6 m	2.2 m	7.8 m
GSNRx™ (L2)	4.6 m	4.2 m	14.2 m

5.5 Ionosphere-free navigation solution

The ionized gas molecules in the ionosphere have a dispersive effect on radio frequency signals including GNSS signals (Misra & Enge 2001). GNSS signal pseudorange can be delayed by ionosphere from 1 m to 100 m depending on the density of free electrons (Cannon 2007). As such, ionosphere effect as a source of error on the navigation solution must be removed or at least be mitigated. One method to mitigate the ionosphere error is using the dual frequency data. In this case, the pseudorange measurement is generated from L1 and L2 signals and then ionosphere-free pseudorange is calculated using the following equation:

$$P_{IonF} = \frac{f_{L1}^2}{f_{L1}^2 - f_{L2}^2} \times P_{L1} - \frac{f_{L2}^2}{f_{L1}^2 - f_{L2}^2} \times P_{L2} \qquad 5\text{-}14$$

where,

- P_{L1} represents L1 pseudorange,

- P_{L2} represents L2 pseudorange,

- f_{L1} represents the frequency of L1 signal,

- f_{L2} represents the frequency of L2 signal, and

- IonF subscript stands for ionosphere-free

Using the above approach, the ionosphere-free pseudorange (P_{IonF}) data was then input into C^3NAVG^{2TM} to see if any improvement in positioning accuracy could be obtained. Figure 5-7 compares the positioning error from L1 and ionosphere-free solution.
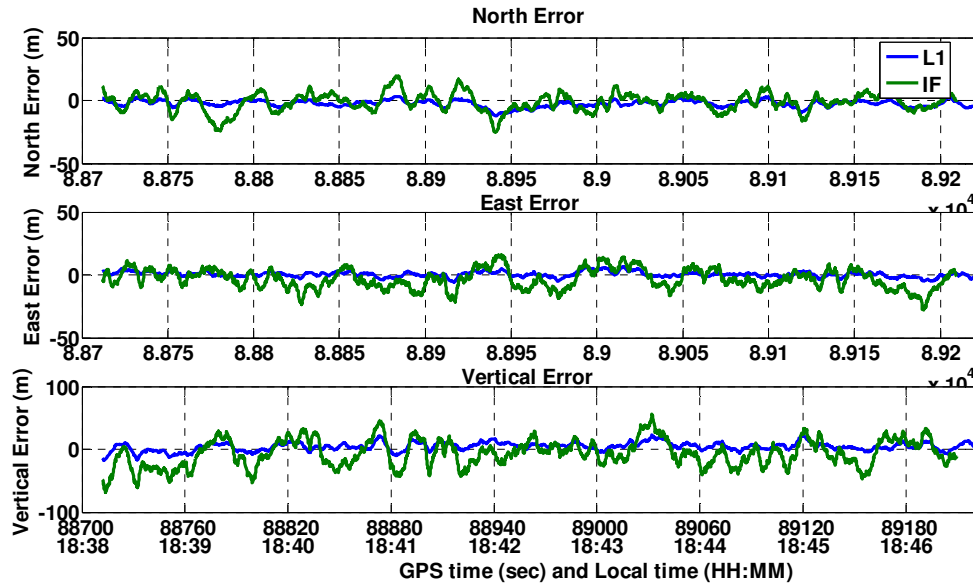

Figure 5-7 L1 and ionosphere-free positioning comparison

In ionosphere-free solution, although the ionosphere error is mitigated, errors due to multipath and noise (i.e., stochastic errors) are increased according to the following equation (Misra & Enge 2001):

$$\sigma_{IonF}^2 = (2.531)^2 . \sigma_{L1}^2 + (1.531)^2 . \sigma_{L2}^2 \qquad \text{5-15}$$

where, σ_{L1} and σ_{L2} are the stochastic errors on L1 and L2 pseudoranges respectively and σ_{IonF} is the corresponding value for the ionosphere-free pseudorange. As such, assuming the same error on L1 and L2 (for simplicity), ionosphere-free pseudorange is approximately three times nosier than L1 pseudorange as it is seen in Figure 5-7.

Table 5-6 compares the mean, root mean square (RMS), and standard deviation (STD) of the positioning error for L1 and ionosphere-free solutions.

Table 5-6 Mean, RMS, and STD of the positioning errors for L1 and ionosphere-free solution

Solution	Mean (m)			Root mean square (m)			Standard deviation (m)		
	North	East	Vertical	North	East	Vertical	North	East	Vertical
L1	-2.5	0.5	4.4	3.6	2.2	7.8	2.6	2.1	6.4
IonF	-1.1	-3.1	-6.1	7.3	8.3	22	7.2	7.7	21.3

In ionosphere-free solution, the large error on vertical direction is caused by the vertical error on L2 solution (see Table 5-5). The deviation of the positioning error from the mean value for ionosphere-free solution is more than L1 solution and is caused by the increased noise generated during ionosphere error mitigation. On the other hand, the inter-frequency biases are a possible source of additional error in the IonF case.

In conclusion, there is a trade-off between noise error and ionosphere error. In calm ionosphere conditions (such as in the current experiment), stochastic errors make the ionosphere-free solution worse.

CHAPTER SIX: GLONASS+GPS SOFTWARE RECEIVER

6.1 Chapter outline

The objective of this Chapter is to present a software receiver capable of simultaneously tracking GPS L1, GLONASS L1 and GLONASS L2 signals (herein termed a "combined software receiver") and providing navigation solution. To begin, there is a brief discussion on the differences and similarities of GPS and GLONASS systems. The Chapter continues with the explanation of the required modifications in GSNRx™. The Chapter concludes some results from the combined software receiver compared with the results from single (GPS alone, GLONASS L1 alone and GLONASS L2 alone) software receivers. At the end of the Chapter, positioning for the combined software receiver is presented and compared to the single systems.

For simplicity, the term "GPS" is used instead of "GPS L1" throughout the Chapter.

6.2 Differences and similarities of GPS and GLONASS

As discussed in Chapter one, the GLONASS system can be used to augment GPS system. With the recent revitalization of GLONASS (constellation status shown in Figure 2-1), the combination of GPS and GLONASS helps achieving more reliable and accurate navigation solutions. Combination of GLONASS L1 and GLONASS L2 helps reducing

the effect of ionosphere error. Furthermore, those interference signals which affect GLONASS L1 may not affect GLONASS L2. As such, GPS, GLONASS L1 and GLONASS L2 combination is an excellent method for achieving the most accurate and reliable navigation solution at this time. Table 6-1 compares relevant parameters between GPS and GLONASS systems.

Table 6-1 GPS and GLONASS comparison

	GPS (nominal constellation)		GLONASS (nominal constellation)	
Number of satellites	24		24	
Number of orbital planes	6		3	
Orbital inclination	55°		64.8°	
Orbital altitude	20,200 km		19,100 km	
Time reference	GPS time		UTC(SU)	
Coordination Reference	WGS-84		PZ-90.02	
Period of revolution	11 h 58 m		11 h 15 m	
Navigation message	Super-frame	12.5 minutes	Super-frame	2.5 minutes
	Page	30 s	Frame	30 s
	Sub-frame	6 s	String	2 s
	Word	600 ms		
Multiplexing	CDMA		FDMA	
RF Signals	L1	1.57542 GHz	L1	1.602 GHz $+K\Delta f_1$
	L2	1.2276 GHz	L2	1.246 GHz $+ K\Delta f_2$
	L5	1.17645 GHz	L3	L1×(3/4)

Ranging code type	Gold Code	M-Length
Civilian ranging code rate	1.023 MHz	0.511 MHz
Civilian ranging code length	1023 bits	511 bits
Civilian ranging code repeat rate	1 ms	1ms

6.3 GPS, GLONASS L1, and GLONASS L2 combination in GSNRx™

At first step, to discriminate between GPS, GLONASS L1 and GLONASS L2 in the combined software receiver, a PRN number is assigned to each signal according to Table 6-2. Moreover, Table 6-3 presents the PRN numbers assigned to each GLONASS satellite according to the orbital slot and channel number.

For the combined software receiver verification, the data collected on 10th of October 2008 is used (see section 3.5). GPS, GLONASS L1 and GLONASS L2 signals are acquired with the method discussed in section 3.4. With this method, 10 GPS, six GLONASS L1 and five GLONASS L2 signals are acquired. The outputs of this acquisition process are summarized in Table 6-4.

Table 6-2 PRN numbers assigned to GPS, GLONASS L1 and GLONASS L2

GNSS	PRN number
GPS	1 to 32
GLONASS L1	33 to 56
GLONASS L2	57 to 80

Table 6-3 PRN numbers assigned to GLONASS L1 and GLONASS L2

Orbital slot	Channel number	PRN number for GLONASS L1	PRN number for GLONASS L2
1	07	33	57
2	…	34	58
3	…	35	59
4	06	36	60
5	…	37	61
6	01	38	61
7	05	39	63
8	06	40	64
9	-2	41	65
10	04	42	66
11	00	43	67
12	…	44	68
13	-2	45	69
14	04	46	70
15	00	47	71
16	…	48	72
17	-1	49	73
18	…	50	74
19	03	51	75
20	02	52	76
21	…	53	77
22	…	54	78
23	03	55	79
24	02	56	80

Table 6-4 Code offset and carrier Doppler from acquisition process

	PRN number	Code offset (Chip)	Carrier Doppler(Hz)
GPS	2	812.2	3825
	4	68.1	3025
	5	23	3625
	9	627.8	825
	11	408.13	-3475
	12	923.73	3125
	17	871.1	-1125
	20	752.84	1575
	28	536.95	-2525
	32	40.42	575
GLONASS L1	45	79.83	-4325
	47	167.32	2925
	49	87.27	3425
	55	441.34	-3025
	39	441.34	3075
	56	508.62	775
GLONASS L2	69	79.80	-3375
	71	167.28	2375
	73	87.27	2775
	79	441.34	-2375
	80	508.67	575

To track GPS, GLONASS L1, and GLONASS L2 signals in the combined software receiver, several changes in the GSNRx™ structure/setup had to be made. The major changes are listed below:

1. Input samples: the software must be able to read real samples from three input files, namely one for GPS, one for GLONASS L1 and one for GLONASS L2.

2. Intermediate frequency: GPS intermediate frequency is different from GLONASS intermediate frequency. As such, according to the PRN number, the correct intermediate frequency must be generated within the software. For GPS, the intermediate frequency is 4.42 MHz and for GLONASS is 4 MHz.

3. Maximum coherent integration time: This value can be extended to 20 ms for GPS and to 10 ms for GLONASS because the received GLONASS navigation data bit is 10 ms.

4. PRN number: presented in Table 6-2, the PRN numbers should be different for GPS, GLONASS L1 and GLONASS L2.

5. Ranging code: the software must be capable of generating both the GPS and GLONASS standard ranging codes, as appropriate, for the satellite signal being tracked.

6. Bit synchronization: referring to section 5.3.1, one GLONASS navigation data bit is divided into 10 1-ms bins for bit synchronization; however a GPS navigation data bit is divided into 20 1-ms bins. This difference must be considered in the software for bit synchronization.

Initial tracking information (initial carrier Doppler and initial code offset) are fed into the software with an option file as explained in section 4.8.2. Other parameters not listed above remain the same for both GPS and GLONASS. For example, the sample rate is

12.5 MSps for GPS, GLONASS L1 and GLONASS L2. Also, the selected tracking loop bandwidths are the same.

The main difference between GLONASS L1 and GLONASS L2 is the final intermediate frequency. It means that 4 MHz intermediate frequency is, in fact, the centre frequency. The final intermediate frequency is generated according to the channel number of each acquired GLONASS signal as follows:

$$\text{Final intermediate frequency for GLONASS} = 4 \text{ MHz} + K \times \Delta f_{1 or 2}$$

where K is the channel number and Δf is different for GLONASS L1 and GLONASS L2 signals (section 2.5.1).

Some of the tracking results are presented in the next section.

6.4 Tracking results

The combined software receiver is capable of tracking GPS, GLONASS L1 and GLONASS L2 satellites using the initial tracking information presented in Table 6-4.

In this section C/N_0 estimation, FLI and PLI results are presented for a single software receiver and the combined software receiver for GPS, GLONASS L1 and GLONASS L2 signals.

6.4.1 C/N$_0$ estimation

The method to estimate C/N$_0$ in the combined software receiver is the same method described in section 4.9.3 for the single software receiver.

The C/N$_0$ for all tracked GPS, GLONASS L1 and GLONASS L2 signals are presented in Figure 6-1. As it is shown, PRN number 9, 17 and 56 have higher C/N$_0$ values on average than the other satellites. PRN number 9 and 17 are related to GPS satellites and PRN number 56 is related to the L1 signal of a GLONASS satellite. None of the GLONASS L2 signals have such a high C/N$_0$ value because GLONASS L2 signals are expected to be weaker compared with GPS and GLONASS L1 (see section 2.5.5).
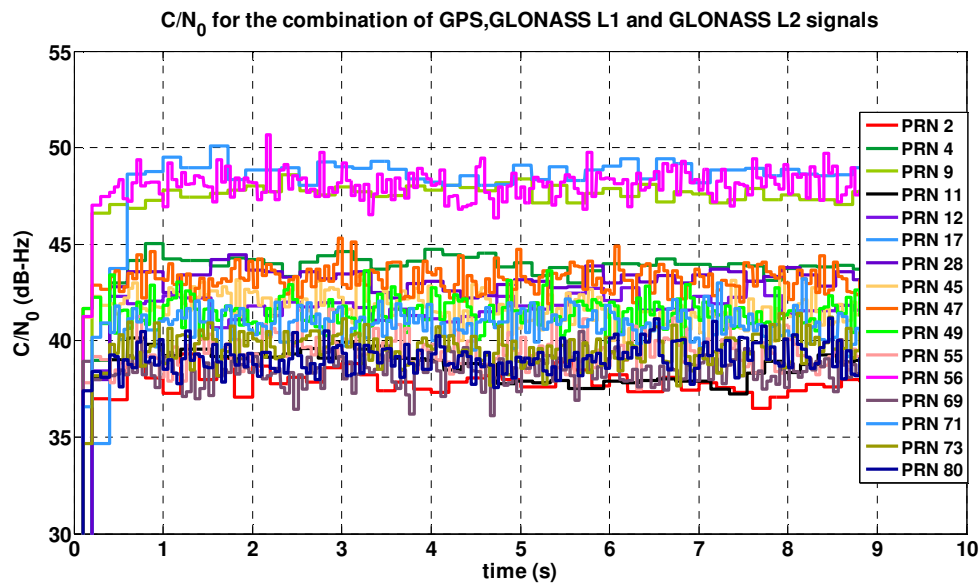

Figure 6-1 C/N$_0$ in combined software receiver for all the GPS, GLONASS L1 and GLONASS L2 signals being tracked

Table 6-5 compares the average value of C/N_0 for GPS, GLONASS L1 and GLONASS L2 signals. GLONASS L2 signals have lowest average C/N_0 in comparison with L1 signal from the same satellite. The highest average C/N_0 belongs to the L1 signal received from GPS satellite with PRN number 17 with the value of 47.6 dB-Hz. These average values are calculated over 10 seconds. Those satellites that are acquired and presented in Table 6-4 but whose C/N_0 values are not presented in Table 6-5 have lost the lock during the tracking process and the software was not able to re-establish the lock. They are mostly those satellite below 10° elevation angle.

Table 6-5 Average C/N_0 for GPS, GLONASS L1 and GLONASS L2

	PRN	Average C/N_0 (dB-Hz)
GPS	2	37.34
	4	43
	9	46.7
	11	38
	12	38
	17	47.6
	28	42.4
GLONASS L1	45	41.4
	47	42.8
	49	41.2
	55	39
	56	46.6
GLONASS L2	69	38.1
	71	40.4
	73	39.3
	80	39

To confirm that the combined receiver is working well, Figure 6-2 shows the C/N_0 for the combined receiver for three signals (GPS, GLONASS L1 and GLONASS L2) and Figure

6-3 shows the same values obtained by tracking each signal in a separate receiver. As can be seen, the results are the same.

6.4.2 PLI and FLI

Referred to sections 4.9.4 and 4.9.5, FLI and PLI are two indicators which have a key role in switching from one tracking status to the other. As such, these two values are checked regularly in the software.

Figure 6-4, Figure 6-5, and Figure 6-6 present some results for PLI and FLI for GPS, GLONASS L1 and GLONASS L2 signal tracked by the single software receiver and the combined software receiver. The figures show that in both software receivers these values have the same results. Therefore, FLI and PLI are working well in the combined software receiver for GPS, GLONASS L1 and GLONASS L2 signals.

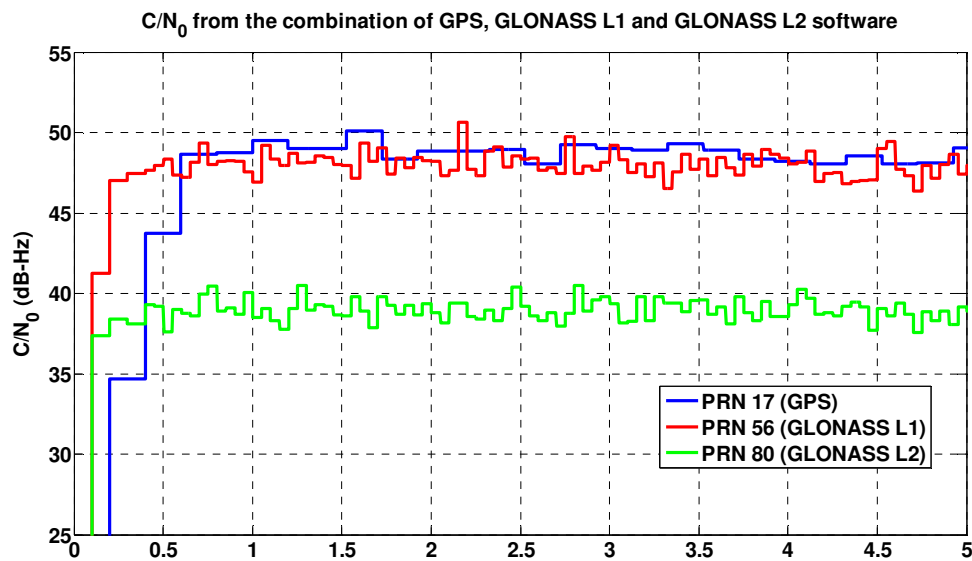**Figure 6-2 C/N$_0$ in combined software receiver**

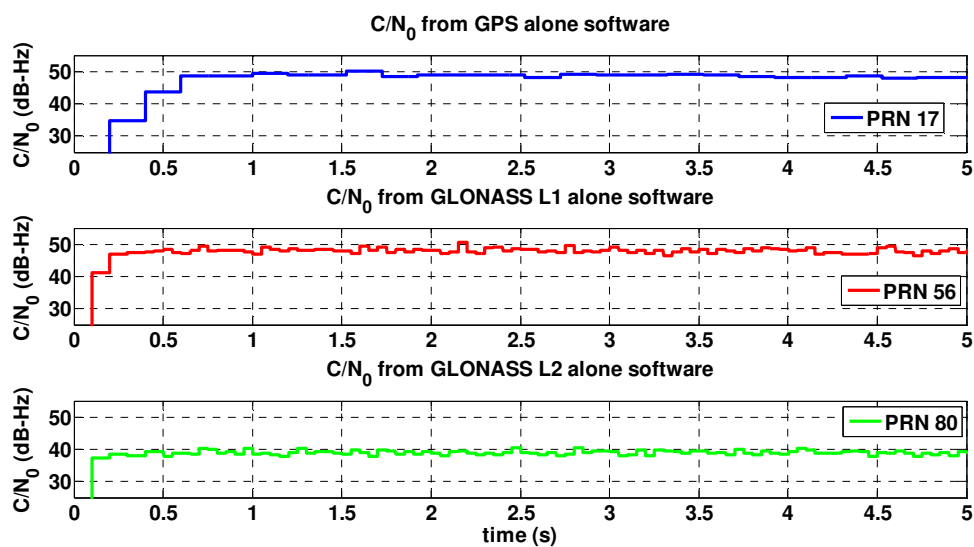**Figure 6-3 C/N$_0$ from GPS alone, GLONASS L1 alone and GLONASS L2 alone software receivers**
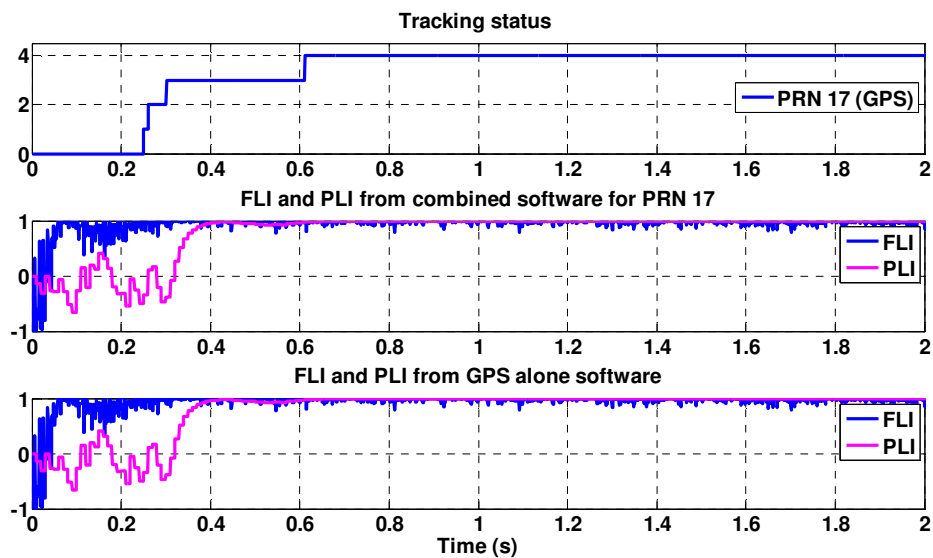

Figure 6-4 PLI and FLI for GPS signal tracked in the combined and single software receiver
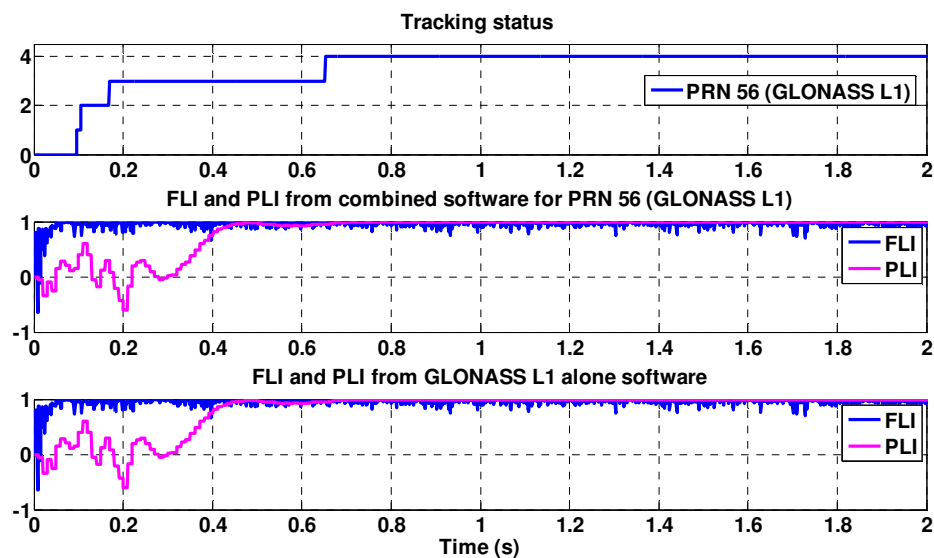
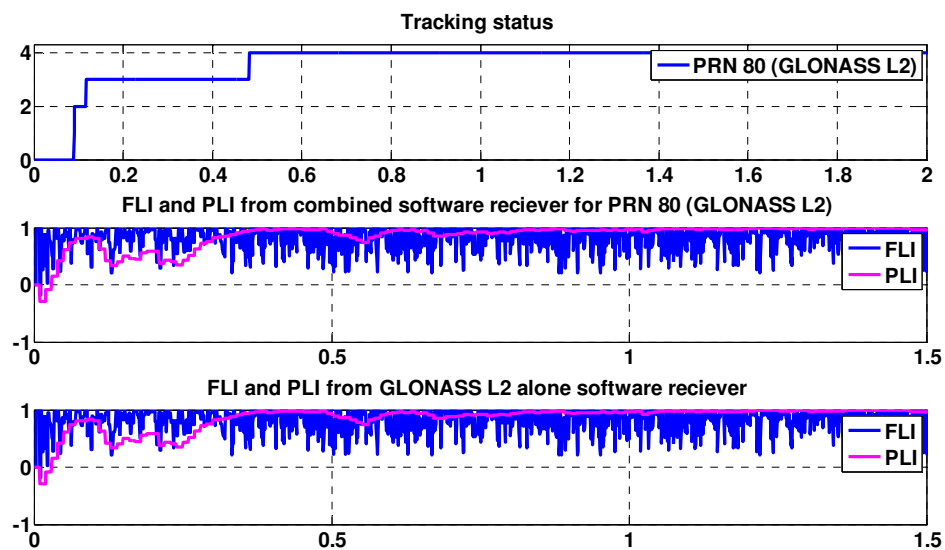**Figure 6-5 PLI and FLI for GLONASS L1 signal tracked in the combined and single software receiver**

Figure 6-6 PLI and FLI for GLONASS L2 signal tracked in the combined and single software receiver

The results presented above verify that the combined software receiver is working properly in case of tracking GPS, GLONASS L1 and GLONASS L2 signals when the samples are fed into the combined software receiver simultaneously. This is the essential step in developing a version of GSNRx™ which can generate navigation solution using GLONASS L1 and GPS L1 signals.

6.5 Navigation solution

The observations output from the combined software receiver were utilized to generate a navigation solution. Similar to the method explained in section 5.4.1, the C^3NAVG^2™ program accepts observation and ephemeris files and outputs navigation solution. The solution can be based on GPS alone, GLONASS alone, or on both GPS and GLONASS. Figure 6-7 illustrates the method which was used to generate navigation solution from the combined software receiver. The method to achieve observation and ephemeris data are explained in the next sections.
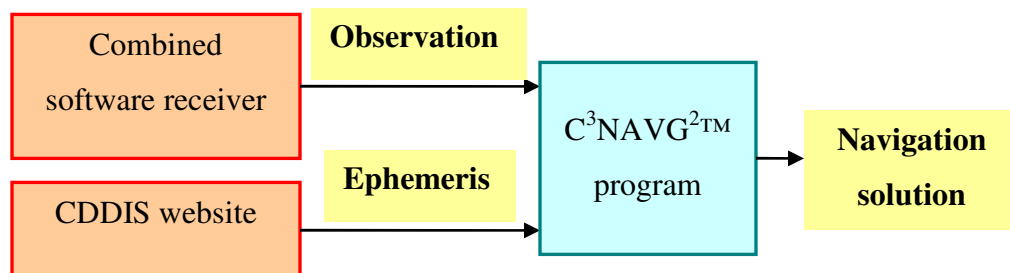
Figure 6-7 Navigation solution generation from the combined software receiver

6.5.1 Observations

The combined software receiver can generate the observation for both GPS and GLONASS L1 and if necessary GLONASS L2. For the purpose of this section, only the observation from GPS and GLONASS L1 are generated. In case of simplicity, the term "GLONASS" is used instead of "GLONASS L1" from now on. The main concern in generation of the observations for the combined GPS and GLONASS is the time difference between GPS and GLONASS system (see section 2.7).

6.5.2 Ephemeris

Although GLONASS ephemeris can be extracted from the navigation message using the algorithm explained in section 5.3.3, for the sake of simplicity, the ephemeris data for GLONASS L1 and GPS L1 signals on 10th of October 2008 was acquired separately from the NASA's Archive of Geodesy Data (CDDIS 2008) website. After being unzipped and conversion from RINEX format, GPS and GLONASS ephemeris were combined in a single file and fed into the C^3NAVG^2™.

6.5.3 Results

Positioning results from the combined software receiver is compared to the positioning results from a GPS alone and GLONASS alone software receiver in Figure 6-8.
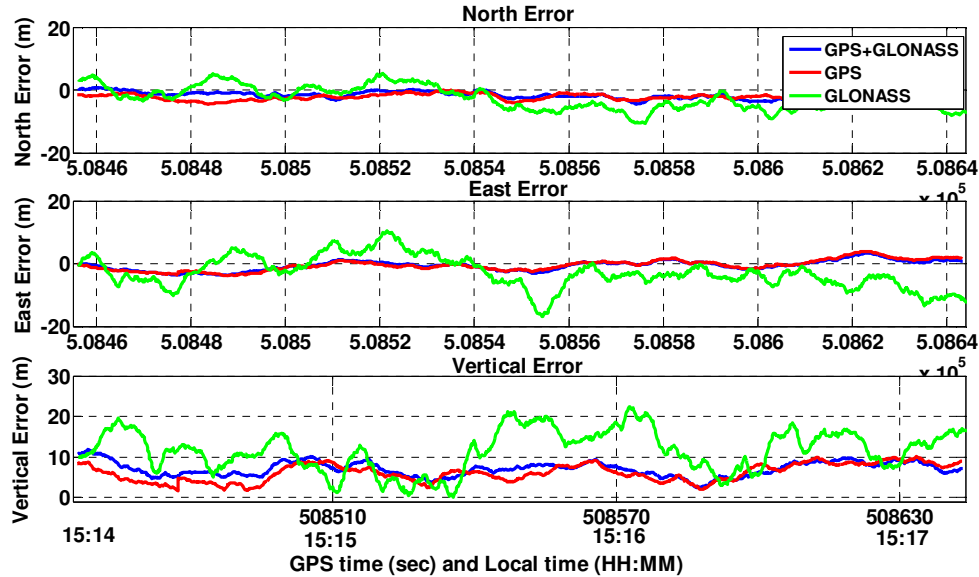
Figure 6-8 Positioning error for GPS, GLONASS and GPS+GLONASS

According to the figure, the combination of GPS and GLONASS solution shows similar result to the GPS alone solution. In the combined solution, seven GPS and five GLONASS satellites are involved. On the other hand, in the C^3NAVG^2™ program, GPS and GLONASS are weighted differently and more weight is on GPS (pseudorange noise assumed to be 2 m for GPS and 4 m for GLONASS). As such, it is expected that the combined solution will closely approximate the GPS alone results. The positioning result for GLONASS alone solution is far from the other two GPS alone and GPS plus GLONASS solutions.

Table 6-6 compares the root mean square (RMS) values of the position error for GPS alone, GLONASS alone and GPS plus GLONASS solutions.

Table 6-6 RMS value of the position error

Solution	North error (m)	East error (m)	Height error (m)
GPS + GLONASS	1.8	1.6	7.2
GPS	2.3	1.8	6.5
GLONASS	4.2	5.7	12.5

According to the table, the RMS value for the north and east error is the least for the combined GPS and GLONASS solution. However, GPS alone solution has the least RMS value of the height error. Totally, there is not that much difference between GPS alone and GPS plus GLONASS solution, as discussed above. The GLONASS alone solution has the worst positioning and is related to the low number of satellites. In addition, these statistics are computed over only a few minutes (~3 minutes) and could therefore exhibit short term biases that would be averaged out over longer periods. It is expected therefore, that the results will be different if considerably longer data sets are considered (e.g., one day or more), where the short term variations in the measurement errors and satellite geometry are averaged out. It is also noted that the GPS solution is better than GLONASS solution because there are more GPS satellites than GLONASS (seven GPS and five GLONASS). To show the geometry of the these three solutions, HDOP and VDOP of GPS+GLONASS, GPS only and GLONASS only solutions are presented in Figure 6-9 and Figure 6-10. It is shown that because of the low number of GLONASS satellites involved in the solution; both VDOP and HDOP of GLONASS only solution are considerably higher than other two solutions. On the other hand, when GLONASS and GPS are combined, the VDOP and HDOP of the combined solution decrease. The

steps of changes in DOP values are related to the increase in the number of the satellites

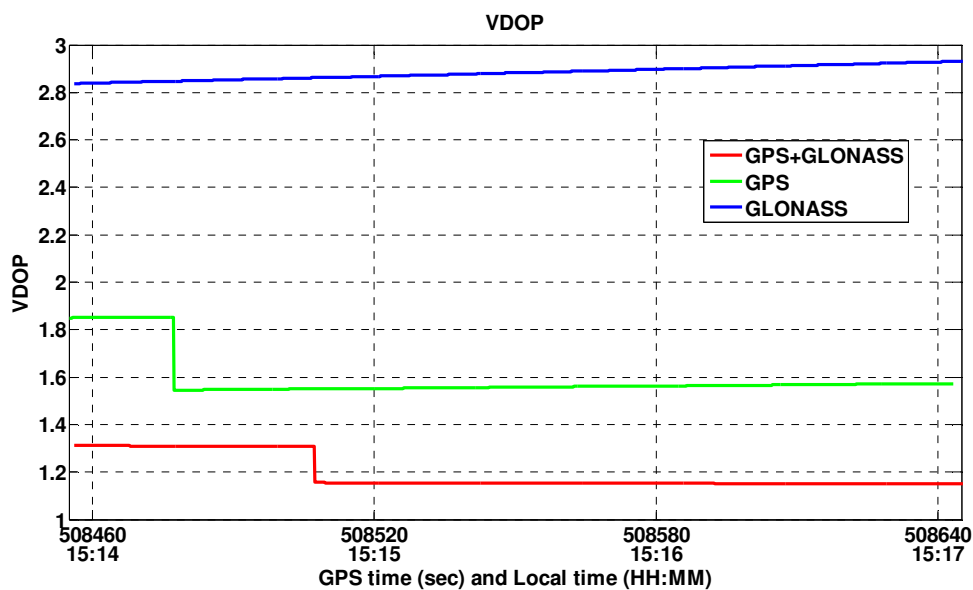involved in the solution.

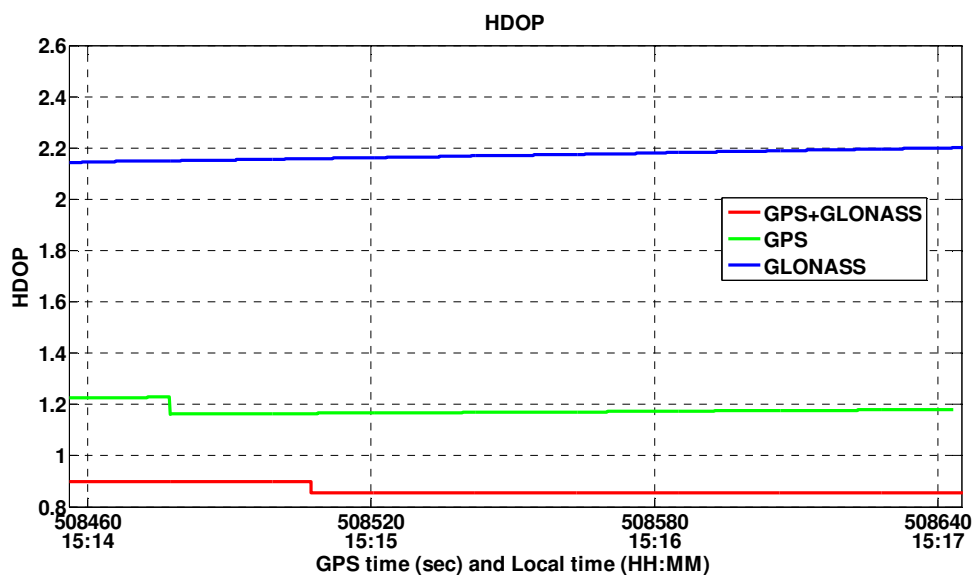**Figure 6-9 VDOP of GPS+GLONASS, GPS only and GLONASS only solutions**

Figure 6-10 HDOP of GPS+GLONASS, GPS only and GLONASS only solutions

Finally, with 20 GLONASS satellites in the constellation in February 2009, more GLONASS signals can be acquired, tracked and utilized in navigation solution and better results are predicted.

CHAPTER SEVEN: SUMMARY, CONCLUSION, AND RECOMMENDATIONS

7.1 Chapter outline

In this Chapter, the research presented throughout this thesis is summarized. The conclusions of this research are presented and possible future work in this field of research is recommended.

7.2 Summary

At the beginning, the GLONASS L1, GLONASS L2 and GPS L1 samples were collected using three channels of an RF front-end on 10th of October 2008. The antenna used for this purpose is capable of receiving GPS L1/L2 and GLONASS L1/L2 signals.

The collected samples were acquired using software implemented in Matlab™. This software was utilized to acquire GPS L1, GLONASS L1 and GLONASS L2 signals. With the mentioned data set, 10 GPS, six GLONASS L1 and five GLONASS L2 signals were acquired. Through the acquisition process, the initial tracking information including initial carrier Doppler frequency and ranging code offset for all the acquired signals were extracted.

After implementing required modifications in GSNRx™, the software was made able to track GLONASS L1 and GLONASS L2 signals for as many channels as possible. Acceptable tracking results showed that tracking process has been accomplished successfully. Moreover, this software was modified in a way that is capable of decoding GLONASS L1 and GLOANSS L2 navigation message. To verify the GLONASS software receiver, the navigation solution from this software was compared with the navigation solution from a commercial receiver. Comparison between the navigation solutions of the software receiver and the commercial receiver confirmed that the GLONASS software receiver was working properly. In addition, tracking both L1 and L2 GLONASS signals allowed for the removal of the effect of ionosphere error.

Considering the differences and similarities of GPS and GLONASS systems in addition to GLONASS L1 and GLONASS L2 signals, necessary modifications was implemented in the software receiver to provide a GPS plus GLONASS software receiver. The combined (GPS L1 + GLONASS L1 + GLONASS L2) version of the GSNRx™ is capable of reading three files containing GPS L1, GLONASS L1 and GLONASS L2 samples, tracking their signals and providing navigation solution.

7.3 Conclusion

Some of the conclusions from this research are presented here:

1. The FFT acquisition algorithm which is commonly used for GPS could also be used for GLONASS by modification of the relevant parameters. FFT method is capable of detecting weak signals which is proper for GLONASS L2 signals but

still is relatively slow in terms of computation. All the GLONASS signals from healthy satellites visible during the data collection were acquired by this method.

2. The tracking algorithm applied to GPS signal is applicable to GLONASS L1 and GLONASS L2 signals as well after updating relevant parameters. The promising results from Doppler frequency, correlator outputs, C/N_0 values, FLI and PLI for both GLONASS L1 and L2 signals confirmed that the tracking process is working properly for all the acquired GLONASS L1 and GLONASS L2 signals.

3. A new algorithm (relative to GPS) for decoding GLONASS navigation message was developed because GPS navigation message structure is completely different from GLONASS navigation message structure. Following the implementation, the algorithm was verified by comparing the extracted ephemeris information with the extracted ephemeris from a commercial receiver.

4. The GLONASS L1-only software receiver is working well. This is confirmed by comparing the navigation solution from the GLONASS L1-only solution of the software receiver (GSNRx™) with the navigation solution from NovAtel™ receiver. With a small difference in the RMS value of the positioning error, both solutions showed similar results in case of north, east and height errors.

5. The GLONASS L2-only software receiver is working well. This is confirmed by comparing the navigation solution from the GLONASS L1-only and GLONASS L2-only solutions of GSNRx™. There is a small difference in case of north and east positioning error but a considerable difference in vertical error which is related to the rejections of one of the GLONASS L2 signals in some epochs of L2 solution processing.

6. Taking the advantage of receiving civilian navigation message on GLONASS L2 signal from GLONASS satellites type M facilitates mitigation of the ionosphere effect on pseudorange. By implementing ionosphere removal algorithm on the pseudorange, although the ionosphere error is mitigated, the stochastic errors increase. As such, the positioning error from the ionosphere-free solution became worse than the positioning error from L1-only solution. Therefore, there is a compromise between mitigation of the ionosphere error and increasing stochastic errors.

7. For a combined GPS and GLONASS software receiver, the similarities of these two systems helps in tracking the signals and providing navigation solution; however, the differences must be considered and applied to the software. The performance of the combined software receiver tracking is checked by comparing the tracking results of the GPS, GLONASS L1 and GLONASS L2 from the combined software receiver with the tracking results of GPS-only, GLONASS L1-only and GLONASS L2-only. The results confirmed that the combined software receiver is properly tacking three types of signals simultaneously.

8. The navigation solution from the combined software receiver is compared with the navigation solution from GPS-only and GLONASS-only software receiver. Because of the small number of GLONASS satellites involved in the navigation solution relative to the number of GPS satellites and also because of the different weighting of the systems in the C^3NAVG^2™ program, the combined navigation solution tend to follow the navigation solution of GPS-only solution. GLONASS-

only solution shows the worse positioning results compared to GPS and GPS+GLONASS solution because of the small number of GLONASS satellites.

7.4 Recommendations

The following are some of the recommendation for future work on this research:

1. By launching the new generation of GLONASS satellites, GLONASS-K, a third civil signal (L3) will be added to pervious L1 and L2 signals. As such, expanding the software receiver to support the new signal is recommended.

2. It is worthy to investigate the performance of the combined software receiver in kinematics mode. All the data collection set-up during this research was in static mode. Although no significant differences in performance are expected, it would still be worth confirming overall performance.

3. Expanding the GPS L1 + GLONASS L1 + GLONASS L2 software receiver in a way that can track signals from other GNSS systems such as Galileo will provide the opportunity of tracking more signals and increasing accuracy and reliability of the navigation solution.

4. Considering the properties of GLONASS ranging codes, the cross-correlation errors that affect GPS do not affect GLONASS. As such, GLONASS software receiver can be used for tracking weaker signals.

5. More advanced architectures such as vector tracking and/or ultra-tight integration with inertial sensors can be applied.

REFERENCES

Bao, J., and Y. Tsui (2000a) *Fundamentals of Global Positioning System Receivers: a Software Approach,* John Wiley & Sons, Inc., pp.4

Bao, J. and Y. Tsui (2000b) *Fundamentals of Global Positioning System Receivers: a Software Approach,* John Wiley & Sons, Inc., pp. 133

Bartenev V., V.E. Kosenko, V.D. Zvonar, V.E. Chebotaryov (2005) "Space vehicle GLONASS-M. Peculiarities of goal designing," *10th International Conference on System Analysis, Controlling and Navigation*, Eupatoria, 3-10 July

Bazlov, Y., V.F. Galazin, B.L. Kaplan, V.G. Maksimov, V.P. Rogozin (2006*) GLONASS to GPS: a new coordinate transformation*, GPS world, January, Vol. 10, No. 1, pp.54-58

Beser, J., and J. Danaher (1993) "The 3S Navigation R-100 Family of Integrated GPS/GLONASS Receivers: Description and Performance Results*," in the Proceedings of Institute of Navigation National Technical Meeting*, 20-22 January, San Francisco CA, pp.25-45

Cannon, M.E. (2007) *Satellite Positioning,* ENGO 465 Lecture Notes, Department of Geomatics Engineering, The University of Calgary, Chapter 6, pp.204

CDDIS (2008) NASA's Archive of Geodesy Data, http://cddis.nasa.gov/ gnss_datasum.html, last access 10 February 2009

Chachis, G.C (2001) "Navigation Professional. Public Policy Positions on GLONASS," *in the Proceedings of Institute of Navigation 57th Annual Meeting/CIGTF 20th Biennial Guidance Test Symposium*, 11-13 June, Albuquerque NM, pp.109-120

Charkhandeh, S., M.G. Petovello and G. Lachapelle (2006) "Performance Testing of a Real-Time Software-Based GPS Receiver for x86 Processors," in *Proceedings of ION GNSS*, 26-29 September, Forth Worth TX, pp2313- 2320, U.S. Institute of Navigation, Fairfax VA

Directorate-General Energy and Transport (2008) *Official Documents*, http:// ec.europa.eu/dgs/energy_transport/galileo/documents/official_en.htm, last accessed 15 January, 2008

Feairheller, S. and R. Clark (2006) *Other Satellite Navigation Systems, Understanding GPS Principles and Applications*, E.D. Kaplan and C. J. Hegarty, eds, Norwood, MA, Artech House, Inc.,Chapter 11

GLONASS ICD (2002), http://www.GLONASS-ianc.rsa.ru, last accessed 3 February, 2008

GLONASS.it (2008) *GLONASS System*, http://www.GLONASS.it, last accessed 30 June, 2008

GLONASS Constellation Status (2009), http://www.glonass-ianc.rsa.ru, last accessed 21 February 2009

GNSS Program Updates (2008), Institute of Navigation Newsletter, Volume 18, Number 1, Spring 2008, pp.12-13

GPS+Reference Manual (2007) *GLONASS Overview,* www.novatel.com/ Documents/ Manuals/GPS+Reference.pdf, Chapter 5, last accessed 15 January, 2008

Heckler, G.W., and J. L. Garrison (2004) "Architecture of a Reconfigurable Software Receiver", *in the Proceedings of Institute of Navigation GPS 2004,* 21-24 September, Long Beach CA, pp.947-955, U.S. Institute of Navigation, Fairfax VA

Heinrichs, G., M. Restle, C. Dreischer, and T. Pany (2007) "NavX®-NSR – A Novel Galileo/GPS Navigation Software Receiver," *in the Proceedings of Institute of Navigation GNSS,* 25-28 September, Fort Worth TX, pp.231-235, U.S. Institute of Navigation, Fairfax VA

Humphreys, T.D., M. L. Psiaki, P.M. Kintner, Jr., and B.M. Ledvina (2006) "GNSS Receiver Implementation on a DSP: Status, Challenges, and Prospects," *in the Proceedings of Institute of Navigation GNSS,* 26-29 September, Fort Worth TX, pp.2370-2382, U.S. Institute of Navigation, Fairfax VA

Inside GNSS (2007) *China Compass,* http://www.insidegnss.com/aboutcompass, last access January 15, 2008

Kovar, P., F. Vejrazka, L. seidl, and P. Lacmarik (2004) "Implementation of the GLONASS Signal-Processing Algorithm to the Experimental GNSS Receiver" *in the European Navigation Conference Proceeding*, 16-19 May, Rotterdam The Netherlands

Kovar, P., F. Vejrazka, L. seidl, and P. Lacmarik (2005) "GNSS Receiver for GLONASS signal reception" *in IEEE A&E System Magazine*, December 2005, pp.21-23

Lachapelle, G. (2007) *Advanced GNSS Theory*, ENGO 625 Lecture Notes. Deparctment of Geomatics Engineering, University of Calgary, Chapter 3

Ledvina, B.M, M.L. Psiaki, D.J. Sheinfeld, A.P. Ceruti, S.P. Powel, and P.M. Kintner (2004) " A Real-Time GPS Civilian L1/L2 Software Receiver," *in the Proceeding Of Institute of Navigation GPS 2004*, 21-24 September, Long beach CA, pp.986-1005, U.S. Institute of Navigation, Fairfax VA

Ledvina, B.M., M. Psiaki, T.E. Humphreys, S.P. Powel, and P.N Kintner (2005) "A Real-Time Software Receiver Tracking of GPS L2 Civilian Signals Using a Hardware Simulator," *in the Proceeding of Institute of Navigation GPS 2005*, 13-16 September, Long beach CA, pp.1598-1610, U.S. Institute of Navigation, Fairfax VA

Ledvina, B.M., M. Psiaki, T.E. Humphreys, S.P. Powel, and P.N Kintner (2006) "A Real-Time Software Receiver for the GPS and Galileo L1 Signal," *in the Proceedings of Institute of Navigation GPS/GNSS* ,26-29 September, Forth Worth TX, pp.2321-2333, U.S. Institute of Navigation, Fairfax VA

Leick, A. (1995) *GPS satellite surveying* (2nd ed.), New York NY, John Wiley & Sons

Ma, C., G. Lachapelle, and M.E. Cannon (2004) "Implementation of a Software Receiver," *in the Proceedings of Institute of Navigation GPS 2004,* 21-24 September, Long Beach CA, pp.882-893, U.S. Institute of Navigation, Fairfax VA

Macchi, F. and M.G. Petovello (2007) "Development of a One Channel Galileo L1 Software Receiver and Testing Using Real Data," *in the Proceedings of Institute of Navigation GNSS,* 25-28 September, Fort Worth TX, pp.2256-2296, U.S. Institute of Navigation, Fairfax VA

Misra, P. and P. Enge (2001) *Global Positioning System Signals, Measurement and Performance,* Lincoln, MA, Ganga-Jamuna Press, pp. 141

Mitrikas, V.V., S.G. Revnivykh, and E.V. Bykhanov (1998) "WGS84/PZ90 Transformation Parameters Determination Based on Laser and Ephemeris Long-Term GLONASS Orbital Data Processing", *in the Proceedings of the 11th International Workshop on Laser Ranging*, Deggendorf, Germany, September 21-25, p. 279

Mumford, P.J, K. Parkinson, and A. Dempster (2006) "The Namuru Open GNSS Research Receiver ," *in the Proceedings of Institute of Navigation GNSS,* 26-29 September, Fort Worth TX, pp.2847-2855, U.S. Institute of Navigation, Fairfax VA

Muthuraman, K., S. K. Shanmugam, and G. Lachapelle (2007) "Evaluation of Data/Pilot Tracking Algorithms for GPS L2C Signals Using Software Receiver," *in the Proceedings of Institute of Navigation GNSS,* 25-28 September, Fort Worth TX, pp.2499-2509, U.S. Institute of Navigation, Fairfax VA

NAVIGADGET (2007) *Navigation Satellite Wars*, http:// www.navigadget.com /index.php/2007/04/10/navigation-satellite-wars/, last accessed January, 2008

Normark, P.L., and C. Ståhlberg (2005) "Hybrid GPS/Galileo Real-time Software Receiver, " *in the Proceeding of Institute of Navigation GPS 2005*, 13-16 September, Long beach CA, pp.1906-1613, U.S. Institute of Navigation, Fairfax VA

O'Driscoll, C. (2007) *Performance Analysis of the Parallel Acquisition of Weak GPS Signals*, PhD Thesis, National University of Ireland, (Available at http://plan.geomatics.ucalgary.ca/)

Parkinson, B. W. (1996) *Introduction and Heritage of NAVSTAR, the Global Positioning System; Global Positioning System: Theory And Application,* .B. Parkinson and J. J. Spilker Jr., eds., volume 1, American Institute of Aeronautics and Astronautics, Inc., Washington D.C., USA, Chapter 1

Petovello, M.G., and G. Lachapelle (2006) "An Efficient New Method of Doppler Removal and Correlation with Application to Software-Based GNSS Receivers," *in the Proceedings of the 19th International Technical Meeting of the Satellite Division of the Institute of Navigation ION GNSS*, September 26 - 29, Fort Worth, Texas, pp.2407–2417

Petovello, M.G. and C. O'Driscoll (2007) *GSNRx™ Algorithm design Document,* Position, Location And Navigation (PLAN) Group, Department of Geomatics Engineering, The University of Calgary, Canada

Petovello, M.G., C. O'Driscoll, G. Lachapelle, D. Borio, and H. Murtaza (2008) "Architecture and Benefits of an Advanced GNSS Software Receiver," *in the Proceeding of International Symposium on GPS/GNSS 2008,* November 11-14, 2008, Tokyo, Japan

Polischuk, G. and S. Revnivykh (2004) *Status and Development of GLONASS*, available at www.sciencedirect.com, last access April, 2008

Psiaki, M.L.(2001)"Block acquisition of weak GPS signals in a software receiver," *In the Proceedings of the 14th International Technical Meeting of the Satellite Division of the Institute of Navigation GPS 2001*, 11-14 September, pp. 2838–2870. Institute of Navigation, Salt Lake City, Utah,

Rambo, J.C. (1989) "Receiver Processing Software Design of the Rockwell International DoD Standard GPS Receivers," in the *proceedings of the Institute of Navigation GPS 89,* 27-29 September, Colorado Springs, CO

Ray, J.K. (2007) *Advanced GNSS Receiver Technology*, ENGO 638 Course Notes, Department of Geomatics Engineering, University of Calgary, Canada, pp.54-83

Revnivykh, S.G. (2007) "GLONASS Status, Development and Application," *International Committee on Global Navigation Satellite System (ICG) Second meeting*, September 4-7, 2007, Bangalore, India

Ryan, S. (2002) *Augmentation of DGPS for Marine Navigation,* PhD thesis, Department of Geomatics Engineering, University of Calgary, Canada, Chapter seven (Available at http://plan.geomatics.ucalgary.ca)

Satellite on the net (2008) *Launch Schedule*, www.satelliteonthenet.co.uk , last access April 2008

Sharawi, M.S., and O.V. Korniyenko (2007) "Software Defined Radios: A Software GPS Receiver Example," *in IEEE/ACS International Conference on Computer Systems and Applications*, 13-16 May, Amman, Jordan, pp.562 – 565

Skone, S., G. Lachapelle, D. Yao, W. Yu and R. Watson (2005) "Investigating the Impact of Ionospheric Scintillation using a GPS Software Receiver," *in the Proceedings of Institute of Navigation GNSS 2005*, 13-16 September, Long Beach CA, U.S. Institute of Navigation, Fairfax VA

Spelat, M., F. Dovis, G. Girau, and P. Mulassano (2006) " A Flexible FPGA/DSP Board for GNSS Receivers Design " , appears in *Research in Microelectronics and Electronics 2006 Ph. D.*, Otranto, pp.77-80

Spilker J.J. Jr., and B.W. Parkinson (1996) Overview of GPS Operation and Design, B. Parkinson and J. J. Spilker Jr., eds., *Global Positioning System: Theory And Applications*, volume 1, Chapter 2, American Institute of Aeronautics and Astronautics, Inc., Washington D.C., USA.

Spilker, J.J., Jr. (1977), Digital communication by Satellite, Prentice Hall, Englewood Cliffs, NJ, Chapter 12, pp.347-357

Tomatis, A., F. Dovis, M. Pini, and M. Fantino (2007) "ITACA: a Scientific GNSS Software Receiver for Innovation Creation and Testing," *in theProceedings of Institute of Navigation GNSS,* 25-28 September, Fort Worth TX, pp.2723-2730, U.S. Institute of Navigation, Fairfax VA

Van Dierendonck, A.J. (1995) *GPS Receivers, Global Positioning System: Theory and Application,* B.W. Parkinson and J.J. Spilker, Jr., volume 1, American Institute of Aeronautics and Astronautics, Chapter 8

Ward, P.W., J.W. Betz and C.J. Hegarty (2006) *Satellite Signal Acquisition, Tracking, and Data Demodulation, Understanding GPS Principles and Applications*, E. D. Kaplan and C.J. Hegarty, Norwood, MA, Artech House, Chapter 5

Won, J., P. Thomas, and B. Eissfeller (2006) "Design of a Unified MLE Tracking for GPS/Galileo Software Receivers," *in the Proceedings of Institute of Navigation GNSS,* 26-29 September, Fort Worth TX, pp.2396-2406, U.S. Institute of Navigation, Fairfax VA

Zheng, B. and G. Lachapelle (2005) "GPS Software Enhancements for Indoor Use," *in the Proceedings of Institute of Navigation GPS 2005*, Long Beach CA, 13-16 September, U.S. Institute of Navigation, Fairfax VA

Zinoviev, A.E (2005) "Using GLONASS in Combined GNSS Receivers: Current Status,"

in the Proceedings of Institute of Navigation GPS/GNSS, 13-16 September 2005, Long

Beach CA, pp.1046-1057, U.S. Institute of Navigation, Fairfax VA